

Characterization of the membrane protein Prat1 in the inner envelope of chloroplasts

Dissertation der Fakultät für Biologie

der

Ludwig-Maximilians-Universität München



vorgelegt von

Carsten Raoni Studte

aus São Paulo, Brasilien

München

2012

Erstgutachter: Prof. Dr. Jürgen Soll
Zweitgutachter: Prof. Dr. Wolfgang Frank

Tag der mündlichen Prüfung: 05. 10. 2012

Eidesstattliche Erklärung

Hiermit erkläre ich eidesstattlich, dass ich diese Dissertation mit dem Titel „Characterization of the membrane protein Prat1 in the inner envelope of chloroplasts“ selbstständig verfasst und keine anderen als die angegebenen Quellen und Hilfsmittel verwendet habe. Die Arbeit wurde in gleicher oder ähnlicher Form keiner anderen Prüfungsbehörde zur Erlangung eines akademischen Grades vorgelegt.

München, den 08. 08. 2012

A handwritten signature in black ink, appearing to read 'Carsten Studte', written in a cursive style.

Carsten Studte

Summary

Almost the entirety of all chloroplast proteins is nuclear-encoded, synthesized in the cytosol and translocated post-translationally across the outer and inner envelope into the chloroplast. This transfer is mainly mediated by the subunits of the Toc and Tic complexes (translocon at the outer/inner envelope membrane of chloroplasts). In addition to the transport of preproteins, the compartmentalisation in eukaryotic cells, which enables metabolic pathways to progress simultaneously, requires abundant shuttling of diverse metabolites. Specific transporter proteins and ion-channels are responsible for this traffic across the membranes. The aim of this study was to further characterize the membrane protein Prat1, a predicted transporter and member of the Prat protein-family (preprotein and amino acid transporters). In earlier studies, a potential transport function of Prat1 was deduced by its ability to complement the function of Tim22 in yeast, a protein responsible for mediating the integration of carrier preproteins into the inner membrane of mitochondria.

In a first approach, the Prat1 protein could be localized to the inner envelope of chloroplasts using *Pisum sativum* as model system, by applying a specifically generated antibody. Biochemical analysis gave rise to a topology model of the protein, consisting of four transmembrane domains connected by hydrophilic loops, with the N- and C-termini both reaching into the stroma of the chloroplast, making possible protein-interactions that might be regulated by a phosphorylation site in the N-terminus accessible from the stromal side. Additionally, it could be shown that all five cysteines that are present in the protein are positioned within the transmembrane domains and are thus not accessible for putative redox regulation. Furthermore, comprehensive phenotypic analyses of a double mutant plant of both Prat1 isoforms present in the model plant *Arabidopsis thaliana* demonstrated retardation in growth in comparison to the wild type. In combination with a metabolic profiling of these plants, off-regulation of key players in the process of photorespiration could be identified that may be responsible for the defects in growth. Analyses of the expression levels of Prat1 resulted in an exemplary circadian rhythm on the RNA level in contrast to constant protein levels. Moreover, the purified Prat1 protein was successfully stably inserted into liposomes that were used for electrophysiological measurements to validate the proposed channel activity of Prat1. Although an extended set of conditions was tested to reveal the optimal conditions for Prat1 to demonstrate channel activity within a lipid bilayer, these analyses have to be continued in future experiments to conclusively measure the transport properties of Prat1. However, the results of the present study contribute to a better understanding of the suggested function of Prat1 as a transporter of preproteins or metabolites.

Zusammenfassung

Fast alle chloroplastidären Proteine sind im Zellkern codiert, werden im Zytosol synthetisiert und posttranslational durch die äußere und innere Hüllmembran in den Chloroplasten importiert. Dieser Transfer wird hauptsächlich durch die Untereinheiten des Toc und Tic Komplexes (translocon at the outer/innner envelope membrane of chloroplasts) ermöglicht. Zusätzlich zum Transport von Vorstufenproteinen erfordert die Kompartimentierung in eukaryotischen Zellen, welche den simultanen Ablauf von Stoffwechselwegen ermöglicht, einen hohen Austausch verschiedenster Metaboliten. Spezifische Transportproteine und Ionenkanäle sind für den Transfer durch die Membranen zuständig. Das Ziel dieser Arbeit lag in der Fortführung der Charakterisierung des Membranproteins Prat1, welches als Transportprotein der Prat Proteinfamilie (preprotein and amino acid transporters) prognostiziert wird. Vorherige Studien haben eine potentielle Transporterfunktion von Prat1 aufgrund seiner Fähigkeit, die Funktion von Tim22 in Hefe zu komplementieren, deduziert, einem Protein, das für die Integration von Carrier-Vorstufenproteinen in die innere Membran von Mitochondrien zuständig ist.

In einem ersten Ansatz konnte Prat1 im Modellsystem *Pisum sativum* mittels eines spezifisch hergestellten Antikörpers in der inneren Hüllmembran des Chloroplasten lokalisiert werden. Biochemische Analysen ermöglichten das Erstellen eines Topologiemodells des Proteins, welches aus vier Transmembrandomänen besteht, die mit hydrophilen Schleifen verbunden sind und dessen N- und C-Terminus in das Stroma des Chloroplasten reichen. Somit können mögliche Proteininteraktionen, die eventuell durch die Phosphorylierung des N-Terminus gesteuert werden, von der stromalen Seite stattfinden. Auch konnte gezeigt werden, dass alle fünf im Protein vorhandenen Cysteine sich innerhalb der Transmembrandomänen befinden und daher für eine putative Redox-Regulierung nicht erreichbar sind. Des Weiteren haben umfangreiche phänotypische Untersuchungen der Doppelmutante beider in der Modellpflanze *Arabidopsis thaliana* existenten Prat1 Isoformen eine Verzögerung der Wachstumsrate im Vergleich zu den Wildtyppflanzen gezeigt. In Verbindung mit einem metabolischen Profil dieser Pflanzen konnten abweichende Regulierungen von Schlüsselkomponenten der Photorespiration festgestellt werden, welche für die Defekte im Wachstum verantwortlich sein könnten. Expressionsanalysen von Prat1 ließen einen charakteristischen circadianen Rhythmus auf der RNA-Ebene im Gegensatz zu einem konstanten Proteinvorkommen erkennen. Darüber hinaus konnte das gereinigte Prat1 Protein erfolgreich stabil in Liposomen eingebaut werden, die in elektrophysiologischen Messungen verwendet wurden um die erwartete Kanalaktivität von Prat1 zu validieren.

Wenngleich eine umfassende Anzahl von Bedingungen getestet wurden um die optimalen Voraussetzungen zur Messung der Kanalaktivität von Pral1 in einer Lipiddoppelschicht feststellen zu können, so müssen diese Studien in weiteren Versuchen fortgeführt werden um endgültig die Kanaleigenschaften von Pral1 zu identifizieren. Dennoch tragen die Ergebnisse dieser Arbeit zu einem besseren Verständnis der angedeuteten Funktion von Pral1 als Transporter für Vorstufenproteine oder Metaboliten bei.

Table of contents

Eidesstattliche Erklärung.....	i
Summary	ii
Zusammenfassung.....	iii
Table of contents	v
Abbreviations	viii
1 Introduction	1
1.1 General import pathway into chloroplasts.....	1
1.2 The Prat protein family.....	4
1.3 Potential function of Prat1	6
1.4 Aim of this work.....	8
2 Materials.....	9
2.1 Chemicals	9
2.2 Enzymes.....	9
2.3 Assay Kits and column materials	10
2.4 Molecular weight markers and DNA standards	10
2.5 Oligonucleotides.....	10
2.6 Vectors, clones and strains	11
2.7 Antibodies.....	12
2.8 <i>E.coli</i> media and plates.....	12
2.9 Plant material.....	13
3 Methods.....	13
3.1 Molecular biological methods	13
3.1.1 General molecular biological methods	13
3.1.2 Polymerase chain reaction (PCR)	13
3.1.3 <i>In vitro</i> transcription and translation.....	14
3.1.4 Genomic DNA isolation from <i>Arabidopsis thaliana</i>	14
3.1.5 RNA extraction from <i>Arabidopsis thaliana</i> and quantitative RT-PCR.....	14
3.1.6 Sequencing.....	15
3.2 Biochemical methods	15
3.2.1 SDS polyacrylamide gel electrophoresis (PAGE) and staining.....	15
3.2.2 Determination of protein and chlorophyll concentration.....	16
3.2.3 Precipitation of proteins with trichloroacetic acid (TCA)	16
3.2.4 Immunoblotting and visualization	16

3.2.5 Protein expression and purification	17
3.2.6 Two-dimensional blue native (BN) electrophoresis	18
3.2.7 Proteolysis assays with thermolysin, trypsin and GluC.....	19
3.2.8 PEGylation assay	20
3.2.9 AMS assay	20
3.2.10 Extraction of inner envelope.....	21
3.2.11 Liposome preparation	21
3.2.12 Flotation assay	22
3.2.13 Thin-layer chromatography.....	22
3.2.14 Swelling assay.....	22
3.2.15 Isoelectric focusing (IEF)	23
3.2.16 Phosphorylation and de-phosphorylation assay.....	24
3.2.17 Cross-linking.....	25
3.2.18 Metabolite analyses.....	25
3.2.19 Protein identification by mass spectrometry (MS)	26
3.3 Cell biological methods	26
3.3.1 Isolation of intact chloroplasts from <i>Pisum sativum</i>	26
3.3.2 Preparation of inner and outer envelope vesicles from <i>Pisum sativum</i>	27
3.3.3 Isolation of stroma from <i>Pisum sativum</i>	27
3.3.4 Isolation and fractionation of <i>Arabidopsis thaliana</i> chloroplasts	27
3.3.5 Protein import experiments.....	28
3.4 Plant growth conditions and phenotyping	28
3.5 Electrophysiological measurements	30
3.6 Cryo-electrotomography.....	31
4 Results	32
4.1 Purification of Prat1	32
4.2 Generating an antibody against psPrat1	33
4.3 Localisation of Prat1	34
4.4 Topology of Prat1 in the inner envelope	35
4.4.1 Prat1 is protease resistant.....	37
4.4.2 PEGylation of Prat1 identifies cysteins in transmembrane helices	38
4.4.3 AMS treatment further supports location of cysteins in transmembrane helices	39
4.4.4 Prat1 can be phosphorylated at the first serine in the N-terminus.....	41
4.5 Prat1 forms small complexes.....	42

4.6 Flootation of Prat1 proteoliposomes demonstrates stable insertion	44
4.7 Electrophysiological measurements	46
4.8 Δ Prat1.1 Prat1.2 represents a true loss of function line in <i>Arabidosis thaliana</i>	48
4.9 Phenotyping of the atPrat1 double mutant	50
4.9.1 Root growth in the Prat1 double mutant is slightly increased	52
4.10 RNA expression is regulated with the circadian clock.....	54
4.11 P1DM is affected in photorespiration, the TCA cycle and the oxidative pentose phosphate cycle (metabolic influences).....	57
5 Discussion	60
5.1 The membrane-spanning protein Prat1 in the IE of chloroplasts	60
5.2 Possible role of Prat1-phosphorylation.....	63
5.3 RNA expression of Prat1 follows a circadian rhythm.....	64
5.4 Prat1 influences certain metabolic pathways.....	67
6 References	70
8 Acknowledgements	80
9 <i>Curriculum Vitae</i>	81

Abbreviations

aa	amino acid
<i>A. thaliana</i>	<i>Arabidopsis thaliana</i>
AMS	4-acetamido-4-maleimidylstilbene-2,2-disulfonic acid
AP	alkaline phosphatase
approx.	approximately
ATP	adenosine-5'-triphosphate
BCIP	5-bromo-4-chloro-3-indolyl-phosphate
BLAST	basic local alignment search tool
bp	base pair
Brij-35	polyoxy-ethylene (23) alkyl-ether or polyoxyethyleneglycol dodecyl ether
BSA	bovine serum albumin
β -ME	β -mercaptoethanol
BN	blue-native
$^{\circ}$ C	degree Celsius
Chl	chlorophyll
Col-0	Columbia-0 (<i>A. thaliana</i> ekotype)
Cys	cysteine
Da	Dalton
cDNA	complementary DNA
DeMa	<i>n</i> -decyl- β -maltoside
DNA	deoxyribonucleic acid
DNase	desoxyribonuclease
dNTP	desoxy-nucleosidtriphosphate
DTT	dithiothreitol
ECL	enhanced chemiluminescence
<i>E. coli</i>	<i>Escherichia coli</i>
EDTA	ethylenediaminetetraacetic acid
EM	electron microscopy
EtOH	ethanol
et al.	and others (latin: et alii)
FBPase	fructose-1,6-bisphosphatase
fwd	forward
H ₂ O	water
Hepes	(4-(2-hydroxyethyl)-1-piperazineethanesulfonic acid
His	histidine
HMW	high molecular weight
IE	inner envelope
IEF	isoelectric focusing
IMS	intermembrane space
k, K	kilo, times 1000
LB	Luria Bertani medium
LBamp	Luria Bertani medium with ampicillin

LS	<i>n</i> -lauroylsarcosine
Mal	maleimide
MeOH	Methanol
mM	millimolar
min	minute
MS	Murashige-Skoog salt
NBT	nitro blue tetrazolium
OD	optical density
OE	outer envelope
PAGE	polyacrylamide gel electrophoresis
PCR	polymerase chain reaction
PEG	polyethylene glycol
PMSF	phenylmethylsulfonyl fluoride
<i>Pst</i> I	type II restriction endonuclease from <i>Providencia stuartii</i>
<i>P. sativum</i>	<i>Pisum sativum</i>
PVDF	polyvinylidene fluoride
rev	revers
RNA	ribonucleic acid
RNase	ribonucleiase
rpm	revolutions per minute
RT	room temperature
RT-PCR	reverse transkriptase- polymerase chain reaction
SDS	sodium dodecyl sulphate
T-DNA	transfer-DNA
<i>Taq</i>	DNA-polymerase from <i>Thermus aquaticus</i>
TCA	trichloroacetic acid
TCEP	tris(2-carboxyethyl) phosphine
Tic	translocon at the inner envelope of chloroplasts
TIM	Translocase of the inner mitochondrial membrane
TM	transmembrane (domain)
Toc	translocon at the outer envelope of chloroplasts
TP	transit peptide
Tris	tris(hydroxymethyl)-aminomethane
v/v	volume per volume
w/v	weight per volume
WT	wild type
x g	times the force of gravity

1 Introduction

Plant cells contain two types of endosymbiotic organelles: plastids and mitochondria (Margulis, 1970). Both evolved from α -proteobacteria. Plastids, including chloroplasts – the most common type of plastids – developed from cyanobacteria, which were engulfed by an ancient mitochondrial eukaryotic host. The ability of plants to convert the energy of light into chemically bound energy generating both biomass and oxygen via a process called photosynthesis (Emerson et al., 1932) takes place within chloroplasts located in the green leaves, making them essential for today's life on earth. Additional crucial functions of chloroplasts include the biosynthesis of fatty acids, porphyrin and amino acids and the assimilation of nitrite and sulphate. To successfully accomplish all these tasks and taking into account that more than 90% of all chloroplast proteins are translated at ribosomes located in the cytosol due to an extensive evolutionary horizontal gene transfer from the plastids to the nucleus, massive traffic (in and out) of metabolites, nutrients and proteins occurs at the two envelope membranes surrounding the plastids. For this purpose specific transporters and ion channels are present in both membrane systems (Philippar and Soll, 2007; Weber and Fischer, 2007).

1.1 General import pathway into chloroplasts

Of the approx. 3000 proteins located in the chloroplast only 50 – 250 (depending on the species) are encoded in the plastome (Gould *et al.*, 2008), meaning that all others need to be imported posttranslationally. Proteins that are destined for the chloroplast are targeted via their transit peptide, which can either be an internal sequence, as it is mainly the case for proteins of the outer envelope (OE; Bölder *et al.*, 1999; Li and Chen, 1996; Pohlmeier *et al.*, 1997; Pohlmeier *et al.*, 1998; Salomon *et al.*, 1990; Seedorf *et al.*, 1995) or a cleavable peptide on the N-terminal end of the preprotein that is removed after the import process. The size and structure of these transit peptides varies considerably (Cline *et al.*, 1985; von Heijne *et al.*, 1989). The machineries responsible for the general import pathway are called Toc (translocase at the outer envelope of chloroplasts) and Tic (translocase at the innner envelope of chloroplasts), located in the OE and the inner envelope (IE) respectively. For proper guidance and to keep the proteins in the necessary unfolded conformation (Ko *et al.*, 1992; May and Soll, 2000; Qbadou *et al.*, 2006) chaperones such as Hsp70 and 14-3-3 proteins (guidance complex) or Hsp90 and Hsp70 support the targeting to the Toc receptor proteins

known as Toc34 and Toc159 (Figure 1; Kessler *et al.*, 1994; Perry and Keegstra, 1994; Hirsch *et al.*, 1994;). Toc34 is anchored into the OE by a single transmembrane domain and can be regulated by phosphorylation and GTP/GDP-binding and hydrolysis. Activation results upon dephosphorylation with an ATP-dependant phosphatase (Sveshnikova *et al.*, 2000). For the larger Toc159, preprotein-binding leads to the activation of the endogenous GTPase activity, triggering a conformational change towards the activation of the translocation channel (Toc75). An alternative receptor protein is constituted by Toc64 that reaches into the cytosol containing a tetratricopeptide repeat domain (TPR; Sohr and Soll, 2000) known to mediate protein-protein interactions, especially with chaperones such as Hsp70 and Hsp90 (Frydman and Hohfeld, 1997; Lamb *et al.*, 1995; Fellerer *et al.*, 2011). The Toc and Tic machineries are considered to be located in close proximity to each other at so called contact sites (Schnell *et al.*, 1990; Schnell *et al.*, 1994; Perry and Keegstra, 1994), where OE and IE are physically near to one another to facilitate the translocation of proteins via the main channels of the Toc (Toc75) and the Tic (Tic110) machineries simultaneously. The intermembrane space (IMS) was postulated to be bridged by a Toc subunit (J-domain protein Toc12), the Tic component Tic22 and Hsp70 (Figure 1; Andrès *et al.*, 2010; Becker *et al.*, 2004). However, recent studies in *Pisum sativum* suggest Toc12 to be a truncated clone of one of the pea J-domain proteins, that it possesses a cleavable transit peptide and is localised in the stroma (Chiu *et al.*, 2010). Whether Tic22 and Hsp70 remain as the only mediators between the Toc and the Tic machineries, still needs to be resolved. Tic20 contains four transmembrane domains and thus shows structural similarities to bacterial amino acid transporters (Reumann *et al.*, 2005) and translocation channels of the inner membrane of mitochondria (Tim17 and Tim23; Rassow *et al.*, 1999). However, biochemical evidence for a function of Tic20 as main IE import channel is missing, even though channel activity has recently been demonstrated *in vitro* (Kovács-Bogdan *et al.*, 2011). Tic110, on the other hand, contains six transmembrane domains (Balsera *et al.*, 2009), reaches an equally high expression level as Toc75 (Vojta *et al.*, 2004) and was found in association with both preproteins and chaperones (Lübeck *et al.*, 1996; Nielsen *et al.*, 1997), indicating that Tic110 plays the major role for protein translocation at the IE. Additionally, channel activity was observed *in vitro* for Tic110 (Balsera *et al.*, 2009; Heins *et al.*, 2002). Further investigations will be necessary to better distinguish between the specific activities of Tic110 and Tic20 within the Tic machinery. Once the preprotein has passed the inner envelope, the stromal processing peptidase (SPP) cleaves off the transit peptide, resulting in the mature form of the protein (Richter and Lamppa, 1998) which is subsequently either inserted into the IE, remains in the stroma or continues its targeting to the

thylakoids. Other Tic components which have so far been described are Tic40, which is believed to provide the driving force together with the stromal chaperones Hsp93 and Hsp70 for the import (“motor complex”; Kovács-Bogdán *et al.*, 2010; Flores-Péres and Jarvis, 2012) and Tic62, Tic55 and Tic32 which present the so-called redox regulon (Figure 1, orange coloured), enabling the redox regulation of the import via their redox-sensitive groups (Küchler *et al.*, 2002; Stengel *et al.*, 2008).

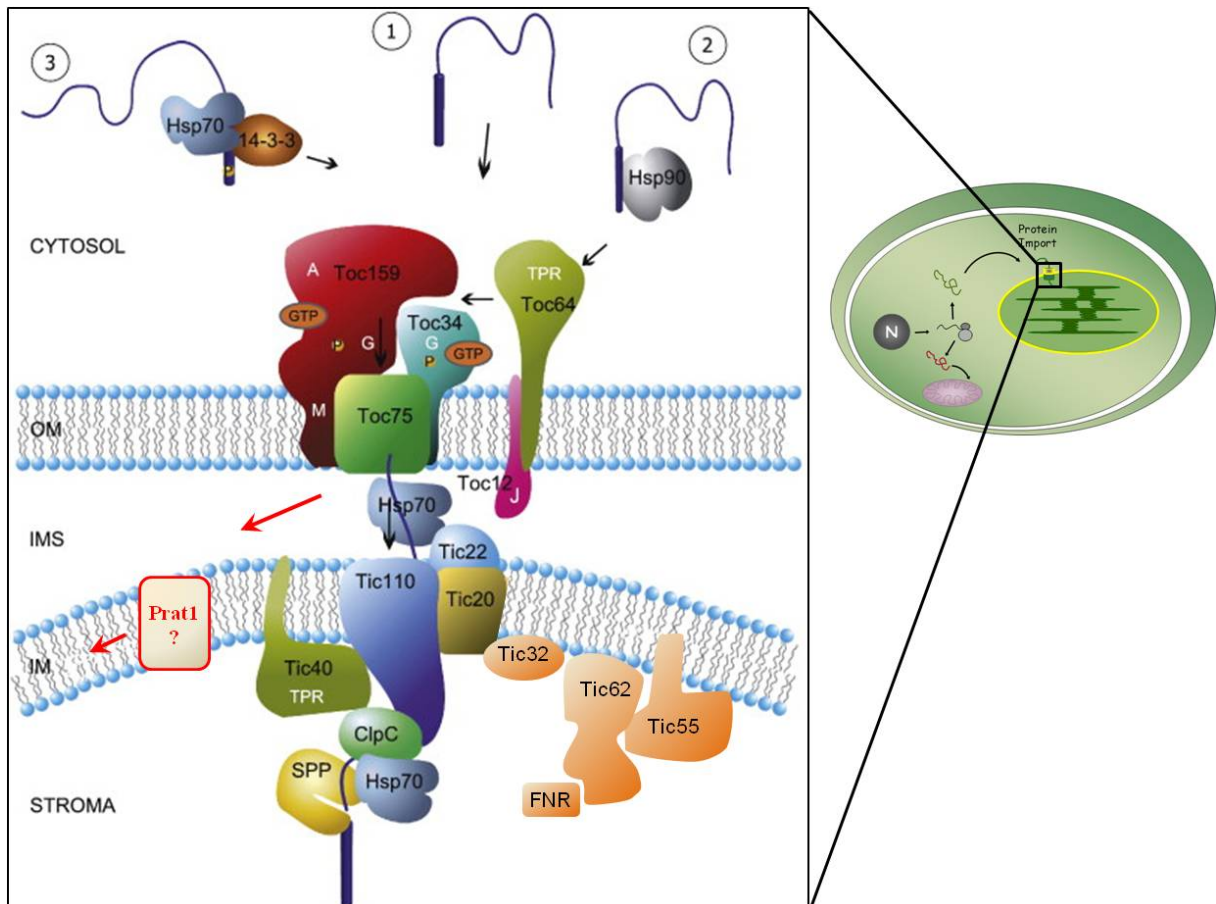


Figure 1: The Toc- and Tic-complex in chloroplasts.

Toc (translocase at the outer envelope of chloroplasts) and **Tic** (translocase at the innner envelope of chloroplasts) mediate the main import pathway for proteins from the cytosol, destined to the stroma or to the thylakoids (Andrès *et al.*, 2010; modified) (1) – (3) = three possible protein classes containing only a transit peptide (1) or additional chaperones (2: Hsp70/14-3-3; 3: Hsp90) targeted to the Toc complex. Toc75 and Tic110 represent the main import channels of the outer and inner envelope respectively. Tic62, Tic55 and Tic32 represent the redox regulon (coloured in orange) Red arrows indicate a speculative alternative pathway for proteins directed to Prat1 that are further inserted into the inner envelope. **FNR** = ferredoxin-NADP⁺ oxidoreductase; **SPP** = stromal processing peptidase; **Hsp** = heat shock protein; **TPR** = tetratricopeptide repeat domain; **OM** = outer envelope membrane; **IM** = inner envelope membrane. For further details, see text.

Beside this general import pathway for the majority of chloroplast-located proteins, several alternative import pathways exist, including translocation of proteins that possess no cleavable transit peptide and are destined for insertion into the IE (Figure 1, red arrows). The import route and participating transport components for these proteins is still speculative;

Prat1 was postulated as a candidate channel protein in this alternative translocation pathway (Rassow *et al.*, 1999). Hence, evolutionary origin and characteristics of the Prat1 protein will be introduced in the following.

1.2 The Prat protein family

The preprotein and amino acid transporters (Prat) were first discovered and described by Rassow *et al.*, 1999. Annotated in the phylogenetic tree for the Prat-family (Figure 2; Murcha *et al.*, 2007) are 17 proteins present in the genome of the model plant *Arabidopsis thaliana*, three from *Saccharomyces cerevisiae* and one from *Pisum sativum*. Common features of these proteins include the lack of a cleavable transit peptide, four predicted transmembrane domains (α -helices) separated by hydrophilic loops and a common sequence motif in the second and third transmembrane domain ($[G/A]_{x_2}[F/Y]_{x_{10}}R_{x_3}D_{x_6}[G/A/S]G_{x_3}G$; Rassow *et al.*, 1999). The sequence motif was defined by comparing the amino acid sequences of the Prat-proteins Tim17, Tim22 and Tim23 (translocase at the inner membrane of mitochondria) from yeast (*Saccharomyces cerevisiae*) with Oep16 (outer envelope protein 16 kDa) from pea (*Pisum sativum*) and the bacterial amino acid transporter LivH. However, further studies demonstrate that this motif is not conserved in all plant members of the Prat-family and that general sequence identity is low especially in the N- and C-termini of the proteins (Murcha *et al.*, 2007). Furthermore, the phylogenetic analysis reveals division of the members into 8 subfamilies (colour coded in Figure 2). Whereas the mitochondrial members of the family such as Tim17, Tim22 and Tim23 (e. g. Moro *et al.*, 1999; Bauer *et al.*, 1999) and the chloroplast localized Oep16 (Pudelski *et al.*, 2012) have been in the focus of numerous studies, only little is known about the two isoforms of Prat1 (Prat1.1 and Prat1.2) in *Arabidopsis thaliana* (highlighted in red, Figure 2) which are the focal point of this work. The remaining three groups in the phylogenetic tree have been subsequently named Prat2, Prat3 and Prat4 (Pudelski *et al.*, 2010). Although all members of the Prat-family are membrane proteins, their sub cellular localisation varies from the OE of chloroplasts for Oep16 to the inner membrane of mitochondria where Tim17, Tim22 and Tim23 are part of the Tim complex (Neupert and Herrmann, 2007) which is partially reminiscent to the Tic machinery (Figure 1; Figure 3). Prat2 has been found to be dually targeted to mitochondria and chloroplast membranes and both Prat3 and Prat4 are inserted into the membrane of mitochondria (Murcha *et al.*, 2007; Philippar *et al.*, 2007).

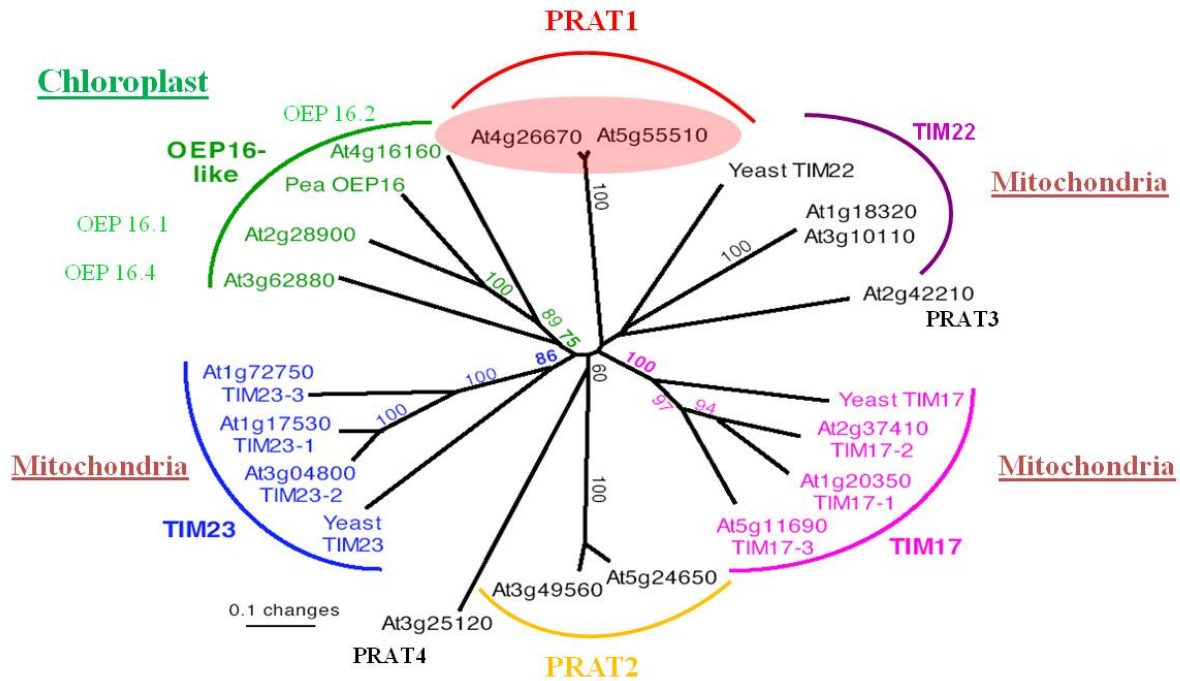


Figure 2: Phylogenetic tree of the Prat-Family.

Phylogenetic tree taken from Murcha *et al.*, 2007. Tim17, 22, 23 from yeast and Oep16 from pea were included in the comparison of the *A. thaliana* proteins. The 82 amino acids between the second and the fourth helix of the membrane proteins were used for the phylogenetic analysis. Included are the AGI codes of the proteins from *A. thaliana* and the subfamily names (Pudelski *et al.*, 2010). Highlighted in red are the Prat1.1 and Prat1.2 homologs.

Functionally, the members of the Prat-family are all proposed to be membrane-spanning channels (Murcha *et al.*, 2007; Pudelski *et al.*, 2010). Best characterised are the Tim17 and Tim23 proteins that form the major translocase at the inner membrane of mitochondria and Tim22 that represents the translocase of the carrier pathway for proteins inserted into the inner membrane of mitochondria (Figure 3). Another well-investigated example is Oep16, an abundant protein in the OE of chloroplasts that possesses channel activity shown by *in vitro* experiments. These studies indicate that Oep16 is selective for amino acids and amines while excluding triphosphates and uncharged sugars (Pohlmeyer *et al.*, 1997). The expression profiles for the three isoforms of Oep16 in *Arabidopsis thaliana* localise the strongest expression for Oep16.1 in mature leaves, Oep16.2 is only expressed in pollen, cotyledons and seeds (Drea *et al.*, 2006; Philippar *et al.*, 2007) and the ubiquitously expressed Oep16.4 is mainly found in seeds and pollen (Duy *et al.*, 2007; Pudelski *et al.*, 2010). Little is known about the Prat2, Prat3 and Prat4 proteins. In the following Prat1 will be the focus of interest.

1.3 Potential function of Prat1

A large scale proteome analysis of the chloroplast envelope membranes (Ferro *et al.*, 2002; Ferro *et al.*, 2003; Froehlich *et al.*, 2003) led to the discovery of Prat1. The two isoforms share an amino acid sequence identity of 77 % (Figure 3). A special feature of Prat1.1 is a high negative net charge (-9) in the N-terminus in (Prat1.2: -5). Like all Prat-family members the Prat1 proteins are structurally characterized by their four predicted transmembrane domains connected by hydrophilic loops, and the lack of a cleavable transit peptide.

At4g26670	PRAT	1.1	MAANDSSNAIDIDGNLDSDSLNTDCEATDNDSSKALVTIPAPAVCLFRFAGDAAGGAV
At5g55510	PRAT	1.2	MAAENSSNAINVDITSLDSDSKPNRDANDMTDHDSSKALVLPAPAVCLVRFAGDAASGAF
At4g26670	PRAT	1.1	MGSIFGYGSGLFKKKGFKGSFADAGQSAKTFAVLSGVHSLVVCLLKQIRGKDDAINVGVA
At5g55510	PRAT	1.2	MGSIFGYGSGLFKKKGFKGSFVDAGQSAKTFAVLSGVHSLVVCLLKQIRGKDDAINVGVA
At4g26670	PRAT	1.1	GCCTGLALSFPGAPQALQSCCLTFGAFSFILEGLNKRQTALAHSVSLRHOTGLFQDHHRA
At5g55510	PRAT	1.2	GCCTGLALSFPGAPQAMLQSCCLTFGAFSFILEGLNKRQTALAHSVSFRQOTRSPQ-HDL
At4g26670	PRAT	1.1	LP LSLALPIPEEIKGAFSSFC KSLAKPRKF-----
At5g55510	PRAT	1.2	PL LSLALPIHDEIKGAFSSFC NSLTKPKLKLKFP HAR

Figure 3: Alignment of Prat1.1 and Prat1.2.

The alignment shows Prat1.1 and Prat1.2 of *A. thaliana*. The black background indicates identical amino acids, grey highlights amino acids which are not identical but possess the same polarity or charge and the white background indicates divergent amino acids. The red bars mark the location of the transmembrane domains.

Using immunodetection, Prat1 could be localised to the chloroplast and more specifically to the envelope fraction containing both inner and outer envelope membrane, thereby confirming the prior proteome analysis (Murcha *et al.*, 2007).

Furthermore, both Prat1 and Prat2 were tested for their ability to complement the Prat-family member Tim22 in yeast (*Saccharomyces cerevisiae*). For this purpose, several vectors (containing either Tim22 or the Prat1 and Prat2 isoform) were each transformed into yeast strains in which the native Tim22 gene was placed under the control of an inducible galactose-dependent promoter (Figure 5A; Murcha *et al.*, 2007). The results clearly demonstrated normal growth of all strains in the presence of galactose (Figure 5C.). However, when the same strains were grown on galactose-free medium, the native Tim22 production was inhibited, leading to a lethal phenotype, since Tim22 is an essential gene (Kovermann *et al.*, 2002). Nevertheless, cell growth can be restored upon transformation with the additional vector containing Tim22 and, to a substantial extent, also by transformation of vectors containing either the Prat1.1 or Prat1.2 proteins (Figure 5B). The Prat2.1 and Prat2.2 proteins on the other hand cannot likewise substitute the function of Tim22 in yeast. The function of

Tim22 has been shown to be the translocation of proteins destined for insertion into the inner membrane of mitochondria called carrier pathway (Figure 4; Kurz *et al.*, 1999; Hasson *et al.*, 2010).

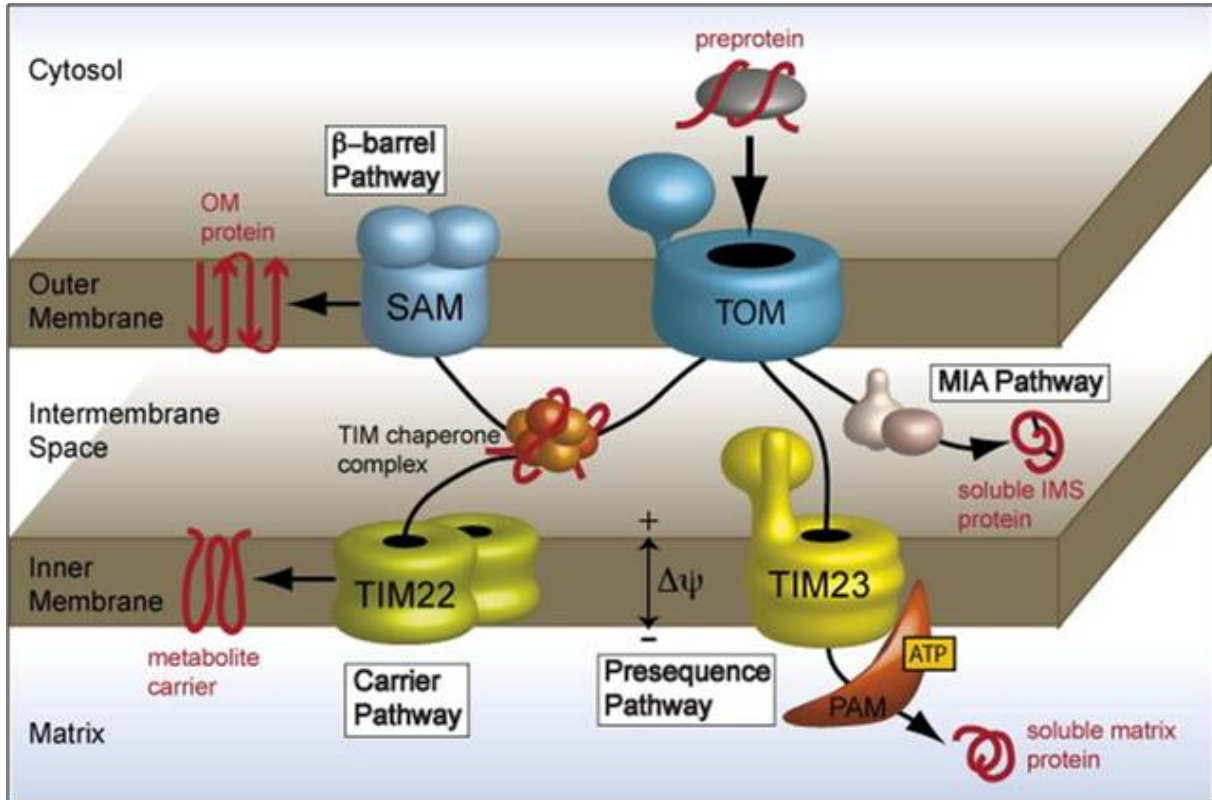


Figure 4: Import pathways for mitochondrial precursor proteins.

Figure taken from Bohnert *et al.*, 2007. **Tom** (translocase at the outer membrane of mitochondria) and **Tim** (translocase at the innner membrane of mitochondria) constitute the main import pathway (Tim23) for proteins from the cytosol, destined to the matrix. Tim22 is part of the carrier pathway, inserting proteins into the inner membrane of mitochondria. Additional pathways are known to insert proteins into the outer membrane of mitochondria (β -barrel pathway) and into the soluble intermembrane space (MIA pathway). **SAM** = sorting and assembly machinery; **MIA** = mitochondrial intermembrane space import and assembly; **PAM** = presequence translocase-associated motor. For further details, see text.

Taking into account that both Prat1 and Tim22 belong to the same protein family, the ability of the two Prat1 isoforms to rescue the lethal $\Delta Tim22$ phenotype in yeast indicates that Prat1 might fulfil a Tim22-related function at the inner envelope of chloroplasts.

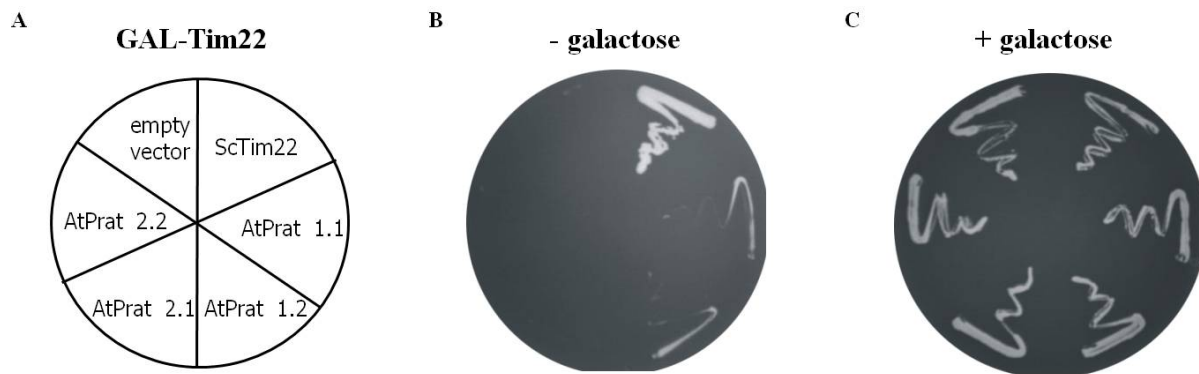


Figure 5: Prati.1 and Prati.2 can functionally complement Tim22 in yeast.

Figure taken from Murcha *et al.*, 2007. Tim22 was placed under the control of an inducible gal-promoter in yeast (*S. cerevisiae*). (A) Setup of the different strains containing the indicated genes in the inserted vector. (B) The lethal phenotype upon removing galactose from the growth medium can be rescued by Tim22 and partially, by both Prati1 isoforms from *A. thaliana*, but not by the Prati2 proteins. (C) When galactose is present in the medium, all strains show normal growth.

1.4 Aim of this work

This work focuses on the functional and structural characterization of Prati1 in chloroplasts. The first objective was to define the exact localisation combined with the topology of the protein within the membrane. Secondly, a loss of function mutant of Prati1 (*A. thaliana*) was analysed with regard to different aspects of plant growth. Thirdly, potential metabolic influences caused by the lack of Prati1 were determined and the expression pattern of the protein was monitored in wild type plants both on RNA- and protein-level. Finally, as Prati1 is known to be a member of the preprotein and amino acid transporter family, one objective focused on putative channel activity of the protein using electrophysiological methods.

2 Materials

2.1 Chemicals

The majority of chemicals used were purchased in high purity from Roche (Penzberg, Germany), Fluka (Buchs, CH), Sigma-Aldrich (Steinheim, Germany), Roth (Karlsruhe, Germany), Merck (Darmstadt, Germany), AppliChem (Darmstadt, Germany) or Serva (Heidelberg, Germany).

Additionally acquired were: Bio-Beads SM-2 Adsorbent from Bio-Rad Laboratories (Hercules, CA, USA), metoxypolyethylenglycol-maleimide 5000 Da (PEG-Mal) from Laysan Bio (Arab, AL, USA), L- α -phosphatidylcholine (PC, Type-IV-S), Tris(2-carboxyethyl) phosphine (TCEP), and iodoacetamide (IAA) from Sigma, 4-acetamido-4'-maleimidylstilbene-2,2'-disulfonic acid (AMS) from Invitrogen (Eugene, Oregon, USA) and radiolabeled amino acids ($[^{35}\text{S}]\text{Met}$) from DuPont-NEN (Dreieich, Germany). All bilayer lipids were obtained from IonoVation (Osnabrück, Germany) or Lipid Products (South Nutfield, England).

The detergents sodium dodecyl sulphate (SDS), and Triton X-100 (TX-100) were obtained from Roth, *n*-decyl- β -maltoside (DeMa) from Glycon (Luckenwalde, Germany), polyoxyethyleneglycol dodecyl ether (Brij-35) from Merck, digitonin from Calbiochem/Merck, *n*-lauroylsarcosine (N-LS) from Sigma and Nonidet P-40 (NP-40) from Fluka.

2.2 Enzymes

Restriction enzymes for cloning, RNA- and DNA-polymerases and T4-DNA ligase were obtained from Roche (Penzberg, Germany), MBI Fermentas (St. Leon-Rot, Germany), New England Biolabs (Frankfurt a. M., Germany), Qiagen (Hilden, Germany), Eppendorf (Hamburg, Germany), Diagonal (Münster, Germany), GeneCraft (Köln, Germany) and Finnzymes (Espoo, Finland). Reverse Transcriptase was purchased from Promega (Madison, USA), RNase-free DNase I from Roche and RNase from Amersham Biosciences (Uppsala, Sweden). The proteases thermolysin, GluC and trypsin were bought at Merck and Sigma-Aldrich.

2.3 Assay Kits and column materials

The “Plasmid Midi Kit” and “Nucleospin Extract II Kit” from Macherey and Nagel (Düren, Germany) were used for DNA purification and purification of DNA fragments from agarose gels, respectively. RNA from plants was isolated using the “Plant RNAeasy Kit” from Qiagen (Hilden, Germany). *In vitro* translation was performed with the “Flexi Rabbit Reticulocyte Lysate System” from Promega (Madison, USA).

Ni Sepharose Fast Flow column material for protein purification was supplied by GE Healthcare (München, Germany). Protein concentration columns (Amicon Ultra 10K and 4K) were purchased from Millipore (Billerica, MA, USA).

2.4 Molecular weight markers and DNA standards

PstI restricted λ -Phage DNA (MBI Fermentas) was used as a molecular size marker for agarose-gel electrophoresis.

For SDS-PAGE the “MW-SDS-70L” and “MW-SDS-200” markers from Sigma-Aldrich (Steinheim, Germany) and for BN-PAGE the “HMW Native Marker Kit” from GE Healthcare (München, Germany) were applied. Additionally in some cases a *prestained* marker from BioRad (München, Deutschland) was used.

2.5 Oligonucleotides

Oligonucleotide primers (Table 1) used in this work were ordered in standard desalted quality from either Invitrogen or Operon (Köln, Germany) or Metabion (Martinsried, Germany).

Table 1: Oligonucleotides used in this study.

Name	Sequence	T _m
PratC1 Xho1 fwd	GATCCTCGAGATGGCGACGGCGGATT	64.3°C
PratC1 Xho1 rev	GATCCTCGAGTCATCGAGATGTAGGATAAGCTACC	65.6°C
PratC1 EcoR1 fwd	GATCGAATTCATGGCGACGGCGGATT	61.1°C
PratC1 EcoR1 rev	GATCGAATTCTCATCGAGATGTAGGATAAGCTACC	63.3°C
RT-psPratC1-fwd	GGGTTCCGTTTTTGGATTCCG	54.4°C
RT-psPratC1-rev	CCAGTGCAGCATCCAGCTAC	55.9°C
RT-atC1.1-fwd	CGAAGCGACCGATAATGATTCC	54.8°C
RT-atC1.1-rev	GCCTCGGATTTGCTTCAGAAG	54.4°C

RT-atC1.2-fwd	GCATTGGTAATCCCTGCTCC	53.8°C
RT-atC1.2-rev	CAGACTGACCCGCATCCAC	55.4°C
RT-atC1.2-fwd neu	GTTGGAGTTGCTGGGTGTTGTAC	57.1°C
RT-atC1.2-rev neu	GCTTCTTGGGTTTCGTTAAGGAG	55.3°C
PratC1 S zu D fwd	CCATGGCGACGGCGGATGACGATGGTATTG	67.1°C
PratC1 S zu D rev	CGTGAGGCGGTGCAATACCATCGTCATCCGC	68.3°C
PratC1 S zu E fwd	CCATGGCGACGGCGGATGAGGATGGTATTG	67.1°C
PratC1 S zu E rev	CGTGAGGCGGTGCAATACCATCCTCATCCGC	68.3°C
pCold rev	CGATCGATTATTTATTTCTGAAAAC	51.7°C
T7 promoter (short)	TAATACGACTCACTATAGGG	47.7°C
at 18S F	AACTCGACGGATCGCATGG	53.2°C
at 18S R	ACTACCTCCCCGTGTCAGG	55.4°C
ps 18SrRNA fwd	CCAGGTCCAGACATAGTAAG	51.8°C
ps 18SrRNA rev1	GAGGGTTACCTCCACATAG	51.1°C
psHistonH4 fwd2	TCACCATGTCTGGAAGAG	48°C
psHistonH4 rev2	ACTGATACGCTTCACACC	48°C
LBa 1	TGGTTCACGTAGTGGGCCATCG	58.6°C

(T_m = melting temperature)

2.6 Vectors, clones and strains

Escherichia coli (*E. coli*) TOP10 (Invitrogen, Darmstadt, Germany) and BL21 (DE3) (Novagen/Merck, Darmstadt, Germany) strains were used for cloning of DNA fragments and heterologous expression of proteins, respectively.

The vectors applied for cloning were pET21d (Novagen/Merck), pCOLDII (Takara-Bio, Kyoto, Japan), pIVEX1.3 and pIVEX1.4 (Roche), pRsetA (Invitrogen) and pGex 6p1 (GE Healthcare; modified by MPI Biochemistry, Martinsried). A description of the DNA constructs generated during or required for this study is presented in Table 2.

Table 2: Plasmid DNA clones used in this work.

Gene	Vector	Organism	Description	Restriction site	Purpose
Prat1 (fl)	pET21d	<i>Pisum sativum</i>	C-terminal HIS-tag	<i>NcoI</i> - <i>XhoI</i>	overexpression
Prat1 (fl)	pColdII	<i>Pisum sativum</i>	C-terminal HIS-tag	<i>XhoI</i> - <i>EcoRI</i>	overexpression

Prat1 (fl)	pIVEX1.3	<i>Pisum sativum</i>	RTS system	<i>NocI - SacI</i>	overexpression
Prat1 (fl)	pIVEX1.4	<i>Pisum sativum</i>	RTS system	<i>NocI - SacI</i>	overexpression
Prat1 (fl)	pGex 6p1	<i>Pisum sativum</i>	C-terminal HIS-tag	<i>EcoRI - XhoI</i>	overexpression
Prat1 (fl)	pRsetA	<i>Pisum sativum</i>	C-terminal HIS-tag	<i>XhoI - EcoRI</i>	overexpression
Tic110 (M1)	pET21d	<i>Arabidopsis thaliana</i>	N-terminal part of mature Tic110 (aa 25- 258)	Balsera <i>et al.</i> 2009a	negative control
Prat1 (fl)	pET21d	<i>Pisum sativum</i>	Ser (aa 6) to Glu	site-directed mutagenesis	mimic phosphorylation
Prat1 (fl)	pET21d	<i>Pisum sativum</i>	Ser (aa 6) to Asp	site-directed mutagenesis	mimic phosphorylation

(**fl** = full-length; **M1** = N-terminal part of mature Tic110 ;**RTS** = rapid translation system)

2.7 Antibodies

A primary antibody against Prat1 (mature protein from *Pisum sativum*) was generated in this work. The overexpressed protein (pET21d/psPrat1 see Table 2) was sent to BioGenes (Berlin, Germany) for immunization of a rabbit.

The following antibodies were already available in the laboratory: Tic62 (C-terminus from *Pisum sativum*), Fructose-1,6- biphosphatase (FBPase; full-length protein from *Arabidopsis thaliana*), Tic110, Tic55, Tic22, Toc75, OE33, VDAC and LFNR1 (leaf isoform from *Arabidopsis thaliana*)

Secondary antibodies, coupled to alkaline phosphatase or horseradish peroxidase, against rabbit were purchased from Sigma-Aldrich.

2.8 *E.coli* media and plates

LB (Luria-Bertani) medium consisting of 1% Trypton (Difco), 0.5% yeast extract (Difco) and 1% NaCl was used for cultivation of *E.coli*. For selection purposes during overexpression 100 µg/ml ampicillin was added after autoclaving to the medium. Solid LB-plates contained additionally 2% of agar and were stored under sterile conditions at 4 °C.

2.9 Plant material

All experiments were performed with *Arabidopsis thaliana* plants, ecotype Col-0 (Lehle Seeds; Round Rock, USA). The T-DNA insertion lines used for generation of the double mutant of *Prat1* were *Prat1.1* (At4g26670 – Salk020671) and *Prat1.2* (At5g55510 – Slak001823). They were purchased from NASC (University of Nottingham, GB).

Peas (*Pisum sativum*) var. “Arvica” were ordered from Bayerische Futtersaatbau (Ismaning, Germany).

3 Methods

3.1 Molecular biological methods

3.1.1 General molecular biological methods

General molecular biological methods like growing conditions of bacteria, preparation of transformation-competent bacteria, DNA precipitation, determination of DNA concentration, and bacterial transformation were performed as described (Sambrook *et al.*, 1989) with slight modifications. Preparation of plasmid DNA, restrictions, ligations, and agarose gel electrophoresis were performed as described (Sambrook *et al.*, 1989) with modifications according to the manufacturer’s recommendations for the corresponding enzymes.

3.1.2 Polymerase chain reaction (PCR)

Polymerase chain reactions (PCR) were performed according to Saiki *et al.* (1988) under the conditions recommended by the manufacturer of the DNA polymerase containing kit (Phusion, Finnzymes, Espoo, Finland). For site directed mutagenesis, clones containing the wild type insert of interest were amplified by PCR using two specific primers, including the desired mutation (see 2.5 Oligonucleotides). The PCR reaction mix was digested with DpnI and transformed in TOP10 cells. The colonies were tested for plasmids containing the mutation by sequencing.

3.1.3 *In vitro* transcription and translation

Transcription of linearized plasmids was carried out as previously described (Firlej-Kwoka *et al.*, 2008). Translation was carried out using the Flexi Rabbit Reticulocyte Lysate System (Promega) following the manufacturer's protocol in presence of [³⁵S]-methionine for radioactive labelling. The samples were analysed by a polyacrylamide SDS-PAGE. Signals were then detected by exposure of the dried gels on X-ray films (Kodak Biomax MR, PerkinElmer, Rodgau, Germany).

3.1.4 Genomic DNA isolation from *Arabidopsis thaliana*

A small *Arabidopsis thaliana* leaf piece (~ 0.5 x 0.5 cm) was cut and transferred to a 1.5 ml microtube. Next, 200 µl extraction buffer (200 mM Tris/HCl (pH 7.5), 250 mM NaCl, 25 mM ethylenediaminetetraacetic acid (EDTA), 0.5% SDS) and one small iron bead was added to the tube and the sample was lysed in a TissueLyser (Qiagen, Hilden, Germany) for three minutes at maximum speed. After pelleting of the debris for 15 min. at 15,000 rpm and room temperature (RT), 100 µl of the supernatant were transferred to a fresh tube. To precipitate the genomic DNA, one volume of -20 °C isopropanol was added to the sample, carefully mixed and centrifuged for another 15 min. at 15,000 rpm and 4 °C. The resulting pellet was washed once with 70% ethanol, subsequently air-dried and finally resuspended in 50 µl of sterilized H₂O or 10 mM Tris/HCl (pH 8.5). The sample was immediately used for PCR-analysis. For this purpose, any residual nondissolved debris was pelleted for 1 min. at full speed in a table-top centrifuge and 0.5 µl of the DNA sample supernatant was then added to a standard 25 µl volume PCR.

3.1.5 RNA extraction from *Arabidopsis thaliana* and quantitative RT-PCR

Total RNA from leaves of three-week-old *Arabidopsis thaliana* plants was isolated using the Plant RNeasy Extraction kit (Qiagen, Hilden, Germany). The RNA was digested with RNase-free DNase I (Qiagen) and transcribed into cDNA using MMLV Reverse transcriptase (Promega, Mannheim). Detection and quantification of transcripts were performed as described previously (Benz *et al.*, 2009).

For quantitative RT-PCR, the FastStar DNA Master SYBR-Green Plus kit was used and the reaction was performed in the iCycler (BioRad) using the appropriate pairs of

oligonucleotides (see 2.5 Oligonucleotides). The relative abundance of all transcripts amplified was normalized to the expression level of 18S rRNA.

3.1.6 Sequencing

All cloned constructs (see Table 2) were sent for sequencing to validate their accuracy. These analyses were performed by the sequencing service of the institute of genetics at the department of biology of the Ludwig-Maximilians-Universität.

3.2 Biochemical methods

3.2.1 SDS polyacrylamide gel electrophoresis (PAGE) and staining

The separation of proteins was performed with electrophoresis, using denaturing gels according to Laemmli (1970). Acrylamide concentrations (ratio of acrylamide to N,N-methylen-bisacrylamide 30:0.8) varied from 10 – 15% in the separating gel as indicated. For the stacking gel, 0.625 ml (two small gels) or 1.25 ml (large gel) of 0.5 M Tris/HCl, pH 6.8 and for the separating gel 1.875 ml (two small gels) or 3.75 ml (large gel) of 1.5 M Tris/HCl, pH 8.8 were used. Prior to loading the gels, the samples were heated for 3 min. at 95°C in solubilising buffer (250 mM Tris/HCl, pH 6.8; 40% glycerine; 9% SDS; 20% β -mercaptoethanol; 1 spatulap bromphenolblue) to denature the proteins. The running buffer consisted of 25 mM Tris, 192 mM glycine and 0.1% SDS.

For a better separation of small proteins, gels according to Schagger and Jagow (1987) were utilized. Separating and stacking gel contained 1.67 ml (4%) to 7.5 ml (15%) of 3 M Tris/HCl, pH 8.45 and 0.3% SDS. Additionally, 13% glycerine were added to the separating gel, leading to altered anode buffer (0.2 M Tris/HCl, pH 8.9) and cathode buffer (0.1 M Tris/HCl, pH 8.25, 0.1 M tricine, 0.1% SDS) compositions.

For coomassie staining, the gels were placed for 15 min in staining solution on a shaker (50% MeOH; 7% HAc; 0.18% coomassie brilliant blue R250; Sambrook et al., 1989). Background staining was removed by incubation in destain solution (40% MeOH, 7% HAc, 3% glycerine).

To carry out a silver staining (Ansorge 1985) the gel was placed overnight in fixing solution (40% MeOH, 7% HAc, 3% glycerine), before briefly (5 – 10 min.) incubating in solutions A (20% TCA, 50% MeOH, 2% CuCl₂, 0.1% formaldehyde), B (10% EtOH, 5%

HAc), D (1% KMnO₄, 40% KOH) B again and C (10% EtOH). Subsequently, the gel was washed for 10 min. with water prior to adding solution F (0.2% AgNO₃) for 10 min. and rinsed with water again. The staining occurred upon the addition of solution G (20% Na₂CO₃, 0.1% formaldehyde) and was stopped with destain solution.

All gels were watered after specific staining procedure and then dried under vacuum.

3.2.2 Determination of protein and chlorophyll concentration

For soluble proteins, the concentration was determined with the help of the Bio-Rad Protein Assay Kit (Bio-Rad, München, Germany; Bradford, 1976). Concentrations of proteins in membrane samples were determined according to Lowry *et al.*, 1951.

Determination of chlorophyll (Chl) concentration was carried out as described by Arnon, 1949.

3.2.3 Precipitation of proteins with trichloroacetic acid (TCA)

For precipitation of proteins from solution, a final concentration of 15% TCA was added to the sample and incubated for 30 min. on ice. The sample was then centrifuged for 30 min. at 20,000 g and 4 °C, subsequently 500 µl of cold acetone were added to the precipitate and incubated for 10 min on ice before centrifugation for 15 min. at 20,000 g and 4 °C. The final precipitate was dried and resuspended in solubilising buffer.

3.2.4 Immunoblotting and visualization

For antibody detection, proteins were electro-blotted onto polyvinylidene fluoride (PVDF; Immobilon-P; Zefa, Harthausen) or nitrocellulose membrane (Protran; Whatman, Dassel) using a semi-dry western blotting system (Hoefer TE 77; GE Healthcare, Freiburg, Germany) and Towbin buffer (25 mM Tris/HCl (pH 8.2-8.4), 192 mM glycine, 0.1% SDS, 20% methanol). Labelling with protein-specific primary antibodies was carried out by standard techniques using 1 – 5% skimmed milk or BSA (albumin fraction V, Roth, Karlsruhe, Germany) and 0.05% Tween 20 in TTBS (100 mM Tris/HCl, pH 7.5, 0.2% Tween 20 0.1% BSA, 150 mM NaCl). Antibody binding after washing of the membranes occurred either for 3 h at RT or overnight at 4 °C. Bound antibodies were visualized either with alkaline phosphatase (AP)- conjugated secondary antibodies (goat anti-rabbit IgG (whole molecule)-AP conjugated; Sigma) or using a chemiluminescence detection system (Enhanced

Chemiluminescence, ECL) in combination with a horseradish peroxidase-conjugated secondary antibody (goat anti-rabbit (whole molecule)-peroxidase conjugated; Sigma). The marker was cut from the blots and stained with amido black (stain: 0.1% w/v Naphthol Blue Black in 50% H₂O, 40% MeOH and 10% acetic acid; destain: 72.5% H₂O, 20% MeOH and 7.5% acetic acid).

ECL detection solution 1 (100 mM Tris/HCl (pH 8.5), 1% (w/v) luminol, 0.44% (w/v) coomarcic acid) and solution 2 (100 mM Tris/HCl (pH 8.5), 0.018% (v/v) H₂O₂) were mixed in a 1:1 ratio and added to the blot membrane (1-2 ml per small gel). After incubation for 1 min at RT (in the dark) the solution was removed and the luminescence detected using a film (Kodak Biomax MR; PerkinElmer, Rodgau, Germany).

Detection of AP signals was performed by incubation of the membrane in a buffer containing 66 µl NBT (nitro blue tetrazolium chloride, 50 mg/ml in 70% N,N-dimethylformamide) and 132 µl BCIP (5-bromo-4-chloro-3-indolyl phosphate, 12.5 mg/ml in 100% N,N-dimethylformamide) in 10 ml 100 mM Tris/HCl (pH 9.5), 100 mM NaCl, 5 mM MgCl₂ buffer.

3.2.5 Protein expression and purification

Prat1 (fl) from *Pisum sativum* with a HIS-tag was overexpressed in BL21 (DE3) cells (Novagen/Merck) in LB medium in the presence of 100 µg/ml ampicillin at 37 °C. For this purpose, a 30 ml pre-culture was first grown overnight to high density. The pre-culture was used for inoculation of four 2 l baffled flasks filled with 500 ml generating a starting OD₆₀₀ of 0.1 in each flask. Induction of the overexpression was performed with IPTG (Isopropyl β-D-1-thiogalactopyranoside) concentrations of 0.2 – 1 mM when the OD₆₀₀ reached approx. 0.5. Overexpression was then continued for 3- 4 h while shaking the flasks at 125 rpm and 37 °C. Afterwards cells were centrifuged for 20 min at 6000 rpm and 4 °C and stored at -20 °C until further use.

For purification cell lysis was performed in 20 mM Tris/HCl (pH 8.0), 150 mM NaCl and 1 mM phenylmethylsulfonyl fluoride (PMSF) by three passages through an M-110L Microfluidizer Processor (Microfluidics, Newton, MA, USA) and two repetitions of ten short impulses with a rod sonifer, while keeping the cells on ice. For purification of insoluble proteins, cell membranes and inclusion bodies were then pelleted by centrifugation at 40,000 g and 4 °C for 20 min and solubilized in 20 mM Tris/HCl (pH 8.0), 150 mM NaCl, 1% *n*-lauroylsarcosine (N-LS) for 1.5 h, rotating at 4 °C, followed by 15 min rotation at RT.

Unsolubilized material was removed by centrifugation at 20,000 g and 4 °C for 15 min, and the cleared supernatant was used for batch Ni-affinity purification using Ni-NTA-Sepharose (GE Healthcare, Munich, Germany). Prati1 was bound to Ni-NTA by rotation for 1 h at 4 °C. During binding to the beads (100 µl) a final concentration of 15 mM imidazole was present in the buffer. The beads were subsequently washed eight times with five volumes each of 20 mM Tris/HCl (pH 8.0), 150 mM NaCl, 0.3% N-LS, 15 mM imidazole. Elution was carried out six times, twice with one volume each of 20 mM Tris/HCl (pH 8.0), 150 mM NaCl, 0.3% N-LS and 100 mM imidazole twice with one bead volume each of 20 mM Tris/HCl (pH 8.0), 150 mM NaCl, 0.3% N-LS and 200 mM imidazole and finally twice with one volume each of 20 mM Tris/HCl (pH 8.0), 150 mM NaCl, 0.3% N-LS and 500 mM imidazole. All elutions were analyzed by SDS-PAGE and coomassie-staining, the elutions containing only minor amounts of contaminating proteins were pooled and concentrated on an Amicon column (Merck Millipore, USA).

For purification of dNTic110 from *Pisum sativum* the respective construct was overexpressed and purified as described previously (Balseira *et al.*, 2009a). Overexpression was performed using BL21 (DE3) cells (Novagen/Merck) at 27 °C in LB medium in the presence of 100 µg/ml ampicillin. When cell density reached an OD₆₀₀ of 0.5, the cells were induced with 0.2 mM IPTG and the temperature was shifted to 12 °C for overexpression at 125 rpm overnight. Next, cells were centrifuged for 20 min. at 6000 rpm and 4 °C and stored at -20°C until further use. Cell lysis was performed in 20 mM Tris/HCl (pH 8.0), 300 mM NaCl, 1 mM phenylmethylsulfonyl fluoride (PMSF), 5 mM β-ME and protease inhibitor cocktail tablet (Roche) using a French pressure cell press (Heinemann, Schwäbisch Gmünd, Germany), followed by centrifugation (40,000 g, 30 min, 4 °C). The supernatant was purified using HisTrap HP column (1 or 5 ml) with an ÄKTA purifier system (GE Healthcare, München, Germany). For wash and elution 20 mM Tris/HCl (pH 8.0), 300 mM NaCl with increasing concentrations of imidazole was used. Aliquots with high purity were collected and concentrated on an Amicon column for gel filtration (20 mM Tris/HCl (pH 8.0), 150 mM NaCl) on a Superdex 200 column to remove aggregates and remaining contaminants.

3.2.6 Two-dimensional blue native (BN) electrophoresis

Blue native gel electrophoresis (BN-PAGE) was carried out essentially as described in Schägger and von Jagow, 1991 and Wittig *et al.*, 2006 with the following modifications: Chloroplasts (equivalent to 25-50 µg of Chl) or IE membranes (50-200 µg protein content)

were solubilized in 50 mM Bis-Tris/HCl (pH 7.0), 750 mM 6-aminocaproic acid, 1% *n*dodecyl- β -D-maltoside by incubation on ice for 10 min. Afterwards the samples were centrifuged at 256,000 g for 10 min at 4 °C. The supernatant was supplemented with 0.1 volume of a coomassie blue G solution (5% coomassie brilliant blue G-250, 750 mM 6-aminocaproic acid) and loaded on a polyacrylamide gradient (5 – 12%) gel for separation in the first dimension. Electrophoresis was carried out at increasing voltage (stacking gel: 100 V max.; separating gel: 15 mA/400 V max. for a 12 x 14 cm gel, 8 mA max. for a 6 x 8 cm gel) at 4 °C. The first cathode buffer (5 mM tricine, 1.5 mM Bis-Tris/HCl (pH 7.0)) additionally contained 0.02% dye (coomassie blue G-250) and was replaced by buffer lacking dye after approximately one-third of the electrophoresis run had been completed. The anode buffer (5 mM Bis-Tris/HCl (pH 7.0)) remained constant for the entire run.

For the second dimension, the lanes of interest were cut out from the gel after the run of the first dimension and incubated in 1% SDS, 1 mM β -mercaptoethanol (β -ME) for 15 min, followed by 15 min in 1% SDS without β -ME and 15 min in SDS-PAGE electrophoresis buffer (25 mM Tris, 192 mM glycine, 0.1% SDS) at RT. Single lanes were then placed horizontally on top of SDS-PAGE gels (10 or 12.5% polyacrylamide content), and the individual complexes were separated into their constituent subunits by denaturing electrophoresis (see 3.2.1).

For detection of proteins using specific antibodies, the gels were electro-blotted and labelling with protein-specific primary antibodies was carried out as described before (see 3.2.4).

3.2.7 Proteolysis assays with thermolysin, trypsin and GluC

For thermolysin (from *Bacillus thermoproteolyticus*) digestion, inner envelope vesicles (IE) (Seigneurin-Berny *et al.*, 2008; Li *et al.*, 1991; see 3.3.2) from *Pisum sativum* (10 μ g total protein content) or Prat1-proteoliposomes (approx. 4 μ g protein content) were pelleted (10 min, 256,000 g, 4 °C) and washed with 25 mM HEPES/KOH (pH 7.6), 5 mM MgCl₂ and 0.5 mM CaCl₂. The samples were incubated with 0.1 μ g/ μ l thermolysin for 5 – 30 min as indicated in the presence or absence of 1% Triton X-100 or 1% SDS at RT. The reaction was stopped by addition of 10 mM EDTA. Additionally, some samples were reduced with 10 mM DTT prior to the incubation with the protease if required. As negative control, 10 mM EDTA was added prior to thermolysin to the reaction mixture to inhibit proteolysis. Prat1 (and Tic110 as control in IE) was visualized by immunoblotting and antibody labelling after SDS-

PAGE. To digest IE from from *Pisum sativum* in a more specific manner, trypsin was applied. The digest leads to a specific pattern for Prat1. The digestion buffer consisted of 50 mM tricine (pH 8.5) and 0.1 mM CaCl₂. The incubation procedure was equal to the thermolysin treatment and the reaction was stopped by addition of 1 mM phenylmethylsulfonyl fluoride (PMSF), 5:1 volumes of trypsin inhibitor and 1:1 volume of α -macroglobulin. Additionally, some samples were reduced with 10 mM DTT prior to the incubation with the protease. As a control, all inhibitors were added before trypsin to the reaction mixture to repress proteolysis. Again, Prat1 (and Tic110 as control in IE) was visualized by immunoblotting and antibody labelling after SDS-PAGE.

Another specific digestion pattern is obtained with GluC (from *Staphylococcus aureus* V8). For this inner envelope from *Pisum sativum* was treated as described above and then resuspended in 50 mM NH₄HCO₃ (pH7.8). The samples were incubated with 0.1 – 4 μ g/ μ l GluC for 5 – 30 min in the presence or absence of 1% Triton X-100 or 1% SDS at RT. The reaction was stopped by addition of 5:1 volumes of α -macroglobulin. Additionally, some samples were reduced with 10 mM DTT prior to the incubation with the protease. As a control, excess α -macroglobulin was added before GluC to the reaction mixture to inhibit proteolysis. Prat1 was visualized as mentioned above.

3.2.8 PEGylation assay

IE vesicles from *Pisum sativum* (approx. 10 μ g protein content) were treated with 10 mM metoxypolyethylenglycol-maleimide 5000 Da (PEG-MAL, Laysan Bio, Arab, AL) in a buffer containing 100 mM Tris/HCl (pH 7.0), 1 mM EDTA, for 0, 5, 10, and 30 min respectively, at 4 °C in the dark in absence or presence of 1% SDS. In the presence of SDS, the incubation took place at RT. The PEGylation reaction, leading to a 5 kDa shift for each attached PEG-MAL on a cystein in Prat1, was stopped by addition of 100 mM DTT and SDS-PAGE solubilising buffer. Bis-Tris gels (0.36 M Bis-Tris/HCl (pH 6.5-6.8), 10% acrylamide), were employed using a MES running buffer (50 mM MES, 50 mM Tris, 1 mM EDTA, 1 mM sodium bisulfite, 0.1% SDS). The protein was detected by immunoblotting with a specific α Prat1 (*Pisum sativum*) antibody.

3.2.9 AMS assay

IE vesicles from *Pisum sativum* (approx. 10 μ g protein content) were treated with 10 mM of the membrane-impermeable sulfhydryl reagent, 4- acetamido -4- maleimidylstilbene -2,2-

disulfonic acid (AMS) in a buffer containing 100 mM Tris/HCl (pH 7.0), 2 mM EDTA for 1 h at RT in the dark. Additionally 1% SDS, 2 mM diamide or 2 mM TCEP (Tris 2-carboxyethylphosphine) was added to the samples if indicated. The reaction with AMS, leading to a shift of approx. 0.5 kDa for each attachment to a reduced cysteine in Prat1, was terminated by the addition of 5 μ l of non-reducing solubilising buffer (250 mM Tris/HCl, pH 6.8; 40% glycerine; 9% SDS; one spatulapip bromphenolblue) and 12.5% SDS-PAGE gels (see 3.2.1) were employed. The protein was detected by immunoblotting with the α Prat1 antibody.

3.2.10 Extraction of inner envelope

Isolated IE (10 μ g protein content) from *Pisum sativum* (see 3.3.2) was centrifuged for 10 min. at 256,000 g and 4 °C and then resuspended in 25 mM Hepes/KOH (pH 7.6) and 5 mM MgCl₂. For alkaline pH conditions 0.5 M Na₂CO₃, for high salt conditions 4 M NaCl and for denaturing conditions 6 M urea were added to the samples and incubated for 10 min. on ice, before being centrifuged for 10 min. at 256,000 g and 4 °C. Both supernatant and pellet were separated on an 10% SDS-PAGE gel and afterwards a selection of proteins (Tic110, Tic62, Prat1 and Tic22) were visualized by immunoblotting with protein specific antibody labelling, using alkaline phosphatase (AP)- conjugated secondary antibodies (see 3.2.4).

3.2.11 Liposome preparation

Phospholipid phosphatidylcholine (PC) was solubilized in chloroform:methanol (1:1) in a concentration of 20 mg/ml. To remove the solvent, samples were dried under a steady flow of nitrogen gas for 30 min and afterwards placed in a vacuum exsiccator for 3 h. PC forms a thin layer at the bottom of the utilized glass tube and was stored at -20 °C under argon. Lipid vesicles (20 mg/ml) were prepared in 10 mM Mops/Tris (pH 7.0), 100 mM NaCl, in the presence or absence of 1% SDS or in 20 mM Tris-HCl (pH 8.0), 100 mM NaCl as indicated. To prepare unilamellar liposome vesicles, samples were frozen and thawed 5 times in liquid nitrogen prior to being carefully extruded 21 times through a polycarbonate filter with a diameter of 100 or 200 nm (Liposofast, Avestin, Ottawa, Canada). For generation of proteoliposomes, purified proteins (Prat1 and Tic110) in a concentration of 0.3-0.6 mg/ml (or the respective buffer only as control) were subsequently mixed with liposomes in a 1:2 protein:lipid volume ratio and incubated for 1.5 h at 4 °C. Samples were dialysed for 16 h at 4 °C against the protein buffer without detergent, and the remaining detergent was removed during 2 h incubation at 4 °C with Bio-Beads (20 mg/ 1 mg detergent). In the presence of SDS, incubation and dialysis was performed at RT.

3.2.12 Flotation assay

To differentiate between liposome-associated and liposome-free proteins, separation by flotation through a sucrose gradient was applied. Samples as described before in 3.2.11 were therefore adjusted to a sucrose concentration of 1.6 M and overlaid with a sucrose step gradient consisting of 0.8 M, 0.4 M and 0.1 M concentrations (to a final volume of 4 ml for the small centrifuge tubes or 12 ml for the larger tubes). After centrifugation at 100,000 g and 4 °C for 19 h, 0.5 ml (small tubes) or 1 ml (large tubes) fractions were carefully collected from the top of the tube, followed by a TCA precipitation (see 3.2.3) and washing of the proteins with 100% acetone. Samples were then resuspended in Laemmli-buffer, separated by SDS-PAGE and proteins were detected by silver-staining (see 3.2.1).

To verify proper insertion of proteins into the liposomes, these proteoliposomes (0.3-0.6 mg/ml protein content) were incubated for 30 min at RT in the presence of different buffer conditions and then subjected to flotation as described before. The following buffers were used: as a control 10 mM MOPS/Tris (pH 7.0) or 20 mM Tris/HCl (pH 8.0), for high salt conditions 1 M MOPS/Tris (pH 7.0) or 1 M NaCl in 20 mM Tris/HCl (pH 8.0), for alkaline pH conditions 10 mM Na₂CO₃ (pH 11.0) and for denaturing conditions 6 M urea in 10 mM MOPS/Tris (pH 7.0) or in 20 mM Tris/HCl (pH 8.0).

3.2.13 Thin-layer chromatography

Isolated chloroplasts from *Arabidopsis thaliana* (see 3.3.4) and *Pisum sativum* (see 3.3.1) (50 – 100 µg chlorophyll. content), inner envelope vesicles from *Pisum sativum* (50 – 100 µg protein content), phosphatidylcholine (PC) (100 – 200 µg lipids) and a mixture of palmitoyl-oleoyl- phosphatidylcholine (POPC) and palmitoyl-oleoyl- phosphatidylethanolamine (POPE) (25 – 50 µg lipids) were applied at the bottom of a silica thin layer chromatography plate. The plate was placed upright in a lid covered beaker containing solvent (65% chloroform and 25% MeOH). The running time for the chromatography amounted to 1 h 45 min. The plate was afterwards sprayed with a staining solution (5 mM FeSO₄, 5 mM KMnO₄ and 3% H₂SO₄) and incubated for 10 min at 120 °C.

3.2.14 Swelling assay

Freshly prepared liposomes and proteoliposomes (see 3.2.11) were diluted to 1 ml, approximating the starting optical density of all samples to 0.5 at OD₅₀₀. The OD₅₀₀ of the

samples was measured with a Shimadzu UV-2401PC Spectrophotometer (Columbia, USA) in time intervals of 1 min or for better disbanding 30 sec. After 2 – 5 min. of measurements 300 mM KCl, sucrose or CsCl were added to the samples and the changes in density recorded. If indicated the Prat1-proteoliposomes and the control liposomes were additionally incubated for 45 min at RT before the measurements. Also treatment with 50 μ M CuCl₂ for 20 min at 20 °C to oxidize the protein, 10 mM DTT for 20 min at RT to reduce Prat1 and the addition of 10 mM ATP which may be needed for proper gating was performed prior to the measurements in the spectrophotometer.

3.2.15 Isoelectric focusing (IEF)

IEF is used to separate proteins based on their overall charge emitted from their amino acids. Isolated stroma samples from wild type and mutant plants (*Arabidopsis thaliana*) of Prat1 were taken and after performing IEF separated on large gels to demonstrate a specific protein pattern. Differences between wild type and mutant help to characterize Prat1.

For the preparation of stroma samples, Rehydration buffer (7 M urea, 2 M thiourea, 0.2% biolytes 3 - 10 (Bio-Rad, München), 2% CHAPS, 100 mM dithiothreitol (DTT), bromophenol blue) was supplemented just before use with protease inhibitors (for 3.0 ml buffer: 2.88 ml urea/thiourea rehydration buffer, 0.06 ml 50x complete (in H₂O), 0.03 ml 100 mM phenylmethylsulfonyl fluoride (PMSF in isopropanol), 0.003 ml pepstatin 1 mg/ml (in pure ethanol)). In the next step, 200 μ g soluble protein (with a concentration of at least 6 mg/ml) from the stromal fraction of isolated chloroplasts (see 3.3.4) was adjusted with this buffer to a total volume of 200 μ l and incubated at RT for 1 h. The samples were centrifuged for 10 min at 20,000 g at RT and the supernatant was loaded into an IEF-tray (Bio-Rad, for 11 cm strips). Subsequently, the protection foil was removed from the strips (ReadyStrip IPG strips, pH range 3 - 10 and 6 - 8, Bio-Rad, München) and gel strips were put on top of the sample located in the tray avoiding air bubbles between the strip and the sample (gel side on bottom, writing on the left hand side). After incubation for 1 h at RT, the strips were covered with mineral oil and the first dimension IEF-run was started (Protean IEF Cell; Bio-Rad; settings: preset method; rapid; rehydration: yes, active; gel length 11 cm; pause after rehydration: yes; hold at 500V: yes). After 12 h of rehydration, the run was paused and wet wicks (use 10 μ l H₂O per wick) were inserted between strips and electrodes, then the program is continued for ~ 9.5 h (35,000 Vh, end voltage: 8000 V). After the run finished, the strips

were drained on a tissue to remove oil and transferred into a clean tray (with gel side facing up). They were either applied directly to the second dimension or stored at -80°C .

For second dimension SDS-PAGE the strips were transferred to a clean tray and equilibrated for 20 min. in equilibration buffer I (6 M urea, 2% SDS, 50 mM Tris (pH 8.8), 20% glycerol, 2% DTT). After incubation in equilibration buffer II (6 M urea, 2% SDS, 50 mM Tris (pH 8.8), 20% glycerol, 2.5% iodoacetamide) for 10 min, the strips were covered with running buffer. SDS-gels (with Rotiphorese Gel 40 (29:1) acrylamide; Carl Roth GmbH, Karlsruhe) contain 0.1% SDS in both the stacking and separating gel and were poured in a Bio-Rad gel system (Criterion Cassette). After application of the IEF strip to the top of the stacking gel, it was directly overlaid with 1% agarose (in running buffer). Electrophoresis is performed in a Criterion Cell (Bio- Rad) at 35 mA per gel.

For staining with colloidal coomassie, the gels were first fixed in 30% ethanol, 2% phosphoric acid (100 ml per gel) for at least 5 h or overnight on a shaker at RT. The gels were then washed in H_2O three times for at least 20 min each. Subsequently, gels were incubated in staining solution (120 ml per gel; 17% ammonium sulfate, 2% phosphoric acid, 34% methanol) for 1 h before 120 mg coomassie blue G-250 (1 mg dye/ml) was sprinkled onto the surface. After incubation for 3 days (on a shaker at RT), the gels were washed for 1 h in H_2O and were then ready for scanning and analysis.

3.2.16 Phosphorylation and de-phosphorylation assay

Samples used for phosphorylation of the first serine in the N-terminus of Prat1 shown by Reiland *et al.* 2011 consisted of either IE vesicles from *Pisum sativum* or *Arabidopsis thaliana* (10 μg protein content), purified Prat1 protein or Prat1 which had undergone site-directed mutagenesis of the serine to aspartic acid or glutamic acid to mimic phosphorylation (see table 2) and pSSU (each protein approx. 2-5 μg) protein in inclusion bodies as a control. The samples were resuspended in 20 mM Tris/HCl (pH7.5), 5 mM MgCl_2 and 0.5 mM MnCl_2 and incubated with 3 μCi ^{32}P -labeled ATP for 10 min. at RT. Additionally, leaf lysate or isolated stroma (approx. 6 mg/ml) from *Pisum sativum* or 1% Triton X-100 were added as indicated to the samples. A thermolysin digest (see 3.2.7) was performed before the phosphorylation was started where indicated. After separation by SDS-PAGE, proteins were detected by immunoblotting (see 3.2.4) with the αPrat1 or αTic110 (*Pisum sativum*) antibodies, respectively. To analyse where phosphorylation had occurred, incorporation of ^{32}P -

labeled ATP was visualized by autoradiography (Kodak BiomaxBLUE, PerkinElmer, Rodgau, Germany) for 5 h, overnight or up to two days.

De-phosphorylation was performed with the same samples also used for phosphorylation, using 50 mM HEPES (pH 7.5), 100 NaCl, 2 mM DTT, 0.01% Brij 35, 10% MnCl₂ and the Lambda Protein Phosphatase (200 units; Lambda PP, New England BioLabs Inc, USA). The samples were incubated for 30 min. at 30 °C and then either phosphorylated as described above or directly loaded onto an SDS-PAGE. The further procedure was identical to the phosphorylation assay.

3.2.17 Cross-linking

To analyse the oligomerization state of Prat1, 10 µg samples of isolated inner envelope from *Pisum sativum* (see 3.3.2) were incubated with 0.1 or 0.5 mM cross-linker for 10 min up to 1 h at RT or on ice in 25 mM HEPES/KOH pH 7.6 buffer. Three different cross-linkers were tested (thiosulfate, 0 Å; dithionite, 0 Å; disuccinimidyl tartrate, 6 Å). The reaction was terminated by the addition of non-reducing solubilising buffer directly onto the sample, which was then loaded on a 10% Schägger gel (see 3.2.1). The gel was blotted onto nitrocellulose membrane (see 3.2.4) and Prat1 was visualized via immunodetection using a specific αPrat1 antibody.

3.2.18 Metabolite analyses

To analyse metabolic changes, leaf material from *Arabidopsis thaliana* wild type (wt) and the double mutant (dm) of Prat1 was collected from plants grown under long-day conditions (16 h light and 8 h dark), short-day conditions (8 h light and 16 h dark) and constant light conditions (24 h light at approx. 100 µmol). The leaves (with three replicas each) were directly frozen in liquid nitrogen, pestled and aliquoted into 50 mg portions. The plant material was extracted with a mixture of H₂O/MeOH/chloroform (1:2.5:1 volumes). As an internal standard for later analysis 50 mM ribitol was added. The samples were mixed using a vortex for 20 sec. and then rotated for 6 min. at 4 °C before being centrifuged for 2 min. at 20,000 g and RT. The supernatant was then carefully removed and used for analyses of metabolites.

The metabolite analyses via gas-chromatography followed by mass spectrometry were performed by Katrin Weber from the group of Prof. Andreas Weber at the Heinrich-Heine-

Universität Düsseldorf (Institute for biochemistry of plants) according to Denkert *et al.* (2008).

3.2.19 Protein identification by mass spectrometry (MS)

Coomassie- or silver-stained protein spots were cut from SDS-PAGE gels and send for identification to the “Zentrallabor für Proteinanalytik” (ZfP, Adolf-Butenandt-Institut, LMU München). There, tryptic peptides were detected either by Peptide Mass Fingerprint (MALDI, Matrix Assisted Laser Desorption/Ionization) or LC-MS/MS (Liquid Chromatography with MS) runs. Protein identification was then accomplished with a Mascot software assisted database search.

3.3 Cell biological methods

3.3.1 Isolation of intact chloroplasts from *Pisum sativum*

To isolate intact chloroplasts (Schindler *et al.*, 1987), seedlings from *Pisum sativum* were grown for 9-11 days on vermiculite in a climate chamber, under 12/12 hours dark/light (160 $\mu\text{mol photons m}^{-2} \text{s}^{-1}$) cycles. The plants were placed in the dark the night prior to conducting the isolation to reduce starch accumulation. All procedures were carried out at 4 °C. About 200 g of pea leaves were collected and ground in a kitchen blender in approximately 300 ml isolation medium (330 mM sorbitol, 20 mM MOPS, 13 mM Tris, 3 mM MgCl_2 , 0.1% (w/v) BSA) and filtered through four layers of mull and one layer of gauze (30 μm pore size). The filtrate was centrifuged for 1 min at 1,500 g and the pellet was gently resuspended in about 1 ml wash medium (330 mM sorbitol, 50 mM Hepes/KOH (pH 7.6), 3 mM MgCl_2). Intact chloroplasts were reisolated via a discontinuous Percoll gradient of 40% and 80% (in 330 mM sorbitol, 50 mM Hepes/KOH (pH 7.6)) and centrifuged for 5 min at 3,000 g in a swing out rotor. Intact chloroplasts were taken from the 40%/80% interface, washed two times, and resuspended in a suitable volume of wash medium. Samples of isolated chloroplasts (3x 1 μl) were taken and resuspended in 1 ml each of 80% acetone. The chlorophyll concentration was estimated by measuring the optical density at three wavelengths (663, 645 and 750 nm) against the solvent (Arnon, 1949). Chloroplasts were used immediately after isolation to ensure functionality.

3.3.2 Preparation of inner and outer envelope vesicles from *Pisum sativum*

For isolation of inner and outer envelope vesicles from chloroplasts, *Pisum sativum* seedlings grown for 9-11 days on sand, under a 12/12 hours dark/light regime, were used. All procedures were carried out at 4 °C. Pea leaves cut from ~ 20 trays were ground in a kitchen blender in 10-15 l isolation medium (330 mM sorbitol, 20 mM MOPS, 13 mM Tris, 0.1 mM MgCl₂, 0.02% (w/v) BSA) and filtered through four layers of mull and one layer of gauze (30 µm pore size). The filtrate was centrifuged for 5 min. at 1,500 g, the pellet gently resuspended with a brush and intact chloroplasts reisolated via a discontinuous Percoll gradient (40% and 80%). Intact chloroplasts were washed twice with wash medium (330 mM sorbitol, Tris-base (~ pH 7.6)), homogenized and further treated according to the modification (Waegemann *et al.*, 1992) of the previously described method (Keegstra and Youssif, 1986). The quality of the isolated inner and outer envelope was checked by comparing the presence of the hallmark proteins on a coomassie stained SDS-PAGE.

3.3.3 Isolation of stroma from *Pisum sativum*

Freshly isolated chloroplasts (see 3.3.1; approx. 600 µg chlorophyll) from *Pisum sativum* were incubated in 5 mM Tris/HCl (pH 7.5) for 30 min. on ice. A first centrifugation for 10 min. at 16,000 g and 4 °C to remove thylakoid fragments was followed by a second centrifugation step (256,000 g, 30 min, 4 °C) to separate the stroma (= supernatant) from the envelope membrane fraction. Protein concentration was determined with the Bio-Rad Protein Assay Kit (Bio-Rad, München, Germany; Bradford, 1976).

3.3.4 Isolation and fractionation of *Arabidopsis thaliana* chloroplasts

Intact *Arabidopsis thaliana* chloroplasts were prepared from two trays (approx. 150 g fresh weight leaf material, harvested from darkness) of three- to fourweek- old plants grown on soil in a climate chamber (see 3.4), essentially as described in Seigneurin-Berny *et al.*, 2008. Chloroplasts were subsequently resuspended in 15 ml of 10 mM Hepes/KOH (pH 7.6), 5 mM MgCl₂ and lysed using 50 strokes in a small (15 ml) Dounce-homogenizer (Wheaton, Millville, NJ, USA). Further separation into stroma, thylakoids, and envelopes was done according to Li *et al.*, 1991 using linear Percoll gradients which were centrifuged for 2 h at 58,000 g and 4 °C. Each fraction, identified by its color (green = thylakoids, yellow/green = IE and outer envelope (OE), clear = stroma) was taken carefully from the gradient. The

envelope fraction was centrifuged again for 1 h at 135,200 g and 4 °C the supernatant removed and the pellet resuspended in a small volume (approx. 100 µl). All samples were either immediately used or frozen in liquid nitrogen and stored at -80 °C. Concentrations were determined according to Lowry *et al.*, 1951.

3.3.5 Protein import experiments

Intact chloroplasts were isolated from 17 to 18-days-old *Arabidopsis thaliana* (grown on plates or on soil) or 9 to 11-days-old *Pisum sativum* (grown on vermiculite) plants according to the protocol by Aronsson and Jarvis, 2002 with the following exceptions: all buffers were supplied with 0.4 M sorbitol, and NaHCO₃ as well as gluconic acid were omitted. An import reaction (containing chloroplasts equivalent to 7.5 µg Chl) was subsequently carried out in 100 µl volume containing 3 mM ATP and 1-5% (v/v) [³⁵S]-labelled translation products (see 3.1.3). Import reactions were initiated by the addition of translation product to the import/chloroplast mix and carried out for the indicated time at 25 °C. Reactions were terminated by the addition of 2 volumes of ice-cold washing buffer (0.4 M sorbitol, 50 mM HEPES/KOH (pH 8.0), 3 mM MgSO₄). Chloroplasts were washed twice and finally resuspended in Laemmli buffer (50 mM Tris/HCl (pH 6.8), 100 mM β-ME, 2% (w/v) SDS, 0.1% bromophenol blue (w/v), 10% glycerol (v/v)). Import products were separated by SDS-PAGE and radiolabeled proteins were analyzed by a phosphorimager or by exposure on autoradiography films (Kodak Biomax-MR).

3.4 Plant growth conditions and phenotyping

Pisum sativum of the type “Arvica” (from Prag, Czech Republic) were purchased at the Bayerische Futtersaatbau (Ismaning, Germany) and grown on vermiculite in a climate chamber regulated in a 12 h day/night-cycle at 20 °C.

Arabidopsis thaliana seed material of the ecotype Col-0 (wild type) was purchased at Lehle Seeds (Round Rock, USA). The T-DNA insertion lines SALK_020671 and SALK_001823 were ordered at NASC (*Nottingham Arabidopsis Stock Center*, Nottingham, UK).

To synchronize germination, all seeds were subjected to vernalization at 4 °C for 2-3 days. Plants were grown on soil or on 0.3% Gelrite medium containing 0.5 x MS salts at pH 5.7 and in the presence or absence of 1% D-sucrose. Before sowing on sterile plates, seeds

Materials and Methods

were surface-sterilized with 70% ethanol, 0.05% Triton X-100 for 10 min and washed four times with 96% ethanol. Unless stated otherwise, plant growth occurred in growth chambers with a 16 h light (22 °C; 100 $\mu\text{mol photons m}^{-2} \text{s}^{-1}$) and 8 h dark (18 °C) cycle.

Phenotyping of the *Prat1* double mutant (*dm*) was performed by comparing growth to wild type (*wt*) *Arabidopsis thaliana* plants (ecotype Col-0) under the various conditions listed in Table 3. *Prat1 dm* plants were retrieved from crossing the two T-DNA insertion lines *Prat1.1* (At4g26670 – SALK_020671) and *Prat1.2* (At5g55510 – SALK_001823) (see 2.9).

Table 3: Phenotyping conditions for *Arabidopsis thaliana* *Prat1* (*wt* vs. *dm*).

location	light duration	light intensity	temperature	humidity
1) Climate chamber	16 h / 8 h	100 μMol	22° / 18°C	50 / 65%
2) Climate chamber	8 h / 16 h	100 μMol	20° / 16°C	60 / 75%
3) Percival 9	16 h / 8 h	100 μMol	10°C	n/a
4) Percival 1	constant	100 μMol	21° / 16°C	n/a
5) Percival 1	constant	10 μMol	21° / 16°C	n/a
6) Percival 4	16 h / 8 h	75 μMol	20° / 16°C	n/a
7) Greenhouse	weather dependant	weather dependant	weather dependant	weather dependant
8) Heat cabinet	16 h / 8 h	80 μMol	28° / 24°C	n/a
9) Climate chamber (no watering)	16 h / 8 h	100 μMol	22° / 18°C	50 / 65%

Root analyses were performed with *wt* and *dm* *Arabidopsis thaliana* seedlings grown on plates containing 0.3% Gelrite medium 0.5 x MS salts at pH 5.7 and 1% D-sucrose. The seedlings were placed in a row at the top end of a vertically positioned plate in a climate chamber with a 16 h light (22 °C; 100 $\mu\text{mol photons m}^{-2} \text{s}^{-1}$) and 8 h dark (18 °C) cycle. The plates were examined regularly and results were documented by photography.

3.5 Electrophysiological measurements

Electrophysiological measurements of channel proteins were performed using the IonoVation Bilayer Explorer (Osnabrück, Germany) according to the supplier's instructions. A disposable bilayer chamber ("bilayer slide"), consisting of two compartments (*cis* and *trans*), separated by a polytetrafluoroethylene (PTFE) septum containing a microhole served for the preparation of the bilayer (Figure 6A and B).

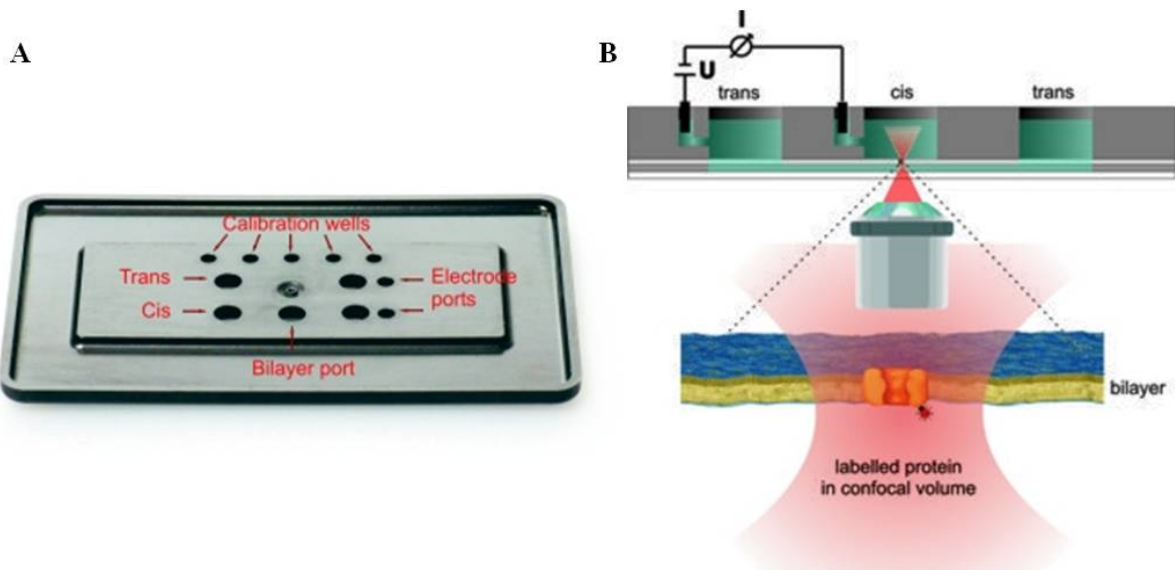


Figure 6: Principles of the IonoVation Bilayer slide.

Figures were taken from IonoVation Bilayer Explorer V01 (2009) Manual from IonoVation. (A) Bilayer slide. Via the bilayer port lipids and proteoliposomes can be added, at the electrode ports the electrodes are inserted into the two chambers and the calibration wells are used to calibrate the system (B) Schematic view of the assembly of the bilayer slide. *Cis* and *trans* chambers are separated by a PTFE septum, serving as a platform for bilayer formation. Inserted proteins allow current flow, which can be measured by the electrodes inserted to each compartment.

Both compartments were filled with approx. 150 μl of saline buffer during measurements (10 mM MOPS/Tris (pH 7.0), 250/20 mM KCl, *cis/trans*). For electrical measurements Ag/AgCl electrodes with salt bridges were connected to the *cis* and *trans* compartments. A perfusion system with two 10 ml syringes was responsible for buffer exchange. For bilayer preparation approx. 0.2 μl of bilayer lipid (phosphatidylcholine and phosphatidylethanolamine) in *n*-decane (5-10 mg/ml) was added directly onto the microhole. A stroking movement with the syringe and the pumping of buffer into and out of the chambers leads to bilayer formation, which was also controlled by light microscopy (Olympus CKX41, Hamburg, Germany) (Figure 7).

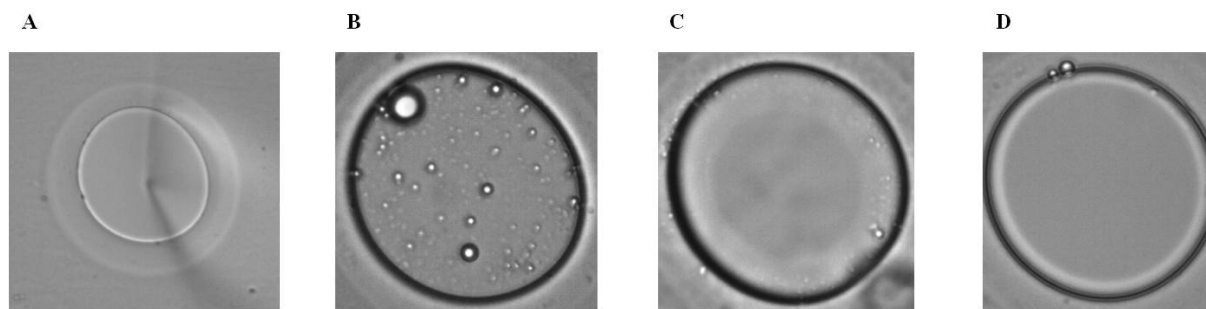


Figure 7: Bilayer formation at the microhole in the PTFE septum.

The pictures show the microhole connecting the two compartments and were kindly provided by Maïke Hellmers. **(A)** No lipids present therefore the buffer flow between the compartments is visible. **(B)** Unordered lipids across the microhole. **(C)** Lipid bilayer with large annulus has formed. **(D)** Large ordered lipid bilayer with a small annulus has formed.

After the formation of a lipid bilayer, 0.3 μl of proteoliposomes (see 3.2.11) were carefully added on top of it in the *cis* chamber (higher salt concentration). Fusion with the lipid bilayer occurred due to the osmotic gradient of 250/20 mM KCl in the buffers between the two chambers (Figure 8).

Patchmaster software (HEKA Elektronik, Lambrecht/Pfalz, Germany) controlled the experiment, by preparing and verifying the bilayer formation and executing the measurements between the two electrodes.

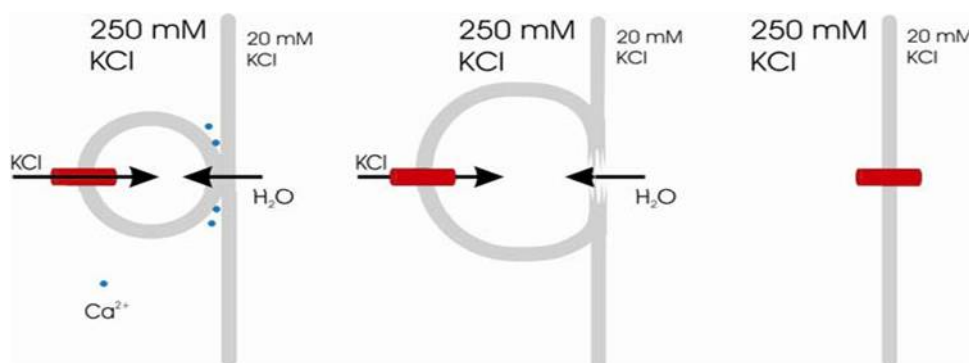


Figure 8: Schematic diagram of the fusion of a proteoliposome to the lipid bilayer.

The figure was taken from Ionovation Bilayer Explorer V01 (2009) Manual from IonoVation. The ionic gradient across the PTFE septum (250/20 mM KCl) allows proteoliposomes to be pulled towards the lipid bilayer and undergo fusion with it, thereby inserting the protein into the lipid bilayer.

3.6 Cryo-electrotomography

For structural analyses of Prat1 and Tic110, 50 μl of proteoliposomes (see 3.2.11) of these proteins were prepared and sent to the group of Prof. Baumeister from the Max-Planck-Institute (Martinsried, Germany). There the samples were shock-frozen in liquid ethane and placed on grids. For images see the supplementary data. The procedure of cryo-electrotomography was performed by Zdravko Kochovski.

4 Results

4.1 Purification of Prat1

To be able to characterise the membrane protein Prat1 (fl) from *Pisum sativum* was overexpressed using the pET21d vector (see 2.6) in *E. coli* at 37 °C as inclusion bodies (see 3.2.5). Bacteria from a 2 l culture were lysed and the pellet solubilised in 1% N-LS and applied to a Ni-column. Samples from load, flow-through, wash (each 1/50) and elution (1/10) after Ni-affinity chromatography were loaded onto an SDS-PAGE gel to control yield and purity. The gel in figure 9 shows a representative result. A large amount of the HIS-tagged protein Prat1 does not bind to the Ni-beads, resulting in a clear band visible at approx. 24 kDa (22.8 kDa = calculated size) in the flow through. The optimal concentration of imidazol was determined in several test purifications as 15 mM during the binding and washing process and 100 mM during elution. After the first elution, the imidazol concentration was raised to 200 mM and 500 mM to clear beads of residual protein. Prat1 was eluted and the protein concentrated via centrifugation on an Amicon ultrafiltration unit. Up-scaling of the bacterial culture to 4 l for overexpression did not lead to a significant increase in protein yield after purification.

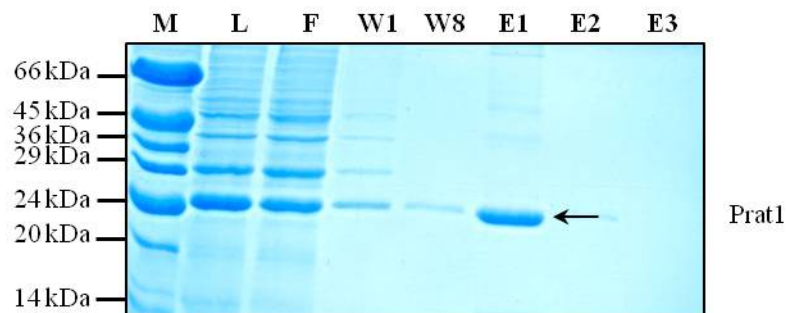


Figure 9: Purification of Prat1 using Ni-affinity chromatography.

SDS-PAGE (12.5%) loaded with 1/50 of load, flow-through and wash and 1/10 of elution samples after Ni-affinity chromatography and coomassie staining **M** = protein marker; **L** = load (prior to Ni-affinity chromatography); **F** = flow through (directly after Ni-affinity chromatography); **W1** = first wash; **W8** = last wash; **E1** = first elution; **E2** = second elution and **E3** = third elution. Prat1 is indicated with an arrow.

4.2 Generating an antibody against psPrat1

An antibody against the heterologously expressed Prat1 protein from *Pisum sativum* (see 4.1) was generated. After overexpression, the lysed samples were loaded onto two large gels (12.5%). The Prat1 bands were excised from the two gels, pooled, 500 μ l of water added and sent to Biogenes (Berlin) to be injected into a rabbit.

The antibodies (used 1 : 500 in 1% skimmed milk and 0.05% Tween 20 in TTBS (100 mM Tris/HCl, pH 7.5, 0.2% Tween 20 0.1% BSA, 150 mM NaCl)) received after the final bleeding (120 days) showed specific reactions with both the native Prat1 and the recombinant protein after overexpression and purification (Figure 10). The antibody is specific for the Prat1 from *Pisum sativum*, an antibody against the homolog in *Arabidopsis thaliana* was already available. Also some cross-reactions with other proteins were detected which might be due to the recognition of other proteins with a similar sequence.

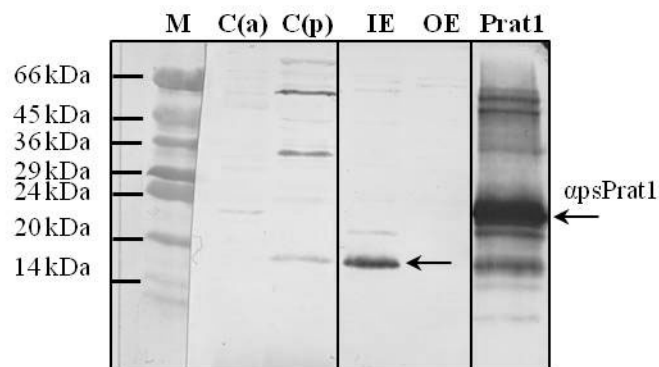


Figure 10: Antibody specificity test.

The immunoblot was incubated with the final bleeding of the psPrat1 antibody (1 : 500 in 1% skimmed milk and 0.05% Tween 20 in TTBS (100 mM Tris/HCl, pH 7.5, 0.2% Tween 20 0.1% BSA, 150 mM NaCl)). The marker was stained separately with amino black. The additional lanes between C(p) / IE and OE / Prat1 were removed. **M** = marker; **C(a)** = chloroplasts from *A. thaliana*; **C(p)** = chloroplasts from *P. sativum*; **IE** = inner envelope from *P. sativum*; **OE** = outer envelope from *P. sativum* and **Prat1** = overexpressed protein which was purified via Ni-affinity chromatography. Prat1 is indicated with arrows.

The running behaviour of Prat1 in its native state at 19 kDa (calculated 22.8 kDa), shown here in the two lanes with isolated chloroplasts and the inner envelope from *Pisum sativum*, differs clearly from the size observed after purification of the overexpressed protein Prat1 using Ni-affinity chromatography, (~24 kDa). This can be attributed to the addition of the His-tag to the overexpressed protein and the presence of inner envelope lipids attached to the native protein. Also it can not be excluded that Prat1 is processed upon import into the chloroplast as can be seen by the weakly predicted transit peptide in the Plant Proteome Database (PPDB; Figure 11, underlined). Also emphasized in red are the peptides that identified Prat1.1 and Prat1.2 using mass spectrometry, which do not represent the extrem N-terminus and therefore

give no indication if the protein is cleaved by a peptidase (Figure 11). In contrast to the PPDB transit peptide prediction, ChloroP (Emanuelsson *et al.*, 1999) forecasts no transit peptide for both Prat1.1 and Prat1.2.

<p><u>MAANDSSNAIDIDGNLSDSNLNTDGDEATDNDSSK</u><u>ALVTIPAPAVCLFRFAGDAAGGAV</u> <u>MGSIFGYGSGLFK</u>KKGFKGSFADAGQSAKTFVLSGVHSLVVCLLKQIRGKDDAINVGVA GCCTGLALSFPGAPQALLQSCLTFGAFSFILEGLNKRQTALAHSVSLRHQTGLFQDHHRA LPSLALPIPEEIKGAFSSFCCKSLAKPRKF</p>	<p>Prat1.1 (At4g26670)</p>
<p><u>MAAENSSNAINVDTSLSDSKPNRDANDMTDHDSSSK</u><u>ALVIPAPAVCLVR</u>FAGDAASGAF MGSVFGYGSGLFKKKGFKGSFVDAGQSAKTFVLSGVHSLVVCLLKQIRGKDDAINVGVA GCCTGLALSFPGAPQAMLQSCLTFGAFSFILEGLNKRQTALAHSVSFRQQTRSPQHDLPL LSLAIPIHDEIKGAFSSFCNSLTKPKKLLKFPHAR</p>	<p>Prat1.2 (At5g55510)</p>

Figure 11: Identified peptides of Prat1.1 and Prat1.2 in *A. thaliana*.

Taken from The Plant Proteome Database (PPDB; Sun *et al.*, 2008). Depicted are the peptide sequences of Prat1.1 (At4g26670) and Prat1.2 (At5g55510). Marked in red are the identified peptides after mass spectrometry. Underlined are weakly predicted transit peptides.

4.3 Localisation of Prat1

To analyse the localization of Prat1, samples of inner and outer envelope (each 10 µg), thylakoids and stroma (each 20 µg) from *Pisum sativum* were subjected to 10% SDS-PAGE. In addition, freshly isolated chloroplasts and mitochondria (each approx. 20 µg) were loaded. Figure 12 exhibits the two resulting immunoblots, whereas the top immunoblot was divided into five separate blots, each incubated with the indicated antibody. Clearly visible is the localisation of the Prat1 protein in the inner envelope and the chloroplast fraction. As controls, antibodies against Toc75 (outer envelope), fructose-1,6-bisphosphatase (FBPase, stroma), OE33 (thylakoids) and the voltage-dependant anion channel (VDAC, mitochondria) were used and the corresponding proteins were each found in the respective fraction. The second immunoblot was run with the same base material as the first and represents a further control for the inner envelope. The αTic110 antibody was applied.

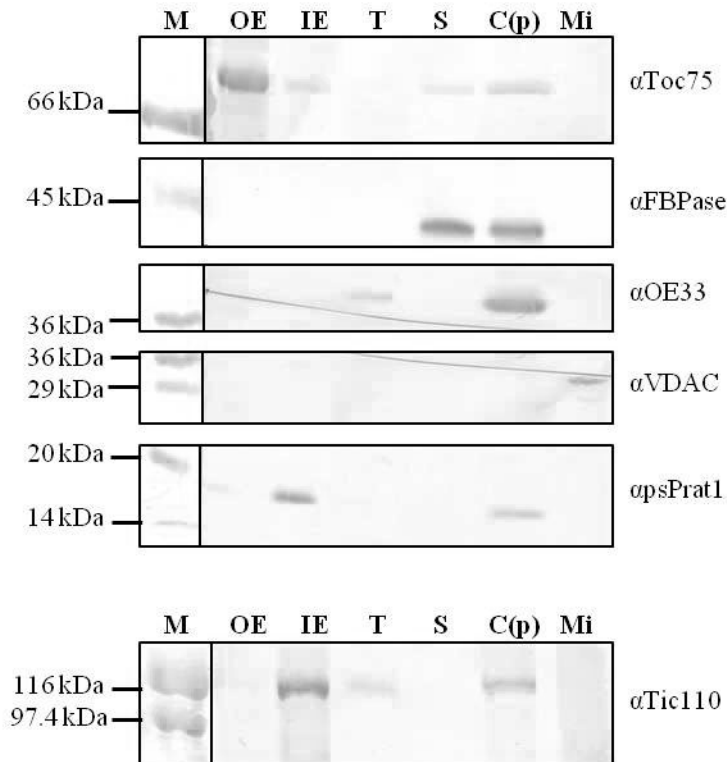


Figure 12: Prat1 is localised at the inner envelope of *Pisum sativum*.

The immunoblot was incubated with the indicated antibodies (each 1 : 1000 in 1% skimmed milk and 0.05% Tween 20 in TTBS (100 mM Tris/HCl, pH 7.5, 0.2% Tween 20 0.1% BSA, 150 mM NaCl)). The marker was stained separately with amino black. Both immunoblots were loaded with identical quantities of the same material. **M** = marker; **OE** = outer envelope; **IE** = inner envelope; **T** = thylakoids; **S** = stroma; **C(p)** = chloroplasts; **Mi** = mitochondria, kindly provided by Sabine Nick. All materials were isolated from *P. sativum*.

4.4 Topology of Prat1 in the inner envelope

In addition to the exact localisation within the chloroplast, the topology of Prat1 within the inner envelope was investigated to determine whether it is an integral membrane protein or if it is merely attached to the inner envelope. For this purpose, a variety of conditions were applied to inner envelope vesicles of *Pisum sativum* by incubating them with buffers containing (i) high salt concentrations (4 M NaCl), (ii) alkaline pH (Na_2CO_3 , pH 11) (iii) 6 M urea (Figure 13). Proteins which are not incorporated into the inner envelope are washed off the membrane when their hydrophobic or electrostatic interactions are disturbed by the conditions listed above. The samples were centrifuged after being incubated for 10 min on ice with the respective buffers and subsequently, supernatant (containing soluble proteins) and pellet (containing membrane-bound proteins) were loaded separately on an SDS-PAGE gel and immunoblotting was performed. Noticeably, Prat1 was exclusively detected in the pellet fraction under all conditions tested, similar to the control membrane protein Tic110. In comparison, Tic62, known to only interact with the inner envelope, can also partly be seen in

the supernatant fractions. This demonstrates that Tic62 was partially washed off the inner envelope, whereas Prat1 seems to be integrated into the inner envelope membrane.

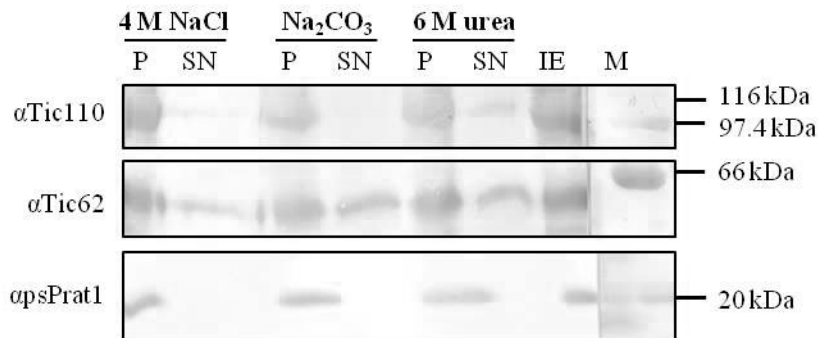


Figure 13: Extraction of inner envelope from *P. Sativum*.

The immunoblot was incubated with the indicated antibodies (each 1 : 1000 in 1% skimmed milk and 0.05% Tween 20 in TTBS (100 mM Tris/HCl, pH 7.5, 0.2% Tween 20 0.1% BSA, 150 mM NaCl)). The marker was stained separately with amino black. IE from *P. sativum* was incubated with buffer conditions as indicated. **4 M NaCl** = high salt condition; **Na₂CO₃** = alkaline pH condition; **6 M urea** = denaturing conditions; **P** = pellet fraction; **SN** = supernatant; **IE** = inner envelope from *P. sativum* with no treatment.

In silico analyses of the Prat1 protein predict the presence of four transmembrane helices that anchor it within the membrane, resulting in a structure with both N- and C-termini facing the same side of the membrane (Figure 14). However, no biochemical experiments had so far been performed to investigate the orientation of the protein in more detail.

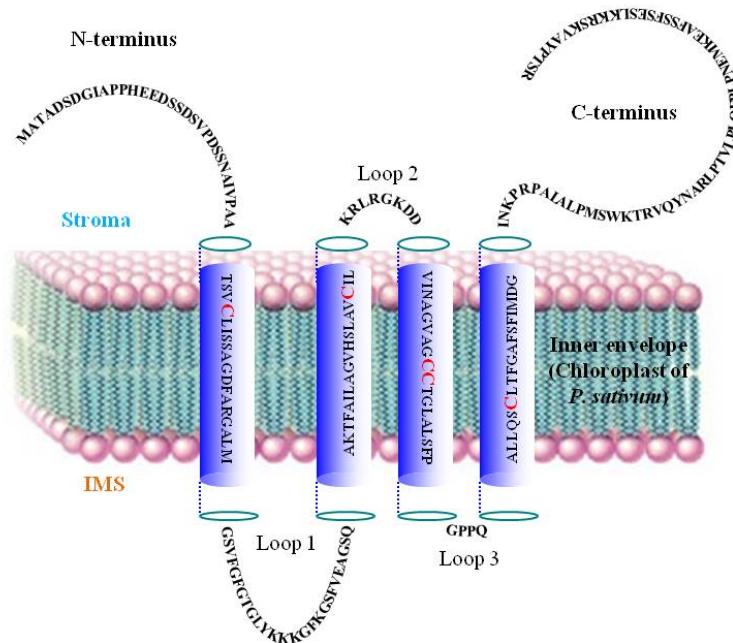


Figure 14: Topology model of Prat1 (*P. Sativum*).

The topology model of Prat1 depicts four transmembrane helices represented as dark blue barrels spanning the inner envelope membrane. Both N- and C-terminus and loop two are reaching into the stroma of the chloroplast. Loops one and three by contrast are facing the inner membrane space. The five cysteines are marked in red and are localised within the transmembrane domains of Prat1.

4.4.1 Prat1 is protease resistant

As a first approach to gain insight into the topological features of Prat1, the protease thermolysin was used to digest the protein in inner envelope vesicles from *Pisum sativum* (Figure 15A). In this approach 1 μg of thermolysin was used for 10 μg protein content and incubated for 10 min on ice. Indicated samples were treated with 1% Triton X-100 or 10 mM dithiothreitol (DTT) prior to the thermolysin digest to solubilize the membranes or reduce the protein.

The results show that the Prat1 protein is hardly affected by thermolysin treatment in the absence of Triton X-100, which demonstrates the protease resistance of the protein under native conditions. The control protein Tic110 on the other hand demonstrates digestion bands already after 2 min of treatment. The addition of DTT seems to hinder the protease activity. Once the samples are solubilised with 1% Triton X-100, both Tic110 and Prat1 are almost completely digested. However, Prat1 is only affected upon solubilisation of IE membranes. Hence, this is a first indication for the N- and C-termini of Prat1 to be localized at the stromal side of the inner envelope. Moreover, it can be concluded that the loops of 26 and 4 amino acids (loops one and three, Figure 14) exposed to the inner membrane space are hardly accessible to thermolysin treatment.

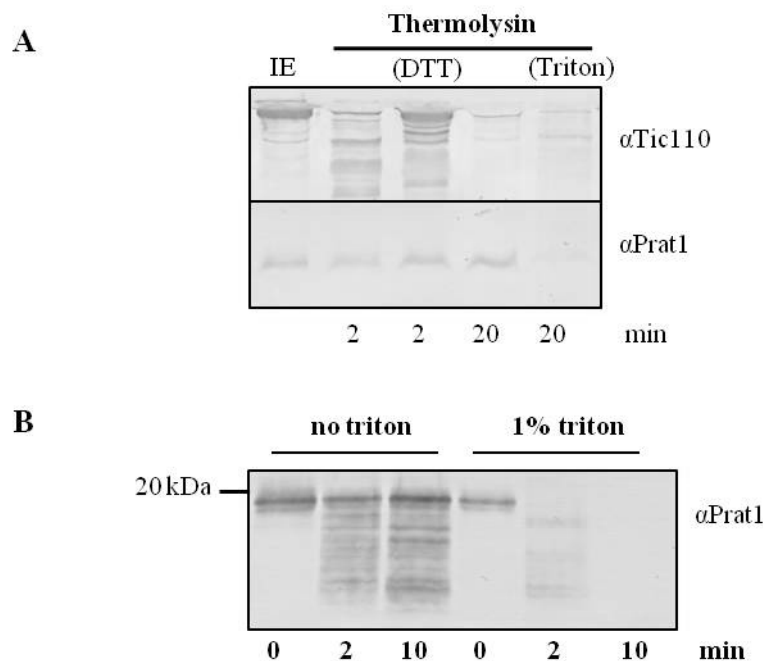


Figure 15: Prat1 from IE vesicles is largely resistant to thermolysin digestion.

(A) Thermolysin digestion of IE vesicles (10 μg) for indicated time. Indicated sample was treated with 10 mM DTT or 1% Triton X-100. The immunoblot was incubated with the psPrat1 antibody and the Tic110 antibody (each 1 : 1000). **IE** = inner envelope, untreated sample. (B) Prat1 proteoliposomes (0.3-0.6 mg/ml protein content) were digested with thermolysin. The three samples on the left remained untreated prior to digestion the three samples on the right were treated with 1% Triton X-100. The time scale on the bottom indicates the digestion time with thermolysin. The immunoblot was incubated with the psPrat1 antibody (1 : 1000).

Additionally, overexpressed and purified Prat1 protein introduced into liposomes (see 3.2.11) was subjected to thermolysin digestion (Figure 15B), with or without pretreatment with 1% Triton X-100. Clearly visible are the degradation bands below the original Prat1 band, demonstrating that thermolysin is able to digest at least part of the protein. A genuine conclusion cannot be drawn from this result, due to the fact that the orientation of the overexpressed protein in the liposomes cannot be controlled and varies. This leads to proteoliposomes that either expose the N- and C-termini and others where the termini are located towards the inside of the proteoliposomes. The addition of 1% Triton X-100 completely dissolves the liposome structure, in contrast to native membranes (Figure 15A). This makes the protein entirely accessible to the protease, leading to a complete digestion (Figure 15B).

Furthermore, digests of IE (10 μg) using the proteases trypsin (0.1 μg) for the indicated time were performed (Figure 16). In addition the indicated sample was reduced with 10 mM dithiothreitol (DTT). As a control the immunoblot was additionally incubated with the αTic110 antibody (Figure 16). Additional digests with the protease GluC lead to comparable results (data not shown).

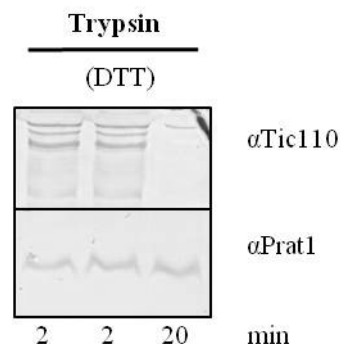


Figure 16: Prat1 from IE vesicles is largely resistant to trypsin digestion.

Trypsin digestion of IE vesicles (10 μg) for indicated time. Indicated sample was treated with 10 mM DTT. The immunoblot was incubated with the psPrat1 antibody and the Tic110 antibody (each 1 : 1000).

4.4.2 PEGylation of Prat1 identifies cysteins in transmembrane helices

Another useful approach to determine the topology of Prat1 is the pegylation of its free cysteins with PEG-Mal. Incubation with this compound leads to its binding to reduced thiol groups that are accessible from outside the membrane. Since PEG-Mal is not membrane permeable, only thiol groups present in the inner membrane space are bound when right-side-out IE vesicles are used. Binding of PEG-Mal to a cystein residue adds 5 kDa to the molecular

weight of the protein. This size shift can then easily be detected on an immunoblot. As highlighted in the topological model, Prt1 contains five cysteine residues, of which two are consecutive (Figure 14). Upon incubation of 10 μ g IE vesicles with 10 mM PEG-Mal for 0, 10 and 30 min, no additional Prt1 bands appear (Figure 17). By contrast, after solubilisation of IE vesicles with 1% SDS, four bands corresponding to higher molecular weight Prt1 forms can be detected. This clearly indicates that all five cysteines (due to sterical hindrance the two consecutive cysteines will bind only one PEG-Mal molecule) are either located on the stromal side of the inner envelope or within the transmembrane regions as predicted in the model. Concomitantly, diminution of the native Prt1 band is observed when PEG-Mal attaches to the cysteines and shifts the protein to a higher molecular weight. Thus the results clearly support the topology model of Prt1 displayed in figure 14.

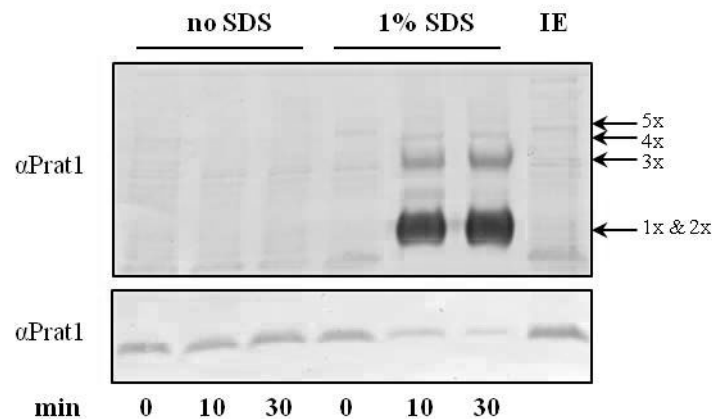


Figure 17: PEGylation of Prt1 cysteines inline with topology model.

Inner envelope vesicles (10 μ g protein content) from *P. sativum* were incubated with 10 mM PEG-Mal for the indicated amount of time. Half of the samples were additionally, prior to PEGylation, solubilised with 1% SDS. The immunoblot was incubated with the psPrt1 antibody (1 : 1000) and divided during staining to better visualise reduction of native Prt1 (lower panel). The arrows indicate size shifts of the protein with one or up to five attachments of PEG-Mal. **IE** = inner envelope from *P. sativum* as a control. The time scale on the bottom indicates the incubation time with PEG-Mal.

4.4.3 AMS treatment further supports location of cysteines in transmembrane helices

Similar to the PEGylation assay shown before, 4-acetamido-4'-maleimidylstilbene-2,2'-disulfonic acid (AMS) is able to attach to reduced cysteines. Hereby, the oxidative state of the protein plays an important factor: only if Prt1 is in a reduced state, alkylation of reduced thiol groups can occur and AMS will attach to cysteines available in the intermembrane space, because AMS can not pass membranes. Modification of the protein with AMS adds 0.5 kDa to the molecular weight, resulting in slower running behaviour. Figure 18 depicts an

immunoblot with inner envelope vesicles from *Pisum sativum* treated as indicated: untreated inner envelope (lane IE; no AMS, no SDS, no reducing or oxidizing agent) shows Prat1 in an oxidized state (all samples were loaded with non-reducing solubilising buffer). Incubating the sample for 1 h in the dark with AMS (lane 1) leads to a slight change in the running behaviour of the protein, indicating that one or two cysteins are accessible to the chemical. This could suggest that cysteins located within the transmembrane domains become available to interact with AMS because they are exposed in a possible channel structure formed by Prat1. Solubilising the inner envelope for 10 min with 1% SDS prior to AMS treatment (lane 2) results in a further upwards shift (approx. 1 – 2 kDa) in the running behaviour, indicating that more cysteins become available to interact with AMS. To better distinguish how AMS interacts with the cysteins in Prat1, the protein was either oxidized (lane 3) with 2 mM diamide or reduced (lane 4) with 2 mM *tris*(2-carboxyethyl)phosphine (TCEP) and afterwards incubated with AMS as before. A clear shift between lane 3 where a similar behaviour to lane 1 can be seen and lane 4 where the chemical bound most likely to all cysteins is visible. Under the applied conditions Prat1 for yet unknown reasons was detected as a double band (Figure 18).

These results further support the topology model of Prat1 (Figure 14). The cysteins require solubilisation for complete accessibility to AMS matching the prediction of the positions of the cysteins in the transmembrane helices as presented in the topology model in figure 14.

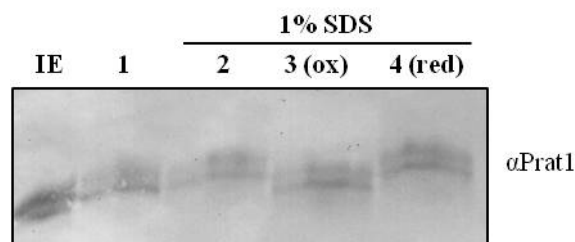


Figure 18: Cysteins only accessible when IE is solubilized.

Isolated IE vesicles (10 µg) were incubated with chemicals as indicated and treated with AMS for 1 h at RT. Proteins were separated on a non-reducing SDS-PAGE gel and Prat1 was detected by immunoblot using a psPrat1 antibody (1 : 1000). **IE** = untreated IE vesicles from *P. sativum*; **1** = IE vesicles incubated with AMS; **2** = solubilised IE vesicles with 1% SDS and incubated with AMS; **3** = IE vesicles solubilised with 1% SDS and oxidized with 2 mM diamide prior to being incubated with AMS; **4** = IE vesicles solubilised with 1% SDS and reduced with 2 mM TCEP and then incubated with AMS.

4.4.4 Prat1 can be phosphorylated at the first serine in the N-terminus

In earlier studies, a single phosphorylation site in Prat1.1 (At4g26670) from *Arabidopsis thaliana* at the first serine residue (position Ser 6) was found (Reiland *et al.*, 2011). Since this is predicted to be the only phosphorylation site present in the protein, the orientation of the N- and C-termini either towards the inter membrane space or the stroma of the chloroplast should be possible to be determined via phosphorylation analysis. Since the serine residue is conserved in Prat1.1 from *Arabidopsis thaliana* and Prat1 from *Pisum sativum*, the experiments were performed with isolated pea inner envelope. To determine the orientation of the protein, a combination of phosphorylation experiment followed by a thermolysin digestion was performed. Inner envelope vesicles (10 µg) were incubated with 3 µCi ³²P-ATP for 10 min at RT before being either treated with or without Triton X-100 followed by thermolysin treatment as indicated. Proteins were separated via SDS-PAGE, transferred on a membrane and the dried blot was placed over night onto an x-ray film for visualisation of phosphorylation (Figure 19A). The corresponding blot (Figure 19B) includes Iep37 as a control because it demonstrates a clear degradational band when cleaved by thermolysin (Figure 19B, lanes 2 & 3). For yet unknown reasons Prat1 was more accessible to thermolysin in this experiment than seen in 4.4.1. The results of the phosphorylation show labelling of Prat1 with ³²P-ATP (Figure 19A, lane 1) that remains to a certain extent when IE vesicles are treated with thermolysin after phosphorylation (Figure 19A, lane 2). This could indicate on one hand that the termini are on the protected stomal side because phosphorylation remains visible on the other hand it could suggest an incomplete digestion of the termini on the side of the intermembrane space. However, after incubation with 1% Triton X-100 to solubilise the vesicles, the phosphorylation site of Prat1 becomes entirely accessible to thermolysin and thus no band can be seen on the x-ray film. Therefore the N-terminus is likely to face the stromal side of the inner envelope, which correlates with the topology model of Prat1 presented before (Figure 14).

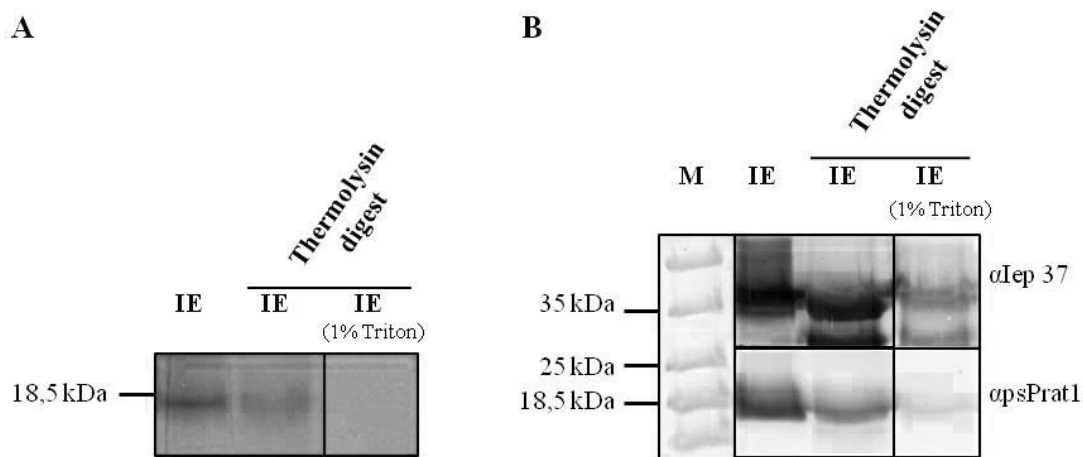


Figure 19: Phosphorylation site accessible to thermolysin only after solubilization.

IE vesicles were incubated with ^{32}P -ATP to phosphorylate the serin residue at the N-terminus of Prat1 before being treated as indicated with Triton X-100 and/or thermolysin for 10 min at RT. After separation of proteins on an SDS-PAGE gel and immunoblotting, labelled proteins were (A) visualized via autoradiography or (B) proteins were detected using the indicated antibodies (1 : 1000). In (B) the marker was stained separately with amino black. **M** = marker; **IE** = inner envelope from *P. sativum*.

Considering all results the topology model for Prat1 in *Pisum sativum* can most likely be concluded as depicted in Figure 14. The N- and C-termini are therefore located on the stromal side of the inner envelope, whereas loop one and three reach into the inner membrane space. Also the position of all cysteins within the transmembrane helices is perfectly in line with the biochemical data presented in 4.4.2 and 4.4.3.

4.5 Prat1 forms small complexes

To analyse the size of native Prat1, which might give evidence on a potential participation in complexes with other proteins, two-dimensional BN/SDS-PAGE analyses were performed. For this purpose, a BN 1st dimension gradient (5 – 12%) loaded with inner envelope from *Pisum sativum* was used. For the 2nd dimension the lane was cut out of the gel and placed horizontally on top of a SDS-PAGE gel. Proteins were subsequently transferred onto nitrocellulose and Prat1 was detected using the respective antibody (Figure 20). A signal for Prat1 is observed in the range from 200 – 100 kDa, thus it seems to be part of a small protein complex with itself or other unidentified partners. Hence, potential interactions that can be detected under the applied conditions occur either with other small proteins or Prat1 itself.

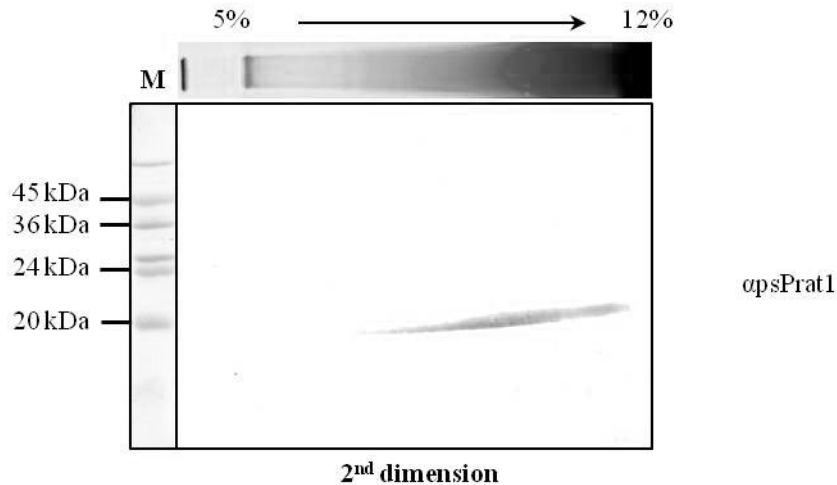


Figure 20: 2nd Dimension of blue-native with inner envelope from *P. sativum*.

Inner envelope from *P. sativum* was run in a 1st dimension gradient gel (5 – 12%) and laterally transferred to a 2nd dimension on a 12.5% SDS-PAGE. The immunoblot was incubated with the psPrat1 antibody (1 : 1000). The marker was stained separately with amino black.

In a next step potential Prt1 interaction partners were searched for. For this purpose overexpressed and purified protein was bound onto a Ni-NTA matrix and a second empty matrix as a control. Both columns were then incubated with solubilised inner envelope from *Pisum sativum*. To identify any specific interaction partners of Prt1 the elutions from both matrixes were loaded on SDS-PAGE gel and the band patterns of the silver staining was compared. However, no differences were detected (data not shown). Furthermore, experiments using iso-electric focusing of envelope from wild type and double mutant plants from *Arabidopsis thaliana* to separate proteins according to their charge and then comparing the colloidal staining of the SDS-PAGE gels showed no differences in general complex formation or protein levels (data not shown). Also silver staining of 2nd dimension blue native gels using envelope or whole chloroplasts from *Arabidopsis thaliana* wild type in comparison to Prt1 double mutant plants demonstrated few distinct spots which do not differ prominently (Figure 21).

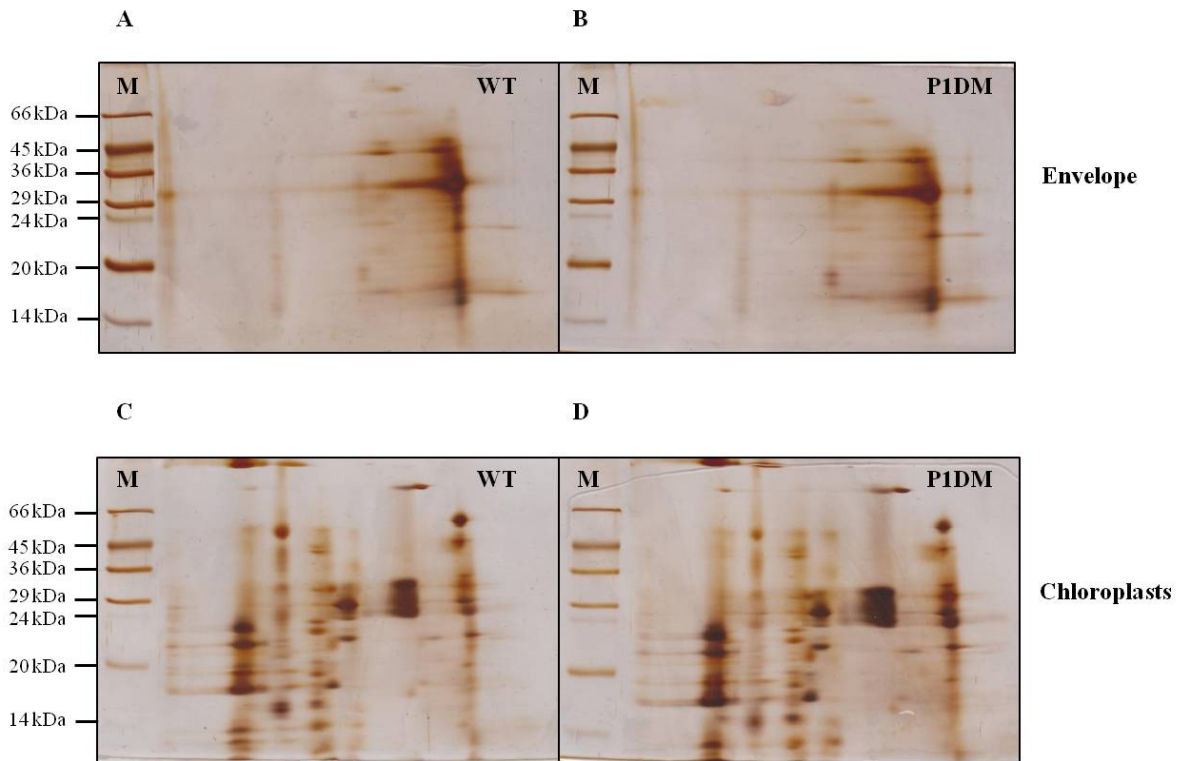


Figure 21: Blue-Native 2nd Dimension of IE and chloroplasts (silver stained).

Depicted are the 2nd Dimension of Blue-Native gels of the indicated samples from either wild type (WT) or double mutant (P1DM) plants from *A. thaliana*. The gels were silver stained. M= marker.

4.6 Flootation of Prat1 proteoliposomes demonstrates stable insertion

A prerequisite for *in vitro* approaches such as channel activity measurements, is the stable integration of Prat1 into liposomes. For this purpose, liposomes prepared as described in 3.2.11 were incubated with purified Prat1 protein (for lipid composition Figure 23). These proteoliposomes were then treated with different buffers to test the quality of insertion: (i) 1 M Mops (high salt conditions), (ii) 10 mM NaCO₃ (alkaline pH conditions) and (iii) 6 M urea were used to wash off proteins which merely attached to the membrane. The samples including an untreated control were loaded at the bottom of separate sucrose gradients and centrifuged at 100.000 g over-night. Fractions of 500 µl each, taken from top to bottom from each gradient, were precipitated using TCA, loaded on SDS-PAGE gels and proteins were visualized with silver staining (Figure 22).

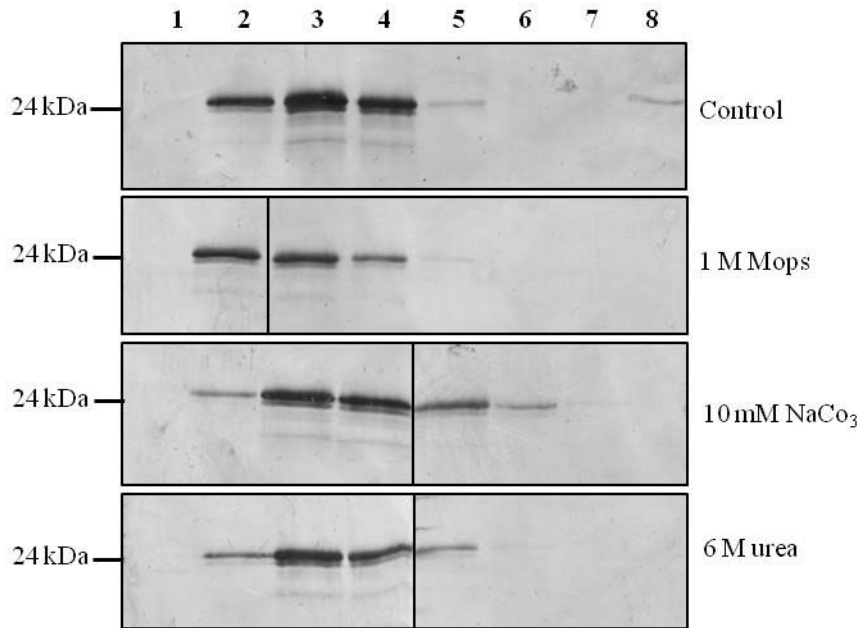


Figure 22: Flootation of proteoliposomes.

Pral1 proteoliposomes were treated with the indicated buffers and centrifuged at 100.000 g o/n at 4 °C at the bottom of a sucrose gradient. Fractions of 500 µl were TCA precipitated, loaded on four SDS-PAGE gels and Pral1 was detected by silver staining. **1 – 8** = top to bottom loading of samples from sucrose gradient.

The results clearly demonstrate that Pral1 is firmly integrated into liposomes. Whereas aggregated protein would accumulate at the bottom of the gradient (corresponding to fraction 8), protein inserted within the liposomes is detected in higher fractions (2 – 5) in the gradient due to the density of the lipids (Morandat *et al.*, 2002). Under all conditions applied, Pral1 colocalises with the liposomes in the gradient, indicating its proper insertion. Thus, these proteoliposomes can be used further for measurements of the channel activity when fused to an artificial lipid bilayer (see 4.7).

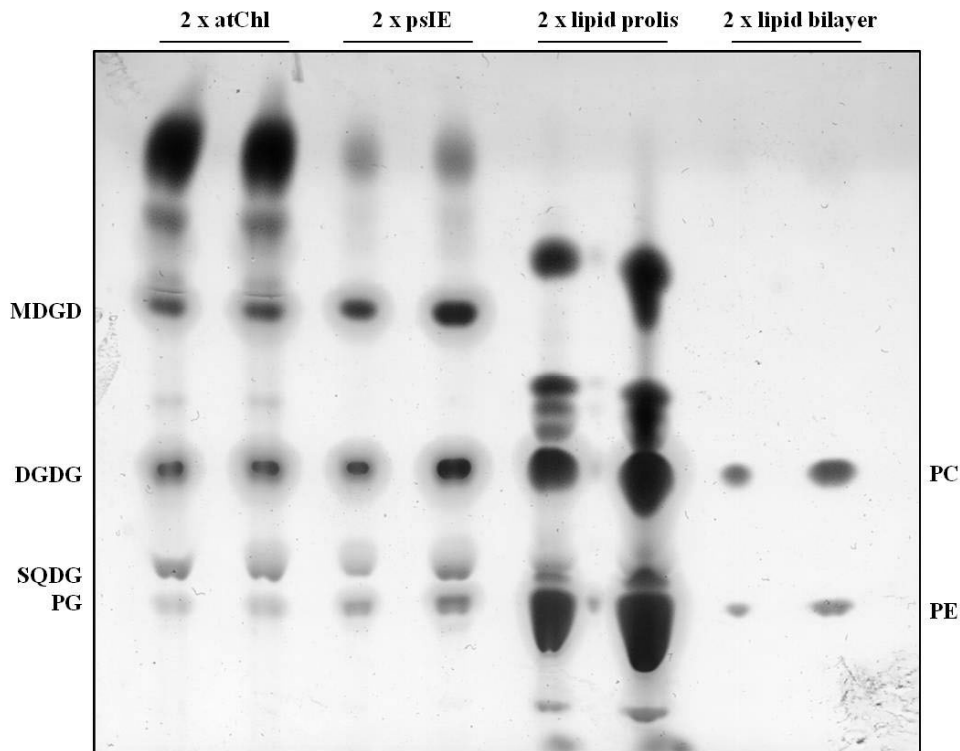


Figure 23: Lipid composition demonstrated via thin-layer-chromatography.

Lipid composition of chloroplasts (Chl) from *A. thaliana*, inner envelope (IE) from *P. sativum*, lipids used for proteoliposome generation (prolis) and lipids used for electrophysiological experiments via the artificial bilayer with the Ionovation Bilayer explorer. Each sample was loaded twice (50 and 100 μg) onto the silica gel plate. Running buffer: 65 ml chloroform, 25 ml methanol and 4 ml H_2O . Staining solution: 2 g $\text{FeSO}_4 \times 7 \text{H}_2\text{O}$, 180 mg KMnO_4 , 6 ml H_2SO_4 and 200 ml H_2O . **MDGD** = monogalactosyldiacylglycerol; **DGDG** = digalactosyldiacylglycerol; **SQDG** = sulfoquinovosyldiacylglycerol; **PG** = phosphatidylglycerol; **PC** = phosphatidylcholine; **PE** = phosphatidylethanolamine

4.7 Electrophysiological measurements

To gain insight into possible channel activities of Prat1, electrophysiological measurements using the Bilayer Explorer from Ionovation GmbH (Osnabrück, Germany) were performed. For this purpose, proteoliposomes containing Prat1 were loaded onto an artificial lipid bilayer (see 3.5; lipid composition see 4.6 Figure 23). When a proteoliposome fuses with the bilayer and the protein is positioned in such a manner that its open channel spans the lipid bilayer, the two electrodes located on each side of the bilayer measure electrical currents passing through the inserted channel protein. From these measurements valuable information about the channel properties can be gathered.

For the overexpression and purification of Prat1 protein from *Pisum sativum*, various conditions were tested including the addition of detergents such as lauryl-sarcosine, n-dodecyl- β -D-maltoside, brij 35, digitonin and Triton X-100. These were analysed in regard to

ideal preparation of the proteoliposomes ensuring proper insertion into the lipid bilayer which was formed between two chambers (see 3.5). The two electrodes separated by the lipid bilayer could then register voltage dependant gating events of Prt1 inserted in the lipid bilayer. In further experiments, recombinant Prt1 protein or its product after translation was loaded directly onto the bilayer to discover optimal insertion properties and conditions. Moreover, giant unilamellar vesicles (GUVs) with multiple Prt1 insertions were tested on a similar machine, the Port-a-Patch from Nanion Technologies GmbH (Munich, Germany; the machine was used with the help of Ana Cosme in the group of Prof. Martin Parniske). The GUVs were allocated onto a small opening between two separated chambers and positioned via mild suction. As described above, electrodes then measured passing currents enabling conclusions regarding to channel activities and properties. Additionally, a deletion construct consisting of only two transmembrane domains of Tic110 was used as a negative control to be able to differentiate between actual measurements of channel activity of Prt1 and unwanted interfering factors.

Further structural analyses were performed using cryo-electron-tomography (see 3.6). Here shock-frozen proteoliposomes are used, which are positioned in an electron microscope and a tomogram is taken by slightly rotating the sample (Prt1 within the proteoliposome) and taking pictures (Figure 24). These can then be reconstructed into a 3D model of the protein similar to crystallization. Various attempts using different conditions for the Prt1 proteoliposomes remained without success. The main reason for this might be the small size of Prt1 (22.8 kDa) making it difficult to detect (proteoliposomes appear empty). The smallest protein that was successfully characterized with this method until now was the major porin of *Mycobacterium smegmatis* MspA (157 kDa; see PhD-Thesis by Christian Werner Hoffmann, TU Munich).

Prat1 and liposomes

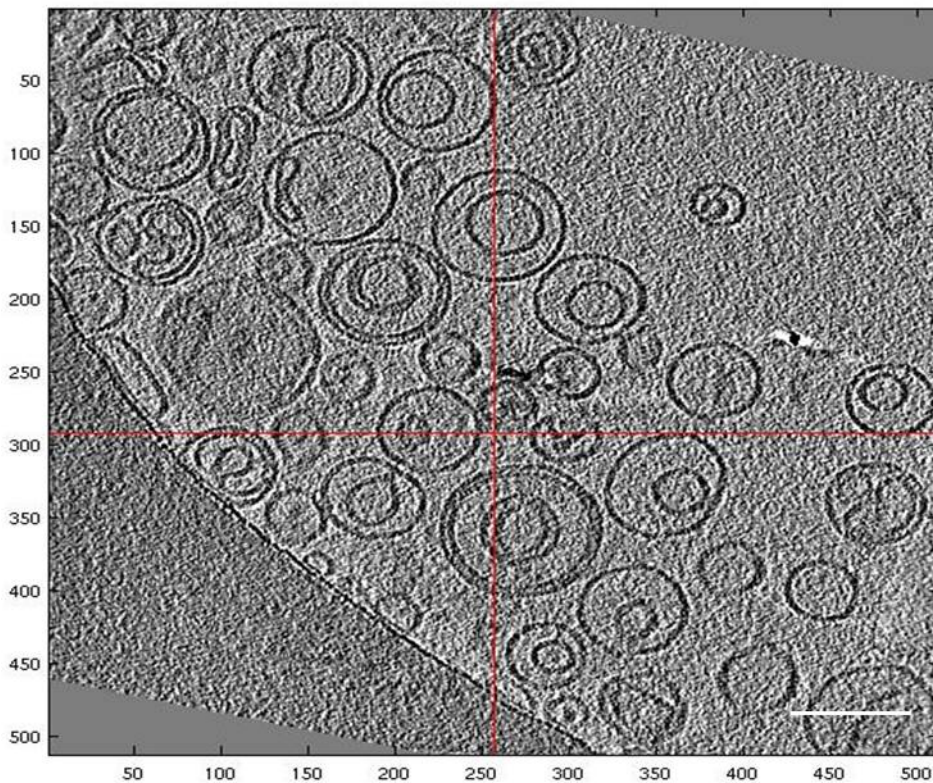


Figure 24: Cryo-electron-tomography.

Cryo-electron-tomogram of shock-frozen (liquid ethane) proteoliposomes. This procedure is able to identify the structure of membrane proteins in their native state localised within the membrane. A) shows Prat1 proteoliposomes but the protein cannot be identified. The picture was provided by Zdravko Kochovski from the AG Baumeister at the MPI in Martinsried. The white scale bar represents 100 nm.

4.8 Δ Prat1.1 Prat1.2 represents a true loss of function line in *Arabidopsis thaliana*

To characterise the Prat1 protein two single knock-out lines for Prat1.1 and Prat1.2 in *Arabidopsis thaliana* were identified from SALK-lines (Manuela Baumgartner, personal communication; Figure 25A, B). The T-DNA insertions are localised within the first intron for Δ Prat1.1 and within the third intron for Δ Prat1.2, respectively. Even though no exon is directly affected by the T-DNA insertions, PCR and RT-PCR analyses revealed the complete lack of both wild type transcripts (Figure 25A).

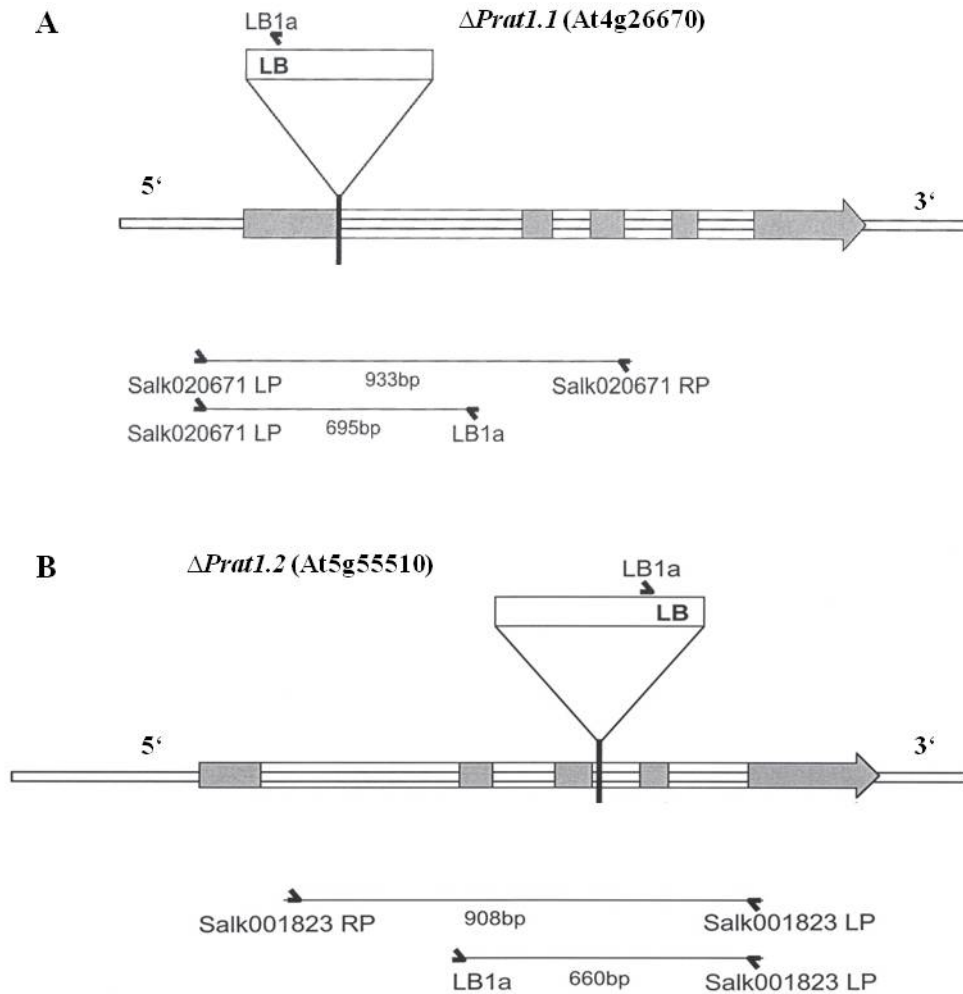


Figure 25: Single knock-out lines of Prati1.1 and Prati1.2 of *A. thaliana*.

A) SALK_020671 line. Depicted is the T-DNA insertion for Prati1.1 and the primer pairs with the indicated PCR products used for verification. **B)** SALK_001823 line. Depicted is the T-DNA insertion for Prati1.2 and the primer pairs with the indicated PCR products used for verification. Exons are marked in grey. **LB** = left border of T-DNA; **RP** = right primer; **LP** = left primer.

These lines were then successfully crossed by Manuela Baumgartner generating a double mutant. To verify the complete loss of function of both genes, RNA was isolated and cDNA was made from wild type and the double mutant plants. Then RT-PCR was performed as described (see 3.1.5) with specific primers (RT-atC1.1 fwd/RT-atC1.1 rev, see Table1). The loss of transcript for Prati1.1 is demonstrated in the lack of a product after RT-PCR (Figure 26A). Furthermore, envelope from wild type (Columbia 0) and the double mutant plants was isolated according to Seigneurin-Berny *et al.*, 2008 and tested for the protein using the atPrati1 peptide antibody. The resulting immunoblot demonstrates the absence of Prati1 in the double mutant (Figure 26B). These results demonstrate that the atPrati1 double mutant does not contain residual Prati1 wild type transcript or protein.

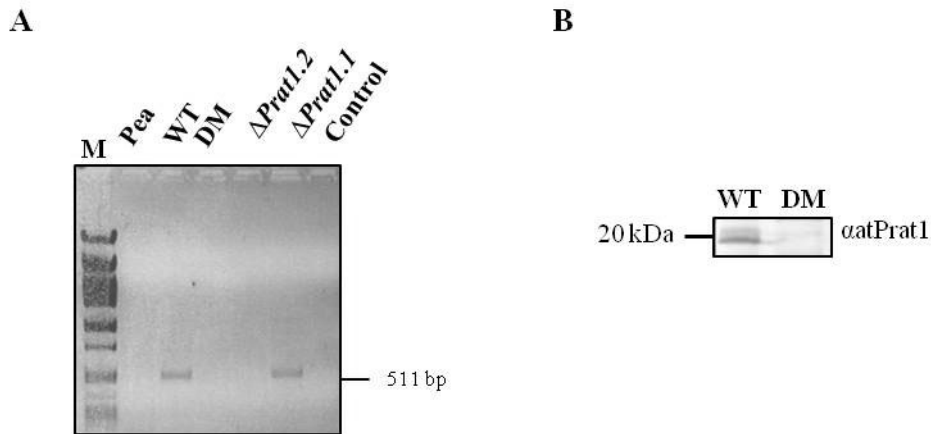


Figure 26: Verification of the Prat1 double mutant in *A. thaliana*.

(A) cDNA from the indicated templates was tested with the RT-atC1.2 fwd neu/RT-C1.2 rev neu (see Table 1) primer pair for the presence of Prat1.2 transcript. Product upon amplification is expected at 511 bp (B) Immunoblot of isolated envelope vesicles (10 μ g) from wild type and Prat1 double mutant upon protein separation on an SDS-PAGE. For detection the atPrat1 peptide antibody (1 : 1000) was used. M = marker.

4.9 Phenotyping of the atPrat1 double mutant

To increase the understanding of the function of a protein, knock-out mutant plants in regard to a specific phenotype were analysed. In this case the Prat1 double mutant (P1DM) plants from *Arabidopsis thaliana* were investigated in comparison to wild type (WT). All plants used for these analyses were grown on soil in flower pots (6.5 x 6.5 cm) with only one seed per pot to allow unhindered growth. All seeds were initially vernalized for approx. three days at 4 °C in the cold room to ensure parallel germination of all seeds. Wild type and double mutant pots were then placed next to each other in the climate chambers and positions switched regularly to enable equal growth conditions at all times. Normal growing conditions included 16 h light and 8 h dark with a light intensity of 100 μ Mol (gradual rise and fall every day from 0 to 100 μ Mol over 30 min), temperatures were held at 22 °C during the day and 18 °C at night and the humidity ranged from 50 to 65%. Under these conditions the P1DM shows retarded growth when compared to the wild type. After 17 days as well as after 33 days of growth, clear differences in size are visible (Figure 27). Additionally, P1DM plants appear slightly paler in color. However, although retarded, the double mutant is able to produce flowers and fertile seeds. Thus, fully grown plants appear identical, and wild type and double mutant cannot be distinguished at these later stages.

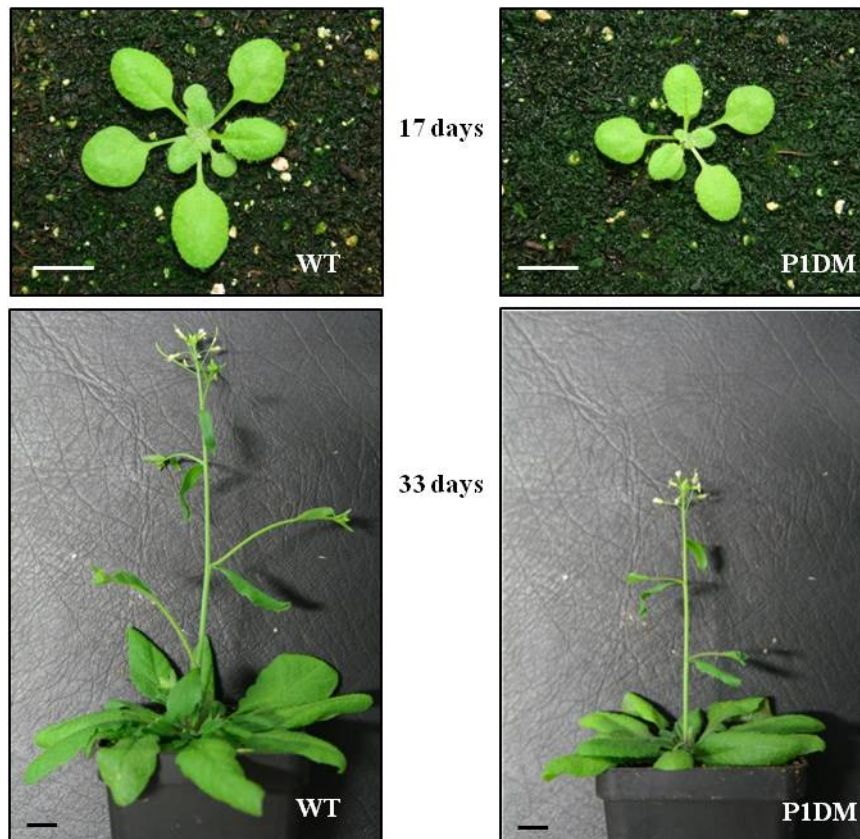


Figure 27: Prat1 phenotype under normal growth conditions.

A. thaliana plants grown on soil in a climate chamber with the following conditions: 16 h light, 22 °C and 50% humidity / 8 h dark, 18 °C and 65% humidity. **WT** = wild type; **P1DM** = Prat1 double mutant. Days indicated were counted after placement of the plants into the climate chamber. The scale bar in each picture represents 1 cm.

In the next step, it was tested whether the so far observed moderate growth phenotype can be maximized by growing the plants under different conditions (see Table 3 in 3.4, Figure 28). Again similar effects can be detected: the double mutant plants are slightly retarded in growth and therefore in development in comparison to the wild type. The general appearance of the plants adapt to the growth conditions (for both wild type and double mutant plants). Additional conditions tested included constant low light (10 μ Mol), heat stress (28 – 30 °C) and drought stress (no further watering after initial identical irrigation; all pots contained equal amounts of soil). However, the phenotypes for these conditions did not alter from the presented ones (data not shown).

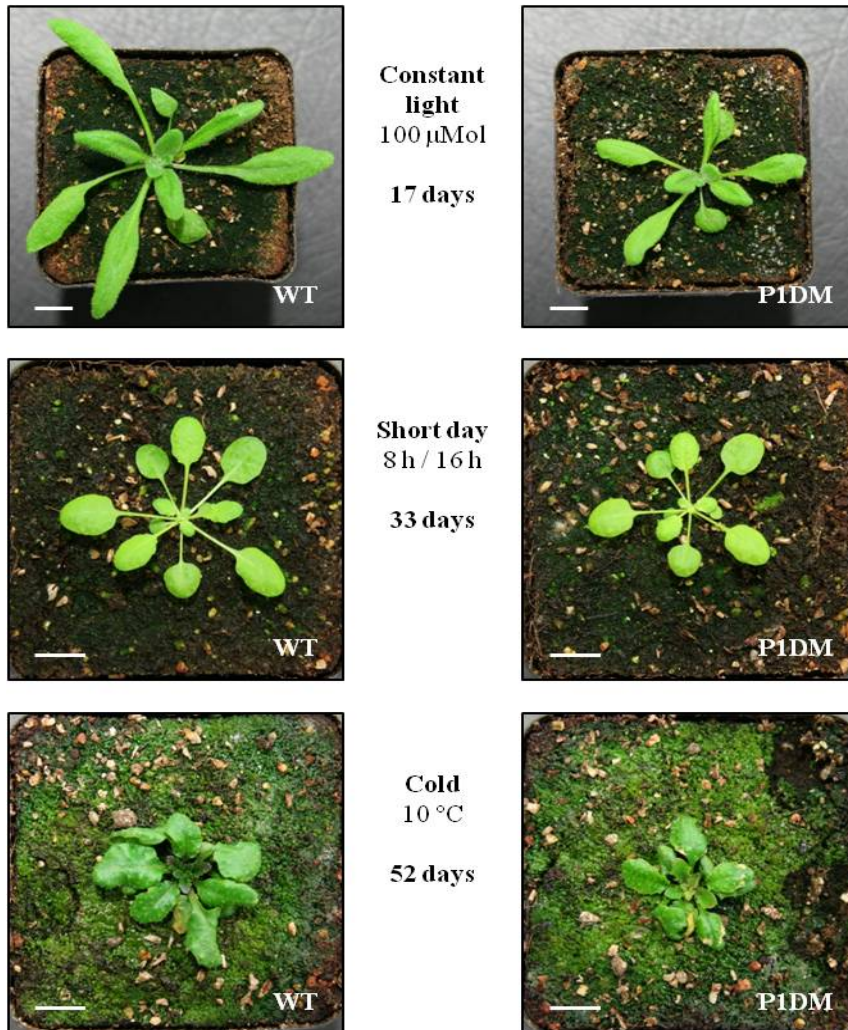


Figure 28: Additional growth conditions for phenotype analyses.

A. thaliana plants were grown on soil in a climate chamber with the indicated growth conditions. **WT** = wild type; **P1DM** = Prat1 double mutant. Days indicated were counted after placement of the plants into the climate chamber. The scale bar in each picture represents 1 cm.

4.9.1 Root growth in the Prat1 double mutant is slightly increased

The visible phenotype of the Prat1 double mutant in *Arabidopsis thaliana* displays a moderate retardation in growth. To analyse possible effects of P1DM mutation on the growth behaviour of the roots, seeds of both the wild type and the double mutant were grown on agar plates, which were placed vertically in the climate chambers. Root growth was monitored for up to 28 days (Figure 29).

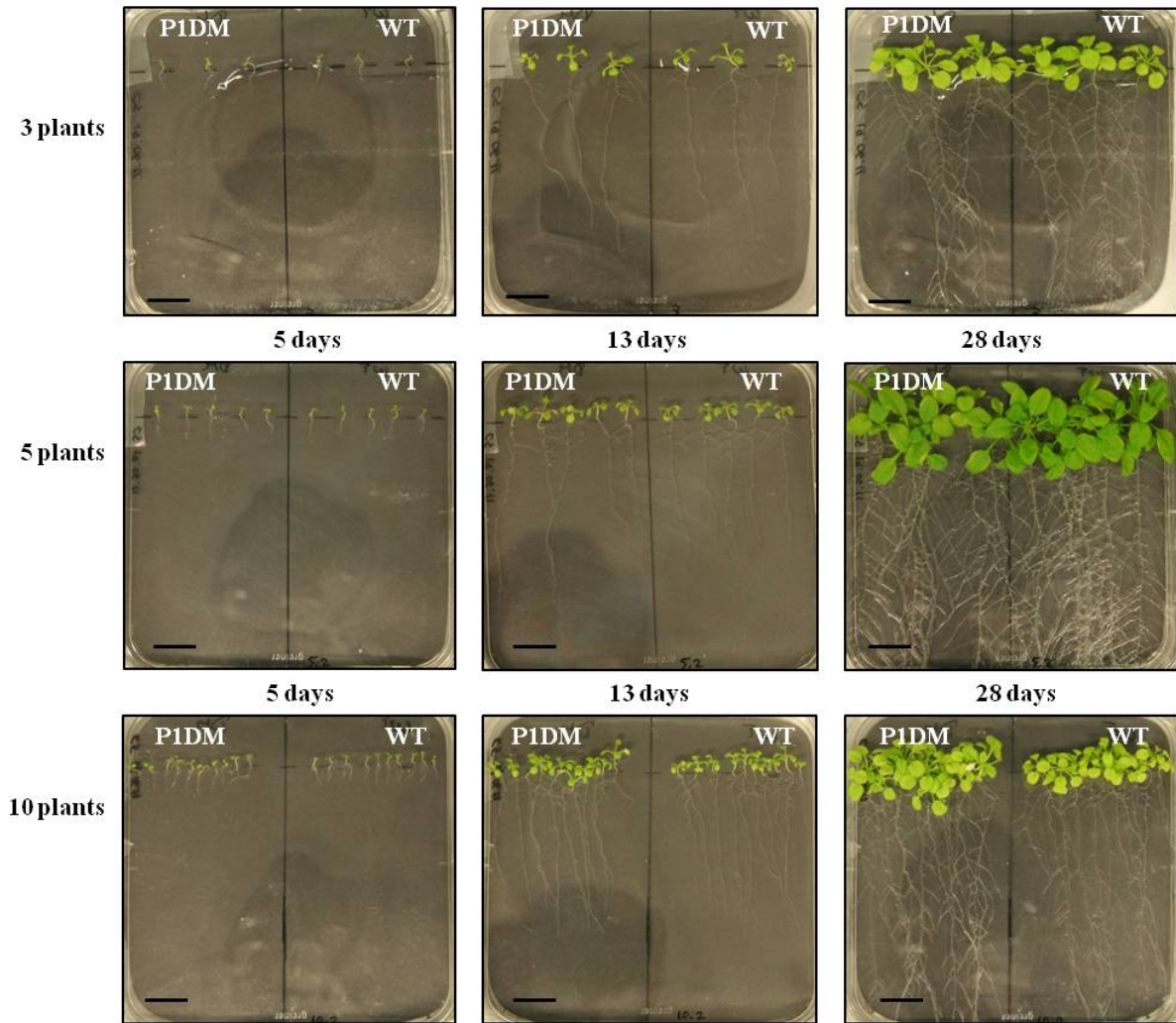


Figure 29: Phenotype analyses of root growth for Prati1.

A. thaliana seedlings (amount indicated) were placed sideways onto vertically positioned plates. **WT** = wild type; **P1DM** = Prati1 double mutant. Days indicated were counted after placement of the plants into the climate chamber. The scale bar in each picture represents 1 cm.

To analyse root growth quantitatively, pictures were taken at regular intervals and the length of the roots was determined digitally using Adobe Photoshop CS3. The data were pooled and are represented in the diagram in figure 30. For wild type plants a mean length of 6.91 +/- 0.62 mm after 5 days, 25.37 +/- 2.25mm after 8 days and 50.79 +/- 6.18 mm after 13 days was measured. For the P1DM, a growth of: 8.89 +/- 0.88 mm after 5 days, 29.17 +/- 1.82 mm after 8 days and 56.56 +/- 5.02 mm after 13 days. Due to excessive branching of roots and the limiting space of the plates, root length analyses were not performed at later timepoints. Taking the standard error bars into account, root growth does not differ significantly between the wild type and the P1DM, although the mean of root length in the double mutant is slightly increased. This indicates a marginally stronger growth of the plants below the soil than above compared to the wild type. (see 4.9).

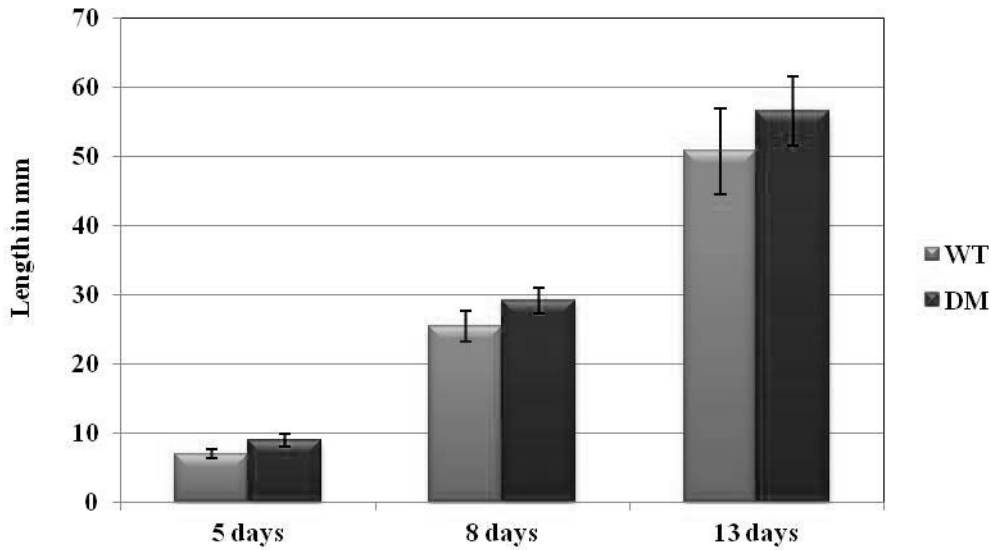


Figure 30: Comparison of the root length between wild type and P1DM plants.

Seedlings were placed on vertically positioned sterile plates in a climate chamber and root growth was regularly photographically documented and digitally measured in Adobe Photoshop CS3. For wild type and PIDM measurements of 18 roots each were pooled. The grey bars represent the mean root length for the **WT** = wild type and the black bars the mean for the **P1DM** = Prat1 double mutant. Standard error bars are included.

4.10 RNA expression is regulated with the circadian clock

In a next step, the RNA expression profiles of the Prat1.1 and Prat1.2 genes were determined (see genome tiling arrays, Winter *et al.*, 2007, Laubinger *et al.* 2008). Interestingly, in a further study, the RNA expression of the Prat1.1 gene from *Arabidopsis thaliana* was analysed using a NASCArray (Nottingham Arabidopsis Stock Centre microarray database, GeneChip analysis) with which the RNA expression behaviour of genes linked to the circadian clock was observed (Steve Smith, E-NASC-49, 2005). The plants used in this analysis for RNA extraction were grown in climate chambers with a 12 h day and 12 h night rhythm. Prat1.1 was found to show an expression pattern independent of the dark/light rhythm (diurnal), but rather anticipating it (Figure 31). During the light phase RNA expression decreases continuously until approx. 3 h before beginning of the dark phase where the expression strongly increases to then slowly drop again during the dark hours. Approx. 2 - 3 h prior to the light phase the strong increase of the expression is observed again, demonstrating that the Prat1.1 RNA expression cycles with the circadian clock present in the plant and is not merely light regulated.

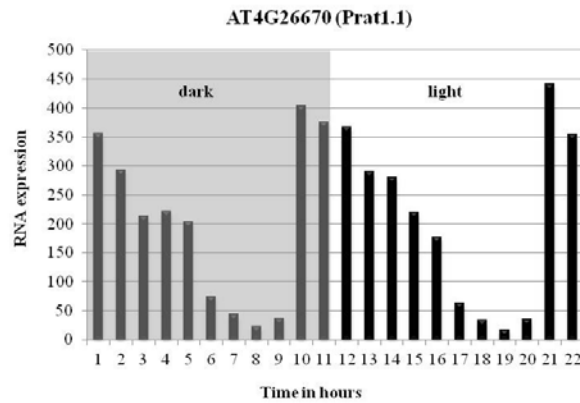


Figure 31: RNA expression pattern of Prat1.1 in *Arabidopsis thaliana* (NASCArray) shows diurnal regulation.

RNA expression levels of atPrat1.1 according to the time. Area in grey represents the 12 h night phase in contrast to the 12 h day phase. Data retrieved from NASCArray (Steve Smith, E-NASC-49, 2005).

To verify these results and to additionally analyse the expression profile of the Prat1.2 gene, RT-PCR experiments were performed. For this purpose, wild type plants as well as the two single mutant plants were grown for 25 days, then leaf samples were taken and directly frozen in liquid nitrogen, followed by RNA isolation and RT-PCR using the primers indicated (Table 1, Figure 32). The results for the RNA expression levels of the Prat1.1 and Prat1.2 genes are not as clear as the ones derived from the NASCArray. However, a distinct tendency is observed, showing gradual decreases and sharp increases of RNA expression levels in regular cycles, as described before. Interestingly, in Δ Prat1.1 and Δ Prat1.2, the expression pattern of the other respective gene remains unaltered (Figure 32). In addition it has to be noted that the light (16 h) and dark (8 h) phases were not identical to the experiment performed by Steve Smith, E-NASC-49, 2005 (12 h / 12 h).

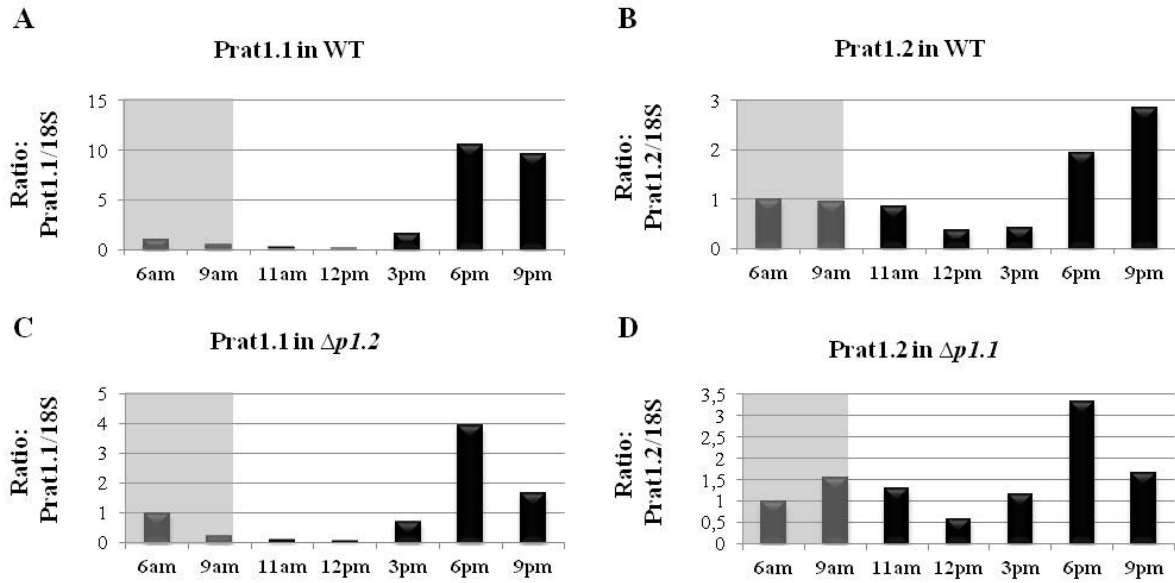


Figure 32: RNA expression pattern of Prat1.1 and Prat1.2 in *Arabidopsis thaliana* (RT-PCR).

Represented is the ratio of RNA expression levels for (A, C) Prat1.1 and (B, D) Prat1.2 from *A. thaliana* to 18S RNA in either wild type or the indicated single mutant plants. Leaf material was taken at indicated timepoints and RNA was isolated for RT-PCR analysis. Area in grey represents the night phase in contrast to the white day phase. Light: 9am – 1am; dark: 1am – 9am.

To determine whether protein expression follows this RNA expression pattern, leaf samples were taken at the indicated times and protein extraction was performed. After separation of proteins via SDS-PAGE and immunoblotting, Prat1 was detected using a specific antibody (Figure 33). Additionally, a Tic110 antibody was applied as a loading control (some sample was lost at timepoint 6 pm, WT). In contrast to the RNA expression levels, the protein amounts remained stable even in the Prat1.1 single mutant (Prat1.2 still present, the antibody detects both isoforms). Thus, the effects of the circadian rhythm on RNA expression do not seem to be directly correlated with protein synthesis and/or stability.

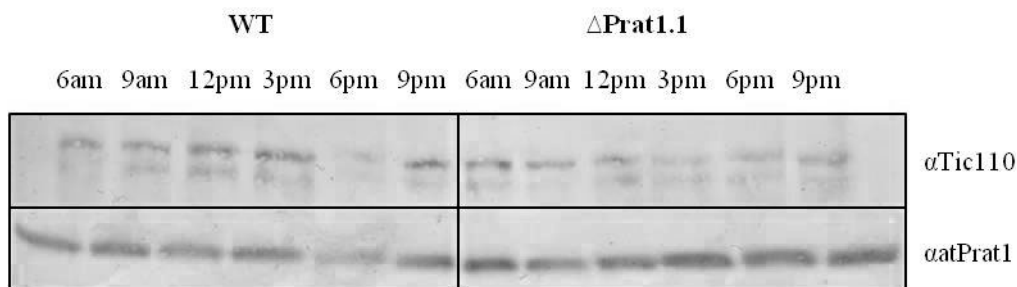


Figure 33: Protein levels of Prat1 remain stable in *A. thaliana*.

Leaf samples were taken at the indicated timepoints and protein extraction was performed. Samples were loaded on a 12.5% SDS-PAGE gel for separation and afterwards blotted onto a PVDF membrane. The immunoblot was incubated with the indicated antibodies (1 : 1000). WT = wild type plants. α Tic110 was used as a loading control.

4.11 P1DM is affected in photorespiration, the TCA cycle and the oxidative pentose phosphate cycle (metabolic influences)

Since the phenotype of the *Prat1* double mutant in *Arabidopsis thaliana* exhibits retarded growth it seems likely that certain metabolic pathways are affected. Thus, the respective substrates might not be synthesized efficiently or their transport to the correct destinations could be influenced, therefore causing retarded growth of the entire plant. Hence, metabolic profiling was performed to gain an overview of the metabolic activities within the double mutant plants, which aids to identify metabolites which are off-regulated in comparison to the wild type.

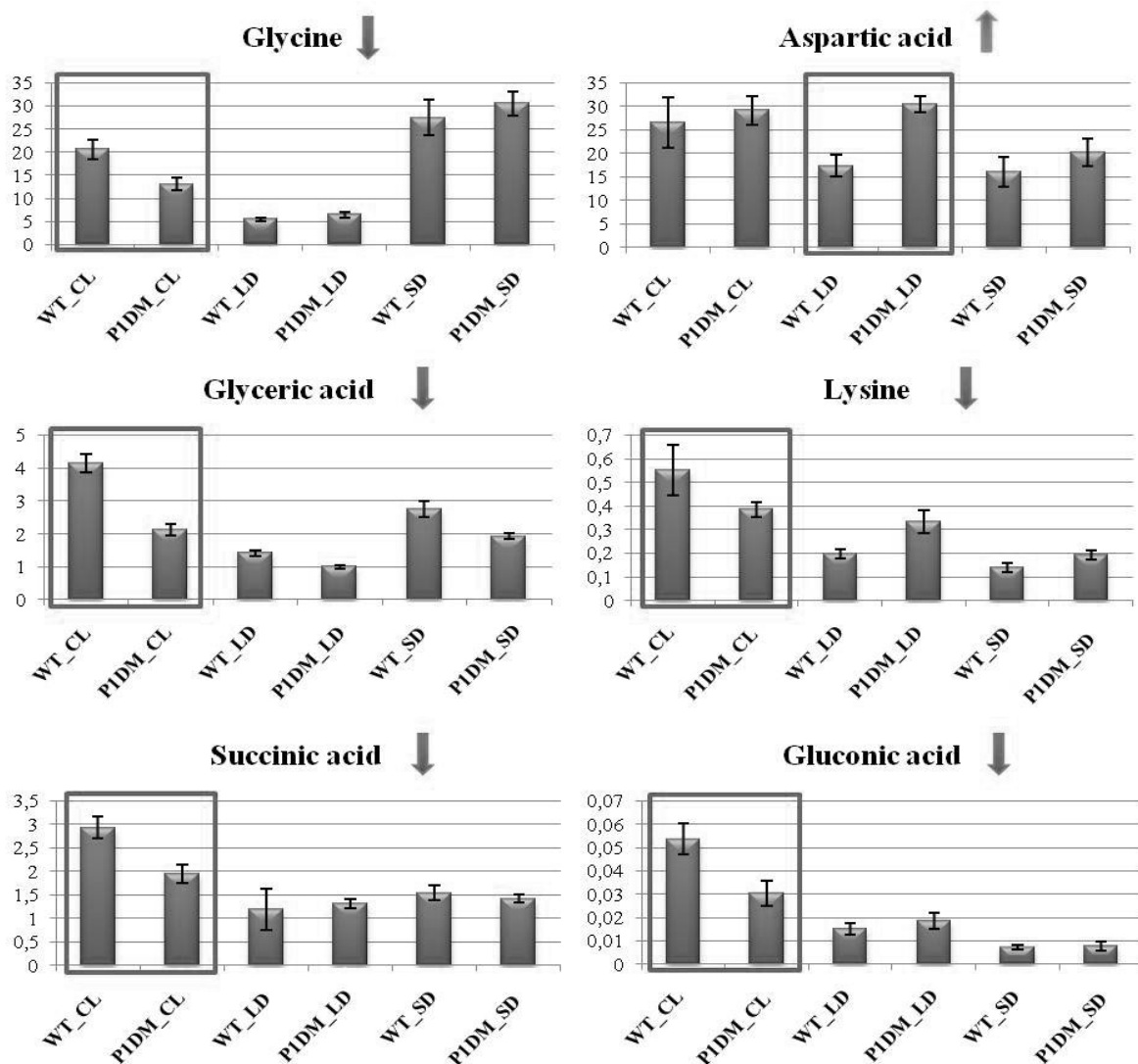


Figure 34: Metabolic profiling data from WT and P1DM.

Leaf samples from indicated 20 days old plants were subjected to metabolic profiling at the University of Düsseldorf in the group of Prof. Andreas Weber. Selected graphs with standard error bars of indicated substances are presented. Framed bars indicate significant up or down regulations. WT = wild type; P1DM = *Prat1* double mutant; CL = constant light; LD = long day; SD = short day. Arrows indicate up or down regulation.

For the metabolic analysis, *Prat1* double mutant and wild type plants were grown under three different conditions: (i) constant light (100 μ Mol), (ii) long day (16 h / 8 h) and (iii) short day (8 h / 16 h). Leaf samples were taken after 20 days of growth and sent to the group of Prof. Andreas Weber at the University of Düsseldorf, Germany where the profiling was performed (Figure 34 and 35). Interestingly, five compounds were found to be slightly down regulated under at least one growth condition (constant light, Figure 34, framed bars). These include glycine, glyceric acid, lysine, succinic acid and gluconic acid. Aspartic acid on the other hand was detected as slightly up regulated under long day conditions. When looking at the relevant metabolic pathways, it can be concluded that the *Prat1* double mutant is affected in photorespiration, the citric acid cycle and the oxidative pentose phosphate cycle. Therefore it is tempting to speculate that *Prat1* might function as a transporter for either amino acids involved or for plastid proteins associated with the described pathways. However, this theory needs to be substantiated by direct evidence.

Results

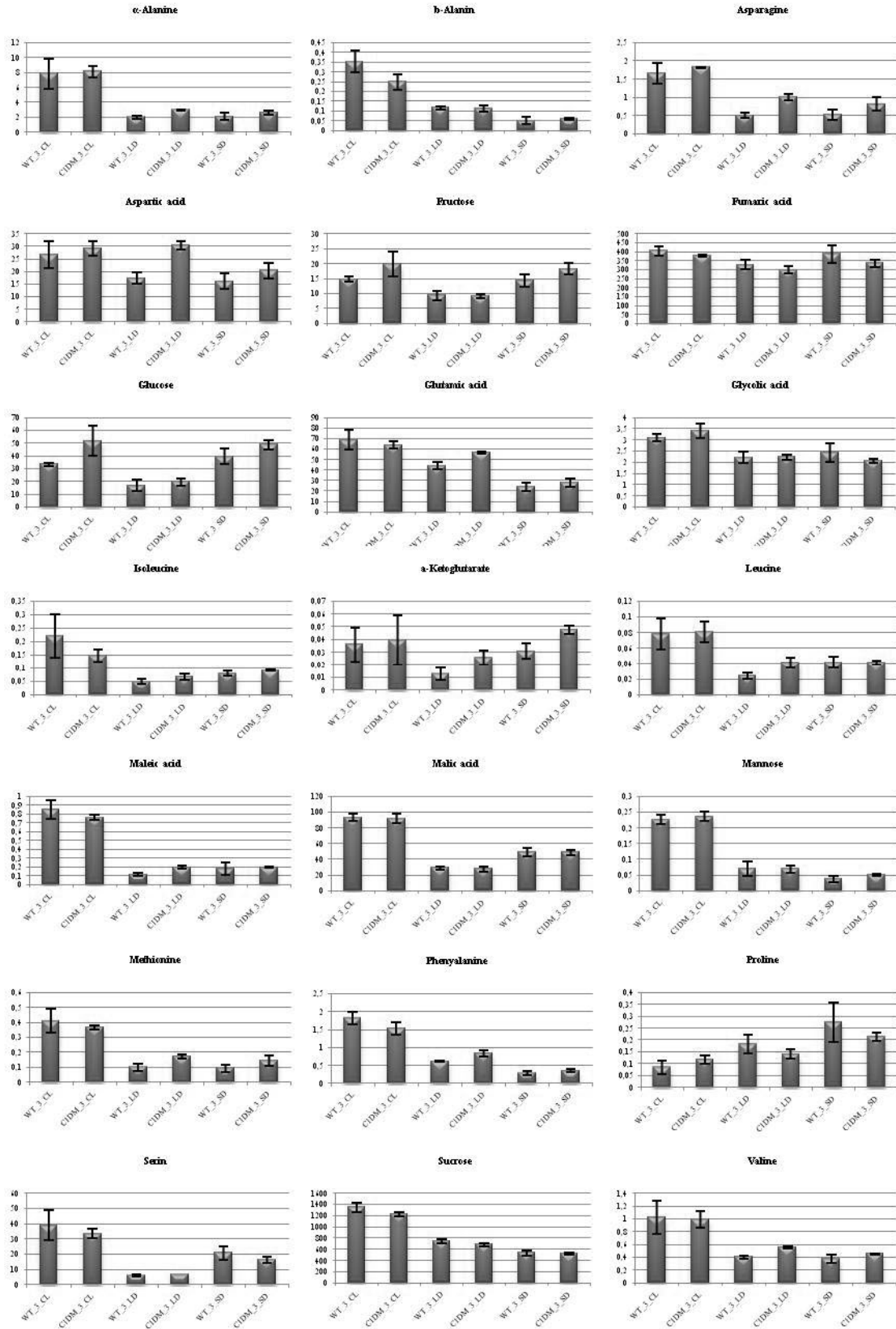


Figure 35: Additional data from metabolic profiling.

Leaf samples from indicated 20 days old plants were subjected to metabolic profiling at the University of Düsseldorf in the group of Prof. Andreas Weber. Selected graphs with standard error bars of indicated substances are presented in alphabetical order. WT = wild type; CIDM = PIDM = Prati double mutant; CL = constant light; LD = long day; SD = short day.

5 Discussion

5.1 The membrane-spanning protein Prat1 in the IE of chloroplasts

The present study focussed on further characterisation of the chloroplast membrane protein Prat1. It was initially discovered in a proteome analysis of the chloroplast envelope membranes from *Arabidopsis thaliana* (Ferro *et al.*, 2002; Ferro *et al.*, 2003; Fröhlich *et al.*, 2003). On the basis of a phylogenetic analysis the protein was confirmed to be a member of the Prat-family (preprotein and amino acid transporter; Murcha *et al.*, 2007), which includes e.g. Tim17, Tim22 and Tim23 from mitochondria (e. g. Moro *et al.*, 1999; Bauer *et al.*, 1999), but also Oep16 from chloroplasts (Pudelski *et al.*, 2012). Moreover, immuno detection assays of Prat1 suggested its localisation within the envelope membrane fraction of chloroplasts from *Arabidopsis thaliana* containing both inner and outer envelope (Murcha *et al.*, 2007). In agreement with this preliminary data, the present study was able to verify this location of the protein using a newly generated specific antibody (see 4.2), which detected the Prat1 homologue in *Pisum sativum* exclusively in the inner envelope membrane of chloroplasts (Figure 12). Furthermore, the bioinformatical prediction for membrane proteins in the ARAMEMNON database (Schwacke *et al.*, 2003) reveals four transmembrane domains of α -helical structure, which is a typical feature of members of the Prat-family. These structural propertise indicate a strong association of the protein to the membrane, which was indeed observed for Prat1 by protease digestion experiments of envelope membranes using thermolysin, GluC and trypsin (see 4.4.1). Even the hydrophilic loops were found to be largely protected from protease degradation (Figure 15 and 16). Additionally, floatation analysis of Prat1 integrated into artificial liposomes further support the predicted membrane localisation of the protein (see 4.6; Hyland *et al.*, 2001).

A question that needed to be solved for generating a more detailed topology model for the protein regards its orientation within the inner envelope of the chloroplast. The predicted structure of Prat1, containing four transmembrane domains connected by hydrophilic loops clearly implies that both N- and C-termini are located towards the same side of the membrane, in this case reaching either into the intermembrane space or the stroma. Other Part-family members such as the Oep16 protein located in the outer envelope membrane demonstrate a topology with both N- and C-termini reaching into the cytosol of the cell (Pudelski *et al.*, 2012). In contrast to this it has been suggested that the Prat2 protein located in the inner envelope of the chloroplast like Prat1 has its termini positioned towards the intermembrane

space (Sabrina Kraus, PhD-Thesis, LMU München 2010). Prat1 contains a single phosphorylation site in the N-terminus of the protein (Ser6; Reiland *et al.*, 2011). It could be shown that approximately 50% of these serines, which are the first in the N-terminus of Prat1, stay phosphorylated after protease treatment, indicating that the phosphorylation site is protected from protease activity and suggesting that both the N- and C-termini are positioned on the stromal side of the inner envelope. However, the lower intensity of the phosphorylation band after thermolysin treatment could also imply an incomplete digestion, placing the termini of Prat1 in the intermembrane space. Nonetheless, a complete solubilisation of the inner envelope membrane is required for a total loss of phosphorylation (Figure 19). Moreover, protease treatment experiments failed to produce clear digestion bands for Prat1 (see 4.4.1), indicating inaccessibility to the proteases used. The present study therefore defines the orientation of the N- and C-termini of Prat1 reaching into the stroma of the chloroplast whereas loop one and three of the protein are located on the side towards the intermembrane space (Figure 14). Possible protein-interaction sites within the termini would therefore be accessible from the stromal side. These interactions could include the recruiting of proteins that will further process or guide preproteins or metabolites which have been transferred by the predicted transporter Prat1 or be part of a signalling pathway yet to be identified. The possible significance of the phosphorylation is discussed in more detail in 5.2. Moreover, the transmembrane domains were also found to include the five cysteines present in the amino acid sequence of Prat1 from *Pisum sativum*, as these could only be chemically labelled after solubilisation of the protein making any redox-regulation unlikely (see 4.4.2 and 4.4.3). The homologue Prat1.1 and Prat1.2 proteins from *Arabidopsis thaliana* contain an additional sixth cysteine in the C-terminus which should be accessible for modification, and which might serve as an excellent control in future analysis. However in the present study, solely the homologue from *Pisum sativum* was employed.

In a next step the question whether Prat1 might form a functional channel which spans the inner envelope of the chloroplast was addressed. When taking a closer look at other members of the Prat-family which have already been investigated to some extent, a channel function is often found. The mitochondrial Tim17 together with Tim23 constitute the main protein import channel proteins of the Tim-complex (Rehling *et al.*, 2001). Prior studies have shown Tim23 to be a 13-24 Å wide voltage-sensitive high-conductance channel with specificity for mitochondrial presequences (Truscott *et al.*, 2001; Mokranjac and Neupert, 2010). Additionally, the Prat-family member Oep16 located in the outer envelope of the chloroplast possesses channel activity and is selective for amino acids and amines while

excluding triphosphates and uncharged sugars (Pohlmeyer et al., 1997). A predicted channel-forming function of the Prat1 protein is therefore a plausible assumption. This hypothetical channel could either be formed by a single or multimer of the Prat1 protein or an assemblage of small proteins clustered together with Prat1 as the main channel protein. The formation of a channel pore by homooligomer or heterooligomer subunits of a membrane protein-family has also been described before (Jeanguenin *et al.*, 2008). Other Prat-family members like Tim23 have been described to possess a pore-stoichiometry consisting of a multiple of three, whereas Oep16 shows dimerisation even though the electrophysiological data point to a channel activity of three or six pores (Truscott *et al.*, 2001; Pohlmeyer *et al.*, 1997; Steinkamp *et al.*, 2000). Results received by BN-PAGE reveal Prat1 to be part of a small protein complex (Figure 20) supporting the hypothesis of oligomerisation. The proposed constellation with two Prat1 proteins could form the basis for a channel-pore.

To test for channel activity, both the Ionovation Bilayer Explorer and the Nanion Port-a-Patch machines were used (see 4.7). Although testing various conditions including the addition of e.g. Ca^{2+} to enable channel activity, the conditions needed for a proper insertion of the Prat1 protein into the lipid bilayer still remain to be optimised for Prat1. Possible misapplications can occur as early as the purification of the overexpressed protein and include the use of inappropriate detergent, being the quantity or the type of detergent (Chiu, 2012; Korepanova and Matayoshi, 2012). Once the purified Prat1 protein is at hand and applied to the lipid bilayer the insertion into the bilayer takes place at random. Nor the orientation of the protein within the bilayer neither an undesirable additional channel-like opening in the bilayer, due to the insertion, can be determined. To minimize these effects a deletion construct, in this case of Tic110, was used as a negative control. The deletion construct consisted of merely two transmembrane domains making it impossible for the protein to form a channel but still integrate into the lipid bilayer. Repetitive trials with both the Prat1 protein and the negative control could then clarify between actual measurements of the channel activity and unwanted interfering factors. Further testing will be necessary for a conclusive statement on the channel activity of Prat1.

Most important for this study is the link between Prat1 and the Prat-family member Tim22 located within the inner membrane of mitochondria where it acts as a channel for proteins without a transit peptide which are inserted into the inner membrane (Hasson *et al.*, 2010). For Tim22 channel activity has been described for a single and a triple pore-unit (Kovermann *et al.*, 2002). In a complementation assay both Prat1 isoforms from *Arabidopsis thaliana* were able to at least partially complement the function of the essential Tim22 protein

in the yeast *Saccharomyces cerevisiae* (Murcha *et al.*, 2007). This is a strong indication that Prat1 adopts a channel function *in vivo* and represents the chloroplast equivalent of the mitochondrial Tim-translocase Tim22 (carrier pathway; Kurz *et al.*, 1999; Hasson *et al.*, 2010). Thereby it might constitute an alternative import pathway for proteins not using the Tic complex (Benz *et al.*, 2009) that are destined to the chloroplast stroma or become integrated into the inner envelope. Another possible hypothesis, given the fact that the chloroplast is the primary compartment for the amino acid biosynthesis (Lam *et al.*, 1996), is a role of Prat1 in transport of amino acids and their derivatives, similarly as has been described for the Oep16 proteins (Pohlmeyer *et al.*, 1997).

5.2 Possible role of Prat1-phosphorylation

During the process of phosphorylation a phosphate group is added to a protein or other organic molecule with the help of a kinase. The mechanism retrieves the supplementary phosphate group usually from an ATP (adenosine-5'-triphosphate) molecule (Figure 36).

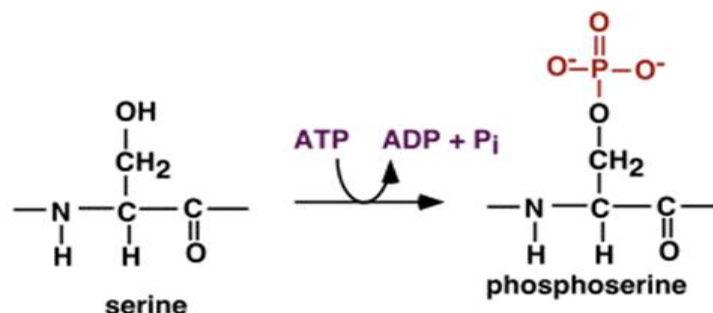


Figure 36: Phosphorylation mechanism of the amino acid serine.

Phosphorylation at the amino acid serine occurs with the help of a serine protein kinase which converts ATP (adenosine-5'-triphosphate) into ADP (adenosine diphosphate) and thereby adds a phosphate group to the serine.

ATP is thereby converted into ADP (adenosine diphosphate), releasing a phosphate group which is transferred to the available phosphorylation site. The primary sites for phosphorylation have been described to be serine, threonine and tyrosine residues although in some cases histidine, arginine and lysine residues may undergo phosphorylation as well (Ciesla *et al.*, 2011). In the case of the Prat1 protein in *Arabidopsis thaliana* Ser6 was described as phosphorylation site in a comparative phosphoproteome profiling performed in *Arabidopsis thaliana* (Reiland *et al.*, 2011).

Phosphorylation is the most widespread posttranslational protein modification, playing a regulatory role in almost every aspect of cell life in both prokaryotic and eukaryotic

organisms (Chang and Stewart, 1998; Ciesla *et al.*, 2011). Many enzymes and receptors are switched “on” or “off” by this reversible process mediated by kinases responsible for phosphorylation them and phosphatases that dephosphorylate. Conformational changes in the involved proteins, signal transduction, protein-protein interactions and even protein degradation are the key effects evoked by phosphorylation (Olsen *et al.*, 2006). For Prat1, the function of the single phosphorylation site remains to be discovered. Most proteins which are phosphorylated contain numerous phosphorylation sites which control and regulate their biochemical properties dependent on which specific site becomes phosphorylated. Due to the location of the sole phosphorylation site at the N-terminus of the Prat1 protein sequence, the site reaches into the stroma of the chloroplast (Figure 14), where it can interact with proteins. Since channel activity is predicted for the Prat1 protein, communication with proteins on the stromal sides of the inner envelope membrane is of substantial importance. The phosphorylation on the stromal side of the protein could cause a specific conformational change inducing an active state of Prat1. Other examples where channel-gating is regulated via phosphorylation sites of the channel protein, include the recently described CaMKII (Ca²⁺/calmodulin-dependent protein kinase II) activity controlling the gating of the cardiac NaV1.5 sodium channel (Ashpole *et al.*, 2012).

Within the scope of the comparative phosphoproteome profiling in *Arabidopsis thaliana* six separate repetitions of the experiment were performed. In four of these experiments the serine at the N-terminus of Prat1 was found in a phosphorylated state and twice in a non-phosphorylated state (Reiland *et al.*, 2011), indicating that the phosphorylation of the Prat1 protein in *Arabidopsis thaliana* is reversible and can therefore adapt to changes in the biochemical capacity or requirements of chloroplasts.

5.3 RNA expression of Prat1 follows a circadian rhythm

Most organisms including higher plants have the innate ability to measure time. Plants do not only respond to sunrise or sunset but rather anticipate dawn and dusk and adjust their biology and metabolism accordingly. The circadian rhythms, are the subsets of biological rhythms divided into periods, defined as the time to complete one cycle of ~ 24 h (Giebultowicz, 2004). Important characteristics of the circadian rhythms include that they are endogenously generated and self-sustained, enabling them to persist under constant environmental conditions such as permanent light (or dark) and/or temperature. Under these controlled conditions, the plant can no longer rely on external time cues to express specific proteins and

therefore it depends on the entrained endogenous timing system which precisely corresponds to the exogenous period of the earth's rotation. The expression of the *Prat1.1* gene from *Arabidopsis thaliana* was analysed using a NASCArray (Nottingham Arabidopsis Stock Centre microarray database, GeneChip analysis) with which the RNA expression behaviour of genes linked to the circadian clock was observed (Steve Smith, E-NASC-49, 2005; Figure 31). Indeed, a typical circadian expression on RNA level was detected for *Prat1.1*. The plants used in this analysis for RNA extraction were grown in climate chambers with a 12 h day and 12 h night rhythm, nonetheless the expression of *Prat1.1* increased 2 h prior to the beginning of the light phase (see 4.10). In the present study similar behaviour could also be detected with RT-PCR analysis for both *Prat1.1* and *Prat1.2* (Figure 32).

The circadian clock is known to regulate many key physiological processes in higher plants, ranging from growth (Dowson-Day and Millar, 1999) and flowering time (Yanovsky and Kay, 2003; Imaizumi and Kay, 2006) to stomatal opening and CO₂ assimilation (Hennessey and Field, 1991). Microarray analyses suggest that more than 10% of all *Arabidopsis thaliana* genes are regulated at the level of mRNA abundance and multiple metabolic pathways have been identified that seem to be under circadian control (Harmer *et al.*, 2000; Schaffer *et al.*, 2001; Michael and McClung, 2003). The current knowledge of the main proteins involved in the circadian rhythm regulation in *Arabidopsis thaliana* are depicted in a simplified model (Figure 37). The evening-expressed *timing of cab expression 1* (*TOC1*) gene forms together with the light/morning-induced transcription factors *circadian clock associated1* (*CCA1*) and its homologous gene *late elongated hypocotyl* (*LHY*) the key players of the main transcriptional feedback loop in *Arabidopsis thaliana* (Ito *et al.*, 2008). Additionally, *CCA1* and *LHY* are regulated by *pseudo response regulatory7* (*PRR7*) and *PRR9* in response to ambient temperatures (Salomé *et al.*, 2010) and function upstream of *TOC1* which they regulate negatively. *TOC1* in turn, serves as a positive regulator of *CCA1* and *LHY*, together they control circadian and morphogenic responses in the plant (Ito *et al.*, 2007).

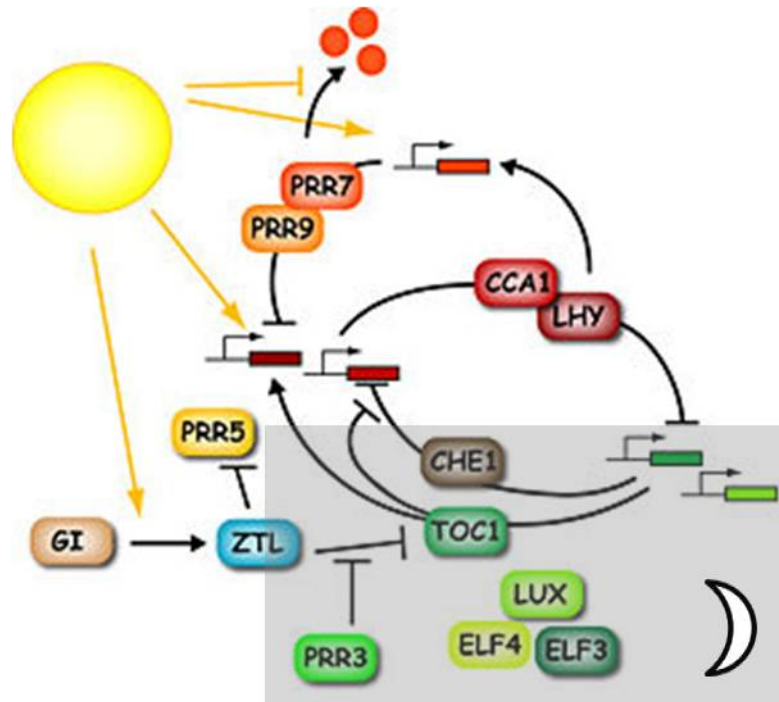


Figure 37: Current knowledge regarding key players of the circadian rhythm in plants.

The figure was taken from the Farré Lab homepage (<http://farrelab.openwetware.org/Research.html>) and modified. Depicted is a basic model of the *Arabidopsis thaliana* circadian oscillator. Proteins are indicated by oval shapes with the indicated protein name. Protein activity is indicated with solid lines, with lines ending in arrowheads indicating positive action and lines ending in perpendicular dashes indicating negative action. CCA1, LHY and TOC1 create the core feedback loop. The shaded area indicates activities peaking in the subjective night and white area indicates activities peaking during the subjective day. **CCA1** = circadian clock associated 1; **LHY** = late elongated hypocotyls; **TOC1** = timing of cab expression 1; **PRR3,5,7,9** = pseudo-response regulators; **GI** = gigantea; **ZTL** = zeitlupe; **CHE1** = CCA1 hiking expedition; **LUX** = lux arrhythmo; **ELF3,4** = early flowering.

Circadian regulated transcripts have been found to be enriched in the subset of transcripts with short half-lives (Gutierrez et al., 2002); hence high transcript stability might conceal transcriptional oscillations when only the steady state transcript level is monitored. Indeed, enhancer trapping, a transgenic construction containing a mobile element (P element) and a reporter gene for the identification of enhancers, suggests that up to 35% of the transcriptome may show clock regulation (Michael and McClung, 2003). Since Prat1.1 does not seem to be regulated in a circadian rhythm on protein level (Figure 33), the function of an oscillating transcript is not yet understood. It could be suggested that a substrate transported by the Prat1.1 protein underlies circadian control but also acts as the main trigger for a signalling pathway inducing Prat1.1 transcription. In this case, changes in the abundance of the circadian regulated substrate would correspond to an altered Prat1.1 transcript level. Whether the Prat1.1 protein would continue to assume its proper function could then be controlled via phosphorylation (see 4.4.4). Hence phosphorylation can also be used as a signal for degradation of a protein (Vlach *et al.*, 1997; Niu *et al.*, 1998; Ke *et al.*, 2003) and hereby

keeping the level of Prat1.1 at a constant amount. The results from experiments performed in plants have shown that post-translational regulation of protein levels plays a key role in the control of the plant circadian clock (Mas *et al.*, 2003; Ito *et al.*, 2007; Kiba *et al.*, 2007; Fujiwara *et al.*, 2008). To what extent this applies for the Prat1 protein still needs to be further investigated.

5.4 Prat1 influences certain metabolic pathways

To generate an overview of the metabolic activities in the Prat1 wild type and double mutant plants from *Arabidopsis thaliana* and analyse the observed phenotype of retardation in growth in more detail, a metabolic profiling experiment was carried out. Taking a closer look at the identified metabolites that are up/down-regulated in the Prat1 double mutant could give insights into the specific substrates of the Prat1 protein and thereby help to further elucidate its function within the inner envelope of the chloroplast. Some metabolites could be identified that depict an altered amount in the double mutant plant in comparison to the wild type. These include the slight but significant down-regulation of glycine, gluconic acid and glyceric acid under constant light conditions, as well as the up-regulation of aspartic acid under long-day conditions. By comparing these results with the phenotype of the Prat1 double mutant plants, a possible explanation could be concluded (see 4.9): retardation in growth in comparison to the wild type plants indicates that the plant metabolism is influenced by the loss of the Prat1 protein, although it can partially be compensated. Thus, the function of Prat1 might be redundant to some extent to that of another protein. Most likely, if Prat1 does display channel activity, the transported substrates are capable of reaching their final destination via other proteins similar to Prat1, however with reduced effectivity. This process is hence more complex and time-consuming resulting in a slower growth of the double mutant plant. As a consequence, some metabolites accumulate because the substrates required for further processing are low abundant, while others become down-regulated due to a missing precursor. The association between other channel proteins in *Arabidopsis thaliana* and plant growth have shown recently that the knock-out mutant of the voltage-dependent anion channel 2 in mitochondria can suffer of severe growth retardation (Tateda *et al.*, 2012).

Glycine, found to be down-regulated under constant light conditions, is synthesized from the amino acid serine, which in turn is derived from 3-phosphoglycerate, an intermediate metabolite in both glycolysis and the Calvin cycle. The lack of either a metabolite or processing enzyme involved in its synthesis pathway will lead to an alteration in its

abundance. One major process in the plant metabolism is photorespiration which occurs when CO₂-levels are low and the enzyme RuBisCO combines O₂ with the sugar Ribulose-1,5-bisphosphate (RuBP) instead of adding CO₂ which is the case during photosynthesis. As a result toxic phosphoglycolate is produced and has to be catabolised before the molecules can re-enter the Calvin cycle. Since photorespiration occurs in the chloroplast (Calvin cycle, oxygen fixation via RuBisCO) the peroxisome (glycolate is converted to glycine) and the mitochondria (glycine is converted to serine; glycolysis, converts glucose to pyruvate), constant shuttling of metabolites and amino acids is mandatory (Bauwe *et al.*, 2010; Figure 38).

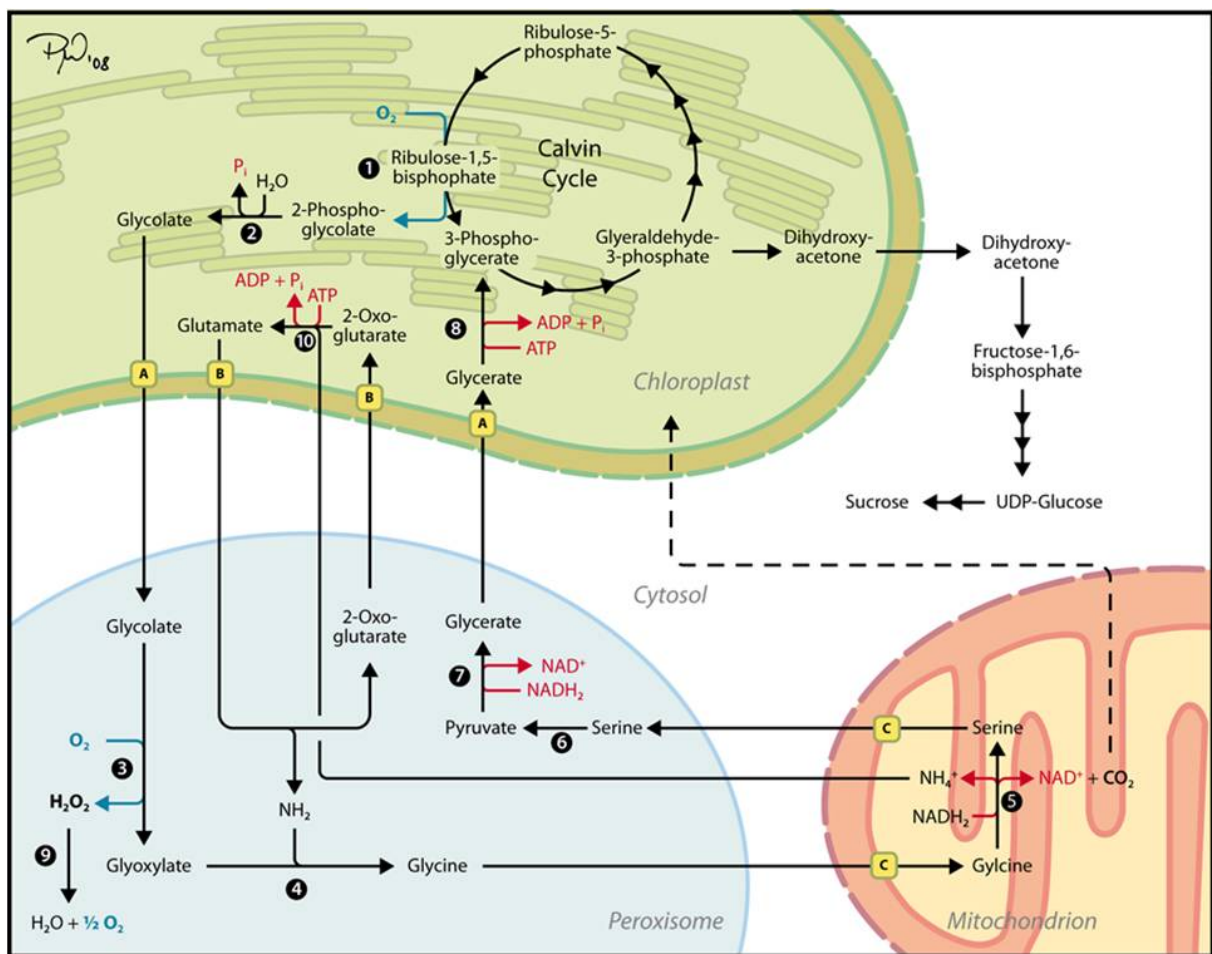


Figure 38: Photorespiration.

The figure was taken from 'Biochemistry and Molecular Biology of Plants' by Buchanan BB, Gruissem W, Jones RL (2000). Depicted is a simplified model of the processes occurring during photorespiration in a plant cell. Black circled numbers represent the enzymes that catalyse the indicated step. 1 = RuBisCO; 2 = phosphoglycolate phosphatase; 3 = glycolate oxidase; 4 = glutamate-glyoxylate aminotransferase; 5 = glycine decarboxylase complex; 6 = serin-glyoxylate aminotransferase; 7 = pyruvate reductase; 8 = glycerate kinase; 9 = catalase; 10 = glutamate synthase and glutamine synthetase. Yellow highlighted letters represent known translocators. A = glycerate-glycolate translocator; B = malate-glutamate/2-oxoglutarate translocator; C = amino acid translocator.

Responsible for the transport of the metabolite glycerate during photorespiration is the glycerate-glycolate translocator with proton/substrate symport activity (Young and McCarty 1993; Figure 38). A conceivable function for the Prat1 transporter could include the translocation of preproteins of the enzymes needed to catalyse the further steps in glycerate processing in the Calvin cycle taking place within the chloroplast. Additionally, the down-regulation of glyceric acid, whose phosphate derivatives are important intermediates in the glycolysis and the lower amount of gluconic acid which arises from the oxidation of glucose seem to be consistent consequences for plants suffering from a loss of the Prat1 protein being active in preprotein transport during photorespiration.

On the other hand, aspartic acid, an acidic amino acid and precursor for lysine and methionine is up-regulated under long-day conditions, leading to a slight increase in the abundance of the essential amino acids lysine and methionine as well. The derivative of aspartic acid, aspartate, participates in the gluconeogenesis (generation of glucose; Leegood and Rees, 1978), indicating that Prat1 double mutant plants seem to be affected in the production (gluconeogenesis) and degradation (glycolysis) of glucose. Slightly elevated levels of glucose (Figure 35) could suggest a higher generation rate, but more likely defects in degradation lead to an accumulation of glucose and a decrease in metabolites downstream in the complex process of photorespiration, demonstrated by the down-regulation of the metabolites mentioned above. Which specific substrate is translocated by the Prat1 protein remains to be the goal of further studies. A strong indication for a function as a transporter of preproteins or metabolites involved in photorespiration has been given in the present study. Nevertheless, more experimental data is needed to confirm this.

6 References

Used references for this work in alphabetical order:

- Andrès C., Agne B., Kessler F.**, (2010). The TOC complex: Proprotein gateway to the chloroplast. *Biochimica et Biophysica Acta - Molecular Cell Research* Vol. 1803 Nr. 6 p. 715 - 723.
- Ansorge W.**, (1985). Fast and sensitive detection of protein and DNA bands by treatment with potassium permanganate. *J. Biochem. Biophys. Methods* 11(1): 13-20
- Arnon D. I.**, (1949). Copper Enzymes in Isolated Chloroplasts - Polyphenoloxidase in Beta-Vulgaris. *Plant Physiology* 24: 1-15.
- Aronsson H., Jarvis P.**, (2002). A simple method for isolating import-competent Arabidopsis chloroplasts. *FEBS Lett* 529: 215-220.
- Ashpole N. M., Herren A. W., Ginsburg K. S., Brogan J. D., Johnson D. E., Cummins T. R., Bers D. M., Hudmon A.**, (2012). Ca²⁺/Calmodulin-dependent Protein Kinase II (CaMKII) Regulates Cardiac Sodium Channel NaV1.5 Gating by Multiple Phosphorylation Sites. *J. Biol. Chem.* 8;287(24):19856-69.
- Balsera M., Goetze T. A., Kovács-Bogdán E., Schürmann P., Wagner R., Buchanan B. B., Soll J., Bölter B.**, (2009). Characterization of Tic110, a channel-forming protein at the inner envelope membrane of chloroplasts, unveils a response to Ca²⁺ and a stromal regulatory disulfide bridge. *J. Biol. Chem.* 284, 2603-2616.
- Bauer M. F., Rothbauer U., Mühlenbein N., Smith R. J., Gerbitz K., Neupert W., Brunner M., Hofmann S.**, (1999). The mitochondrial TIM22 preprotein translocase is highly conserved throughout the eukaryotic kingdom. *FEBS Lett.* 24;464(1-2):41-7.
- Bauwe H., Hagemann M., Fernie A. R.**, (2010). Photorespiration: players, partners and origin. *Trends Plant Sci.* 15(6):330-6.
- Becker T., Hritz J., Vogel M., Caliebe A., Bukau B., Soll J., Schleiff E.**, (2004). Toc12, a novel subunit of the intermembrane space preprotein translocon of chloroplasts. *Molecular Biology of the Cell* 15: 5130-5144.
- Benz J. P., Soll J., Bölter B.**, (2009). Protein transport in organelles: The composition, function and regulation of the Tic complex in chloroplast protein import. *FEBS Journal*, 276, 5, 1166-76.
- Benz M., Bals T., Gügel I. L., Piotrowski M., Kuhn A., Schünemann D., Soll J., Ankele E.**, (2009). Alb4 of Arabidopsis Promotes Assembly and Stabilization of a Non Chlorophyll-Binding Photosynthetic Complex, the CF₁CF₀-ATP Synthase. *Molecular Plant* Vol. 2 Nr. 6 p. 1410-1424.
- Bölter B., Soll J., Hill K., Hemmler R., Wagner R.**, (1999). A rectifying ATP-regulated solute channel in the chloroplastic outer envelope from pea. *EMBO J.* 18: 5505-5516.

- Bohnert M., Pfanner N., van der Laan M.**, (2007). A dynamic machinery for import of mitochondrial precursor proteins. *FEBS Lett.* 19;581(15):2802-10.
- Bradford M. M.**, (1976). A rapid and sensitive method for the quantitation of microgram quantities of protein utilizing the principle of protein-dye binding. *Anal. Biochemical.*, 72, 248-254.
- Chang C., Stewart R. C.**, (1998). The two-component system. Regulation of diverse signalling pathways in prokaryotes and eukaryotes. *Plant Physiol.* 117(3):723-31.
- Chiu C. C., Chen L. J., Li H. M.**, (2010). Pea chloroplast DnaJ-J8 and Toc12 are encoded by the same gene and localized in the stroma. *Plant Physiol.* 154(3):1172-82.
- Chiu M. L.**, (2012). Introduction to membrane proteins. *Curr. Protoc. Protein Sci.* Chapter 29:Unit 29.1.
- Ciesla J., Fraczyk T., Rode W.**, (2011). Phosphorylation of basic amino acid residues in proteins: important but easily missed. *Acta Biochim. Pol.* 58(2):137-48.
- Cline K., Werner-Washbourne M., Lubbe T. H., Keegstra K.**, (1985). Precursors to two nuclear-encoded chloroplast proteins bind to the outer envelope membrane before being imported into the chloroplasts. *J.Biol.Chem.* 260: 3691-3696.
- Denkert C., Budczies J., Weichert W., Wohlgemuth G., Scholz M., Kind T., Niesporek S., Noske A., Buckendahl A., Dietel M., Fiehn O.**, (2008). Metabolite profiling of human colon carcinoma--deregulation of TCA cycle and amino acid turnover. *Mol. Cancer* 18; 7:72.
- Dowson-Day M. J., Millar A. J.**, (1999). Circadian dysfunction causes aberrant hypocotyl elongation patterns in Arabidopsis. *Plant J.* 17, 63–71.
- Drea S. C., Lao N. T., Wolfe K. H., Kavanagh T. A.**, (2006). Gene duplication, exon gain and neofunctionalization of OEP16-related genes in land plants. *Plant J.*, 46, 723–735.
- Duy D., Soll J., Philippar K.**, (2007). Solute channels of the outer membrane: from bacteria to chloroplasts. *Biol. Chem.*, 388, 879–889.
- Emanuelsson O., Nielsen H., von Heijne G.**, (1999). ChloroP, a neural network-based method for predicting chloroplast transit peptides and their cleavage sites. *Protein Science.*, 8, 978-984.
- Emerson R., Arnold W.**, (1932). The Photochemical Reaction in Photosynthesis. *J. Gen. Physiol.* 20;16(2):191-205.
- Fellerer C., Schweiger R., Schöngruber K., Soll J., Schwenkert S.**, (2011). Cytosolic Hsp90 cochaperones HOP and FKBP interact with freshly synthesized chloroplast preproteins of Arabidopsis. *Mol. Plant.* 4(6):1133-45.
- Ferro M., Salvi D., Riviere-Rolland H., Vermat T., Seigneurin-Berny D., Grunwald D., Garin J., Joyard J., Rolland N.**, (2002). Integral membrane proteins of the

- chloroplast envelope: identification and subcellular localization of new transporters. *Proc Natl Acad Science USA*, 99:11487-11492.
- Ferro M., Salvi D., Brugiare S., Miras S., Kowalski S., Louwagie M., Garin J., Joyard J., Rolland N.**, (2003). Proteomics of the chloroplast envelope membranes from *Arabidopsis thaliana*. *Molecular and Cellular Proteomics*, 2, 325–345.
- Firlej-Kwoka E., Strittmatter P., Soll J., Bölder B.**, (2008). Import of preproteins into the chloroplast inner envelope membrane. *Plant Mol.Biol.* 68: 505-519.
- Fischer W. N., Loo D. D. F., Koch W., Ludewig U., Boorer K. J., Tegeder M., Rentsch D., Wright E. M. Frommer W. B.**, (2002). Low and high affinity amino acid H⁺-cotransporters for cellular import of neutral and charged amino acids. *Plant Journal*. 29, 717–731.
- Flores-Péres U., Jarvis P.**, (2012). Molecular chaperone involvement in chloroplast protein import. *Biochim. Biophys. Acta*. Apr. 12. [Epub ahead of print]
- Foyer C. H, Bloom A., Queval G., Noctor G.**, (2009). Photorespiratory Metabolism: Genes, Mutants, Energetics, and Redox Signaling, *Annu. Rev. Plant Biology*. 60, 455–84.
- Froehlich J.E., Wilkerson C.G., Ray W.K., McAndrew R.S., Osteryoung K.W., Gage D.A., Phinney B.S.**, (2003). Proteomic study of the *Arabidopsis thaliana* chloroplastic envelope membrane utilizing alternatives to traditional two-dimensional electrophoresis. *Journal Proteome Research*, 2, 413-425.
- Frydman J., Hohfeld J.**, (1997). Chaperones get in touch: the Hip-Hop connection. *Trends Biochem.Sci.* 22: 87-92.
- Fujiwara S., Wang L., Han L., Suh S. S., Salome P. A., McClung C. R., Somers D. E.**, (2008). Post-translational regulation of the Arabidopsis circadian clock through selective proteolysis and phosphorylation of pseudo-response regulator proteins. *J Biol Chem* 283, 23073-23083.
- Giebultowicz J.**, (2004). Chronobiology: biological timekeeping. *Integr. Comp. Biol.* 44(3):266.
- Gould S. B., Waller R. F., McFadden G. I.**, (2008). Plastid evolution. *Annu Rev Plant Biol* 59:491-517.
- Gutierrez R. A., Ewing R. M., Cherry J. M., Green P. J.**, (2002). Identification of unstable transcripts in Arabidopsis by cDNA microarray analysis: Rapid decay is associated with a group of touch- and specific clock-controlled genes. *Proc. Natl. Acad. Sci. USA* 99, 11513–11518.
- Harmer S. L., Hogenesch J. B., Straume M., Chang H. S., Han B., Zhu T., Wang X., Krops J. A., Kay S. A.**, (2000). Orchestrated transcription of key pathways in Arabidopsis by the circadian clock. *Science* 290, 2110-2113.
- Hasson S. A., Damoiseaux R., Galvin J. D., Dabir D. V., Walker S. S., Koehler C. M.**, (2010). Substrate specificity of the Tim22 mitochondrial import pathway revealed

- with small molecule inhibitor of protein translocation. *Proc. Natl. Acad. Sci. USA*, 25;107(21):9578-83.
- Heins L., Mehrle A., Hemmler R., Wagner R., Kuchler M., Hörmann F., Sveshnikov D., Soll J.**, (2002). The preprotein conducting channel at the inner envelope membrane of plastids. *EMBO J.* 21: 2616-2625.
- Hennessey T. L., Field C. B.**, (1991). Circadian Rhythms in Photosynthesis: Oscillations in Carbon Assimilation and Stomatal Conductance under Constant Conditions. *Plant Physiol* 96, 831-836.
- Hirsch S., Muckel E., Heemeyer F., von Heijne G., Soll J.**, (1994). A receptor component of the chloroplast protein translocation machinery. *Science* 266: 1989-1992.
- Hoffmann C. W.**, (2010). Strategies for cryo-electron tomography of the mycobacterial cell envelope and its pore proteins and functional studies of porin MspA from *Mycobacterium smegmatis*. *PhD-Thesis*, TU München, MPI für Biochemie, Abteilung für Molekulare Strukturbiologie.
- Hyland C., Vuillard L., Hughes C., Koronakis V.**, (2001). Membrane interaction of Escherichia coli hemolysin: flotation and insertion-dependent labeling by phospholipid vesicles. *J. Bacteriol.* 183(18):5364-70.
- Imaizumi T., Kay S. A.**, (2006). Photoperiodic control of flowering: not only by coincidence. *Trends Plant Sci.* 11(11):550-8.
- Ito S., Nakamichi N., Nakamura Y., Niwa Y., Kato T., Murakami M., Kita M., Mizoguchi T., Niinuma K., Yamashino T., Mizuno T.**, (2007). Genetic linkages between circadian clock-associated components and phytochrome-dependent red light signal transduction in *Arabidopsis thaliana*. *Plant Cell Physiol.* 48(7):971-83.
- Ito S., Nakamichi N., Kiba T., Yamashino T., Mizuno T.**, (2007). Rhythmic and Light-Inducible Appearance of Clock-Associated Pseudo-Response Regulator Protein PRR9 Through Programmed Degradation in the Dark in *Arabidopsis thaliana*. *Plant Cell Physiol.*, pcm122.
- Ito S., Niwa Y., Nakamichi N., Kawamura H., Yamashino T., Mizuno T.**, (2008). Insight into missing genetic links between two evening-expressed pseudo-response regulator genes TOC1 and PRR5 in the circadian clock-controlled circuitry in *Arabidopsis thaliana*. *Plant Cell Physiol.* 49(2):201-13.
- Jeanguenin L., Lebaudy A., Xicluna J., Alcon C., Hosy E., Duby G., Michard E., Lacombe B., Dreyer I., Thibaud J.B.**, (2008). Heteromerization of *Arabidopsis* K_v channel α -subunits. *Plant Signaling & Behavior*, 3(9), 622-625.
- Ke P. Y., Yang C.C., Tsai I. C., Chang Z. F.**, (2003). Degradation of human thymidine kinase is dependent on serine-13 phosphorylation: involvement of the SCF-mediated pathway. *Biochem J.* 15;370(Pt 1):265-73.

- Keegstra K., Youssif A. E.,** (1986). Isolation and characterization of chloroplast envelope membranes. In: Weissbach A., Weissbach H. (Eds.), *Methods Enzymology – Plant Molecular Biology*, Vol 118, pp. 316-325.
- Kessler F., Blobel G., Patel H. A., Schnell D. J.,** (1994). Identification of two GTP-binding proteins in the chloroplast protein import machinery. *Science* 266: 1035-1039.
- Kiba T., Henriques R., Sakakibara H., Chua N. H.,** (2007). Targeted Degradation of PSEUDO-RESPONSE REGULATOR5 by an SCFZTL Complex Regulates Clock Function and Photomorphogenesis in *Arabidopsis thaliana*. *Plant Cell* 19, 2516-2530.
- Ko K., Bornemisza O., Kourtz L., Ko Z. W., Plaxton W. C., Cashmore A. R.,** (1992). Isolation and characterization of a cDNA clone encoding a cognate 70-kDa heat shock protein of the chloroplast envelope. *J Biol Chem* 267: 2986-2993.
- Korepanova A., Matayoshi E. D.,** (2012). HPLC-SEC characterization of membrane protein-detergent complexes. *Curr. Protoc. Protein Sci.* Chapter 29:Unit 29.5.1-12.
- Kovács-Bogdán E., Soll J., Bölder B.,** (2010). Protein import into chloroplasts: the Tic complex and its regulation. *Biochim. Biophys. Acta.* 1803(6):740-7.
- Kovács-Bogdán E., Benz J. P., Soll J., Bölder B.,** (2011). Tic20 forms a channel independent of Tic110 in chloroplasts. *BMC Plant Biol.* 30;11:133.
- Kovermann P., Truscott K. N., Guiard B., Rehling P., Sepuri N. B., Muller H., Jensen R. E., Wagner R.,** (2002). Tim22, the essential core of the mitochondrial protein insertion complex, forms a voltage-activated and signal-gated channel. *Molecular Cell* 9, 363-373.
- Küchler M., Decker S., Hörmann F., Soll J., Heins L.,** (2002). Protein import into chloroplasts involves redox-regulated proteins. *Embo Journal* 21: 6136-6145.
- Kurz M., Martin H., Rassow J., Pfanner N., Ryan M. T.,** (1999). Biogenesis of Tim proteins of the mitochondrial carrier import pathway: differential targeting mechanisms and crossing over with the main import pathway. *Mol. Biol. Cell.* 10(7):2461-74.
- Laemmli U. K.,** (1970). Cleavage of Structural Proteins During Assembly of Head of Bacteriophage-T4. *Nature* 227: 680-&.
- Lam H. M., Coschigano K. T., Oliveira I. C., Melo-Oliveira R., Coruzzi G. M.,** (1996). The molecular genetics of nitrogen assimilation into amino acids in higher plants. *Annual Review Plant Physiology*, 47, 569–93.
- Lamb J. R., Tugenreich S., Hieter P.,** (1995). Tetratricopeptide repeat interactions: to TPR or not to TPR? *Trends Biochem.Sci.* 20: 257-259.
- Laubinger S., Zeller G., Henz S. R., Sachsenberg T., Widmer C. K., Naouar N., Vuylsteke M., Schölkopf B., Rättsch G., Weigel D.,** (2008). At-TAX: a whole genome tiling array resource for developmental expression analysis and transcript identification in *Arabidopsis thaliana*. *Genome Biology*, 10.1186/gb-2008-9-7-r112

- Leegood R. C., Rees T.,** (1978). Identification of the regulatory steps in gluconeogenesis in cotyledons of *Cucurbita pepo*. *Biochim. Biophys. Acta.* 3;542(1):1-11.
- Li H. M., Chen L. J.,** (1996), Protein targeting and integration signal for the chloroplastic out-er envelope membrane. *Plant Cell* 8: 2117-2126.
- Li H. M., Moore T., Keegstra K.,** (1991). Targeting of proteins to the outer envelope membrane uses a different pathway than transport into chloroplasts. *Plant Cell* 3: 709-717.
- Lowry O. H., Rosebrough N. J., Farr A. L., Randall R. J.,** (1951). Protein Measurement with the Folin Phenol Reagent. *Journal of Biological Chemistry* 193: 265-275.
- Lübeck J., Soll J., Akita M., Nielsen E., Keegstra K.,** (1996). Topology of IEP110, a component of the chloroplastic protein import machinery present in the inner envelope membrane. *EMBO J.* 15: 4230-4238.
- Margulis L.,** (1970). Origin of eukaryotic cells. *New Haven, CT, USA: Yale University Press*
- Mas P., Kim W. Y., Somers D. E., Kay S. A.,** (2003). Targeted degradation of TOC1 by ZTL modulates circadian function in *Arabidopsis thaliana*. *Nature* 426, 567-570.
- May T., Soll J.,** (2000). 14-3-3 proteins form a guidance complex with chloroplast precursor proteins in plants. *Plant Cell* 12: 53-63.
- Michael T. P., McClung C. R.,** (2003). Enhancer trapping reveals widespread circadian clock transcriptional control in *Arabidopsis*. *Plant Physiol* 132, 629-639.
- Mokranjac D., Neupert W.,** (2010). The many faces of the mitochondrial TIM23 complex. *Biochim Biophys. Acta.* 1797(6-7):1045-54.
- Morandat S., Bortolato M., Roux B.,** (2002).Cholesterol-dependant insertion of glycosylphosphatidylinositol-anchored enzyme. *Biochim Biophys Acta* 31;1564(2):473-78.
- Moro F., Sirrenberg C., Schneider H. C., Neupert W., Stuart R. A.,** (1999). The TIM17,23 preprotein translocase of mitochondria: composition and function in protein transport into the matrix. *EMBO J.* 1;18(13):3667-75.
- Murcha M. W., Elhafez D., Lister R., TontiFilippini J., Baumgartner M., Philippar K., Carrie C., Mokranjac D., Soll J., Whelan J.,** (2007). Characterisation of the preprotein and amino acid transporter gene family in *Arabidopsis*. *Plant Physiology*, 134, 199–212.
- Neupert W., Herrmann J.M.,** (2007). Translocation of proteins into mitochondria. *Annual Review of Biochemistry*, 76, 723-749.
- Nielsen E., Akita M., Dávila-Aponte J. A., Keegstra K.,** (1997). Stable association of chloroplastic precursor with protein translocation complexes that contain proteins

- from both envelope membranes and a stromal Hsp100 molecular chaperone. *EMBO J.* 16: 935-946.
- Nui H., Ye B. H., Dalla-Favera R.,** (1998). Antigen receptor signaling induces MAP kinase-mediated phosphorylation and degradation of the BCL-6 transcription factor. *Genes Dev.* 1;12(13):1953-61.
- Olsen J. V., Blagoev B., Gnad F., Macek B., Kumar C., Mortensen P., Mann M.,** (2006). Global, in vivo, and site-specific phosphorylation dynamics in signaling networks. *Cell* 3;127(3):635-48.
- Perry S. E., Keegstra K.,** (1994). Envelope membrane proteins that interact with chloroplastic precursor proteins. *Plant Cell* 6: 93-105.
- Philippar K., Ivashikina N., Ache P., Christian M., Luthen H., Palme K., Hedrich R.,** (2004). Auxin activates KAT1 and KAT2, two K⁺-channel genes expressed in seedlings of *Arabidopsis thaliana*. *Plant Journal* 37: 815-827.
- Philippar K., Soll J.,** (2007). Intracellular transport: solute transport in chloroplasts, mitochondria, peroxisomes and vacuoles, and between organelles. In: Yeo A.R., Flowers T.J. (Eds), Plant solute transport. *Blackwell Publishing, Oxford, UK*, 133–192.
- Pohlmeier K., Soll J., Steinkamp T., Hinnah S., Wagner R.,** (1997). Isolation and characterization of an amino acid-selective channel protein present in the chloroplastic outer envelope membrane. *Proc.Natl.Acad.Sci.U.S.A* 94: 9504-9509.
- Pohlmeier K., Soll J., Grimm R., Hill K., Wagner R.,** (1998). A high-conductance solute channel in the chloroplastic outer envelope from Pea. *Plant Cell* 10: 1207-1216.
- Pudelski B., Kraus S., Soll J., Philippar K.,** (2010). The plant PRAT proteins - preprotein and amino acid transport in mitochondria and chloroplasts. *Plant Biology* 12 Suppl 1:42-55
- Pudelski B., Schock A., Hoth S., Radchuk R., Weber H., Hofmann J., Sonnenwald U., Soll J., Philippar K.,** (2012). The plastid outer envelope protein OEP16 affects metabolic fluxes during ABA-controlled seed development and germination. *J Exp Bot.* 63(5): 1919-36.
- Qbadou S., Becker T., Mirus O., Tews I., Soll J., Schleiff E.,** (2006). The molecular chaperone Hsp90 delivers precursor proteins to the chloroplast import receptor Toc64. *Embo Journal* 25: 1836-1847.
- Rassow J., Dekker P. J., van Wilpe S., Meijer M., Soll J.,** (1999). The preprotein translocase of the mitochondrial inner membrane: function and evolution. *J.Mol.Biol.* 286: 105-120.
- Rehling P., Wiedemann N., Pfanner N., Truscott K. N.,** (2001). The mitochondrial import machinery for preproteins. *Crit. Rev. Biochem. Mol. Biol.* 36(3):291-336.

- Reiland S., Finazzi G., Endler A., Willig A., Baerenfaller K., Grossmann J., Gerrits B., Rutishauser D., Gruissem W., Rochaix J. D., Baginsky S.,** (2011). Comparative phosphoproteome profiling reveals a function of the STN8 kinase in fine-tuning of cyclic electron flow (CEF). *Proc Natl Acad Sci U S A*;108(31):12955-60.
- Reumann S., Inoue K., Keegstra K.,** (2005). Evolution of the general protein import pathway of plastids (review). *Mol.Membr.Biol.* 22: 73-86.
- Richter S., Lamppa G. K.,** (1998). A chloroplast processing enzyme functions as the general stromal processing peptidase. *PNAS* 95: 7463-7468.
- Saiki R., Gelfand D., Stoffel S., Scharf S., Higuchi R., Horn G., Mullis K., Erlich H.,** (1988). Primer-directed enzymatic amplification of DNA with a thermostable DNA polymerase. *Science* 239: 487-491.
- Salomé P. A., Weigel D., McClung R. C.,** (2010). The Role of the *Arabidopsis* Morning Loop Components CCA1, LHY, PRR7 and PRR9 in Temperature Compensation. *The Plant Cell* vol. 22 no. 11 3650-3661.
- Salomon M., Fischer K., Flugge U. I., Soll J.,** (1990). Sequence analysis and protein import studies of an outer chloroplast envelope polypeptide. *Proc.Natl.Acad.Sci.U.S.A* 87: 5778-5782.
- Sambrook J., Fritsch E. F., Maniatis T.,** (1989). Molecular Cloning - A Laboratory Manual. *Cold Spring Harbour Laboratory Press*, New York.
- Schaffer R., Landgraf J., Accerbi M., Simon V., Larson M., Wisman E.,** (2001). Microarray analysis of diurnal and circadian-regulated genes in *Arabidopsis*. *Plant Cell* 13, 113-123.
- Schagger H., von Jagow G.,** (1987). Tricine-sodium dodecyl sulfate-polyacrylamide gel electrophoresis for the separation of proteins in the range from 1 to 100 kDa. *Anal. Biochem.* 166, 368–379.
- Schagger H., von Jagow G.,** (1991). Blue native electrophoresis for isolation of membrane protein complexes in enzymatically active form. *Anal Biochem* 199: 223-231.
- Schindler C., Hracky R., Soll J.,** (1987). Protein transport in chloroplasts: ATP is prerequisite. *Z. Naturforsch.* 42c, 103-108.
- Schnell D. J., Blobel G., Pain D.,** (1990). The chloroplast import receptor is an integral membrane protein of chloroplast envelope contact sites. *J Cell Biol* 111: 1825-1838.
- Schnell D. J., Kessler F., Blobel G.,** (1994). Isolation of components of the chloroplast protein import machinery. *Science* 266: 1007-1012.
- Schwacke R., Schneider A., van der Graaff E., Fischer K., Catoni E., Desimone M., Frommer W.B., Flügge U.I., Kunze R.,** (2003). ARAMEMNON, a novel database for *Arabidopsis* integral membrane proteins. *Plant Physiology*, 131, 16–26.

- Seedorf M., Waegemann K., Soll J.,** (1995). A constituent of the chloroplast import complex represents a new type of GTP-binding protein. *Plant J.* 7: 401-411.
- Seigneurin-Berny D., Salvi D., Dorne A. J., Joyard J., Rolland N.,** (2008). Percoll-purified and photosynthetically active chloroplasts from *Arabidopsis thaliana* leaves. *Plant Physiology and Biochemistry* 46: 951-955.
- Smith S.,** (2005). Transcription profiling by array of Arabidopsis over the diurnal cycle. (22 assays) E-NASC-49.
- Sohrt K., Soll J.,** (2000). Toc64, a new component of the protein translocon of chloroplasts. *J. Cell Biol.* 148: 1213-1221.
- Steinkamp T., Hill K., Hinnah S. C., Wagner R., Rohl T., Pohlmeier K., Soll J.,** (2000). Identification of the pore-forming region of the outer chloroplast envelope protein OEP16. *Journal Biological Chemistry*, 275, 11758-11764.
- Stengel A., Benz P., Balsera M., Soll J., Bölter B.,** (2008). TIC62 redox-regulated translocon composition and dynamics. *J Biol Chem* 283: 6656-6667.
- Strittmatter P., Soll J., Bölter B.,** (2010). Chloroplast protein import machinery. *Springer Verlag, Protein Sekretion* 2: 307-321.
- Sun Q., Zybailov B., Majeran W., Friso G., Olinares P. D., van Wijk K. J.,** (2008). PPDB, the Plant Proteomics Database at Cornell. *Nucleic Acids Res.* Oct 2 [Epub].
- Sveshnikova N., Soll J., Schleiff E.,** (2000). Toc34 is a preprotein receptor regulated by GTP and phosphorylation. *Proc. Natl. Acad. Sci. U.S.A* 97: 4973-4978.
- Tateda C., Kusano T., Takahashi Y.,** (2012). The Arabidopsis voltage-dependent anion channel 2 is required for plant growth. *Plant Signal Behav.* 7(1):31-3.
- Truscott K. N., Kovermann P., Geissler A., Merlin A., Meijer M., Driessen A. J., Rassow J. Pfanner N., Wagner R.,** (2001). A presequence- and voltage-sensitive channel of the mitochondrial preprotein translocase formed by Tim23. *Nat. Struct. Biol.* 8(12):1074-82.
- Vlach J., Hennecke S., Amati B.,** (1997). Phosphorylation-dependent degradation of the cyclin-dependent kinase inhibitor p27. *EMBO J.* 1;16(17):5334-44.
- Vojta A., Alavi M., Becker T., Hormann F., Kuchler M., Soll J., Thomson R., Schleiff E.,** (2004). The protein translocon of the plastid envelopes. *J. Biol. Chem.* 279: 21401-21405.
- von Heijne G., Streppuhn J., Herrmann R. G.,** (1989). Domain structure of mitochondrial and chloroplast targeting peptides. *J. Biochem.* 180: 535-545.
- Waegemann K., Eichacker S., Soll J.,** (1992). Outer envelope membranes from chloroplasts are isolated as right-side-out vesicles. *Planta* 89-94.

Weber A. P., Fischer K., (2007). Making the connections - the crucial role of metabolite transporters at the interface between chloroplast and cytosol. *FEBS Letter*, 25, 2215-22.

Winter D., Vinegar B., Nahal H., Ammar R., Wilson G. V., Provart N. J., (2007). An "Electronic Fluorescent Pictograph" browser for exploring and analyzing large-scale biological data sets. *PLoS ONE* 2: e718.

Wittig I., Braun H. P., Schagger H., (2006). Blue native PAGE. *Nat Protoc* 1: 418-428.

Yanovsky M. J., Kay S. A., (2002). Molecular basis of seasonal time measurement in Arabidopsis. *Nature* 419, 308–312.

Young X. K., McCarty R. E., (1993). Assay of Proton-Coupled Glycolate and D-Glycerate Transport into Chloroplast Inner Envelope Membrane Vesicles by Stopped-Flow Fluorescence. *Plant Physiology* vol. 101 no. 3 793-799.

8 Acknowledgements

First of all I would like to thank Prof. Dr. Jürgen Soll for entrusting me with the possibility to realize my PhD work in his lab, with his support and his ever open door.

Also I would like to thank my supervisor PD Dr. Bettina Bölter for always having answers to my flood of questions and continually helping me to improve my work.

I am grateful to everyone who contributed to this work with experiments, samples and discussions: The group of Prof. Richard Wagner (Osnabrück), especially Anke, for introducing me into the field of electrophysiology; Ana (Prof. Martin Parniske) for her help with the Nanion machine; Roland (Ionovation GmbH) for his support with the Bilayer Explorer; the group of Prof. Andreas Weber (Düsseldorf) for performing the metabolic profiling; Zdravko (Prof. Wolfgang Baumeister) for his relentless tries to get a structure of Prat1; Giorgia for her introduction of phosphorylation assays, and Manuela for her prior work that initiated this project.

Special thanks go to Anna and Philipp for all the help and advice they offered to get me started in the lab and the proofreading by Anna at the end.

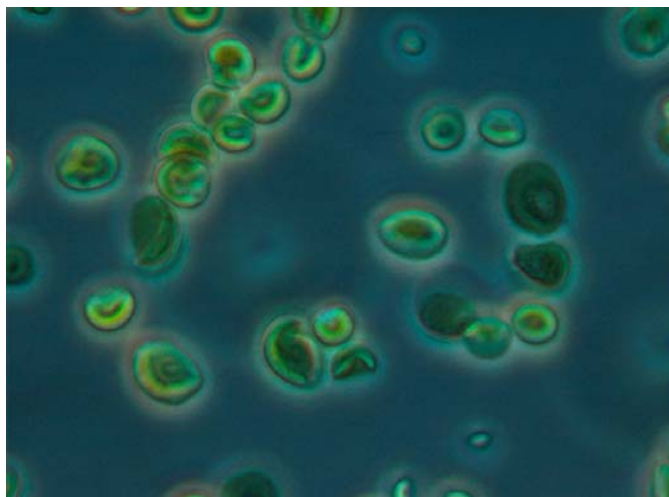
Thank you Eike and Katja for supporting me in my daily challenges. It was a lot of fun working with and next to you two. A big thank you also to Erika and Maike - the best team to tackle any electrophysiological problem.

Many thanks to the entire lab for creating such a positive atmosphere and bringing a bit of laughter and fun into so many lab situations. In particular the 'Tic'-lab: Andi, Angela, Natalie, Penelope and WaiLing. You guys (eh girls) are great company to have.

Thanks also to Ingo – there is no better lunchtime companion.

I would also like to thank the members of the ENB-graduate-program for the stimulating discussions on numerous scientific (and non-scientific) subjects and the great retreats. I have found many friends there.

My greatest thanks are dedicated to my parents and family (worldwide) who supported me every step of the way, and of course my lovely wife for giving me the strength and faith to meet any challenge.



9 Curriculum Vitae

Carsten Studte

19. November 1980 in São Paulo, Brasilien
Deutsch, Brasilianisch

Akademischer Werdegang

- 11/2008 – 10/2012 **Dissertation**, Lehrstuhl Prof. Dr. J. Soll
Ludwig-Maximilians-Universität, München
Titel: “Characterization of the membrane protein Prat1 in the inner envelope of chloroplasts”
- 10/2007 – 10/2008 **Diplomarbeit**, Lehrstuhl Prof. Dr. R. Reski
Albert-Ludwigs-Universität, Freiburg im Breisgau
Titel: “Functional Genomics of WOX-Homologs in *Physcomitrella patens*”
- 08/2004 – 08/2005 **Austauschstudent**
Genetik- und portugiesische Sprachkurse
Universidade Federal de Santa Catarina, Florianópolis, Brasilien
- 10/2001 – 09/2007 **Biologiestudium (Diplom)**
Albert-Ludwigs-Universität Freiburg im Breisgau
Hauptfach: Genetik / Nebenfächer: Biotechnologie, Zellbiologie
Zusätzliches Nebenfach: BWL

Schulischer Werdegang

- 07/2000 **Abitur** (Leistungskurse: Biologie und Englisch)
Klettgau Gymnasium Tiengen, Waldshut-Tiengen
- 06/1998 **High-School Diploma (Diplôme d'études secondaires)**
Alexander von Humboldt Schule, Montréal, Kanada

Auslandsaufenthalte

- | | |
|--------------------------|-------------|
| Florianópolis, Brasilien | 2004 – 2005 |
| Montréal, Kanada | 1991 – 1998 |
| São Paulo, Brasilien | 1980 – 1985 |

08. August 2012

